Biomimetic Approach to Cardiac Tissue Engineering

by
Milica Radisic

B.Eng. Chemical Engineering
McMaster University, 1999

Submitted to the Department of Chemical Engineering
in Partial Fulfillment of the Requirements for the Degree of

Doctor of Philosophy in Chemical Engineering

at the
Massachusetts Institute of Technology
September 2004

Signature of Author_____
Department of Chemical Engineering

Certified by_____
Robert S. Langer
Thesis Supervisor
Kenneth J. Germeshausen Professor of Chemical and
Biomedical Engineering

Accepted by_____
Daniel Blankschtein
Professor of Chemical Engineering
Chairman, Committee of Graduate Studies

This Doctoral Thesis has been examined by the following Thesis Committee:

Robert Langer, Sc.D._____
Thesis Advisor
Germeshausen Professor of Chemical and Biomedical Engineering
Department of Chemical Engineering
Massachusetts Institute of Technology

Charles L. Cooney, Ph.D._____
Professor of Chemical Engineering
Department of Chemical Engineering
Massachusetts Institute of Technology

William M. Deen, Ph.D._____
Carbon P. Dubbs Professor of Chemical Engineering
Department of Chemical Engineering
Massachusetts Institute of Technology

Lisa E. Freed: M.D., Ph.D._____
Research Scientist
Division of Health Sciences and Technology
Massachusetts Institute of Technology

Gordana Vunjak-Novakovic, Ph.D._____
Research Scientist
Division of Health Sciences and Technology
Massachusetts Institute of Technology

To Anastasia

ACKNOWLEDGEMENTS

I would like to acknowledge my thesis advisor Prof. Robert Langer and thesis committee members: Prof. William Deen, Prof. Charles Cooney, Dr. Lisa Freed and Dr. Gordana Vunjak-Novakovic for their valuable mentorship throughout the course of this Ph.D. thesis. I am especially thankful to Prof. Langer and Dr. Vunjak-Novakovic for their insight and advice not only in scientific but also in personal and professional matters.

I would like to thank Dr. Hyoungshin Park for making the tedious laboratory procedures seem like fun. I am thankful to my parents Vukosava and Branislav and my brother Milos for their love and encouragement. Finally, I would like to thank my husband Zoran for his constant and selfless support in both good and bad times.

Biomimetic Approach to Cardiac Tissue Engineering

by
Milica Radisic

Submitted to the Department of Chemical Engineering
On July 19th 2004 in Partial Fulfillment of the Requirements for the Degree of

Doctor of Philosophy in Chemical Engineering

Heart disease is the leading cause of death in the Western world. Tissue engineering may offer alternative treatment options or suitable models for studies of normal and pathological cardiac tissue function *in vitro*. Current tissue engineering approaches have been limited by diffusional oxygen supply, lack of physical stimuli and absence of multiple cell types characteristic of the native myocardium.

We hypothesized that functional, clinically sized (1-5 mm thick), compact cardiac constructs with physiologic cell densities can be engineered *in vitro* by mimicking cell microenvironment present in the native myocardium *in vivo* .

Since cardiac myocytes have limited ability to proliferate we developed methods of seeding cells at high densities while maintaining cell viability. Cultivation of cardiac constructs in the presence of convective-diffusive oxygen transport in perfusion bioreactors, maintained aerobic cell metabolism, viability and uniform distribution of cells expressing cardiac markers. To improve cell morphology and tissue assembly cardiac constructs were cultivated with electrical stimulation of contraction in a physiologically relevant regime. Electrical stimulation enabled formation of tissue with elongated cells aligned in parallel and with organized ultrastructure remarkably similar to the one present in the native heart. To investigate the effect of multiple cell types on the properties of engineered cardiac tissue cardiac fibroblasts and cardiac myocytes were cultivated synchronously, separately or serially (pretreatment of scaffolds with fibroblasts followed by the addition of myocytes). Presence of fibroblasts remarkably improved contractile response of the engineered cardiac constructs with the superior biochemical and morphological properties in the pretreated group. Finally, in order to mimic capillary structure cardiac fibroblasts and myocytes were co-cultured on a scaffold with a parallel channel array that was perfused with culture medium supplemented with synthetic oxygen carrier (PFC emulsion). Presence of the PFC emulsion resulted in significantly higher cell density and improved contractile properties compared to the constructs cultivated in the culture medium alone, by increasing total oxygen content and effective diffusivity.

Thesis Supervisor: Robert Langer
Title: Germeshausen Professor of Chemical and Biomedical Engineering

Table of Contents

List of Tables

List of Figures

1. INTRODUCTION

Cardiovascular disease is the leading cause of death in the Western world. It kills more people than next five leading causes of death including cancer. (AHA update 2004) Diseases related to myocardium, heart muscle, contribute to a significant portion of this death toll. Nearly 8 million people in the United States alone have suffered from myocardial infraction, with 800,000 new cases occurring each year [1].

Conventional treatment options, including drugs and assist devices are limited by inability of myocardium to regenerate after injury. Cell based therapies have been considered as a novel and potentially curative treatment option [2], either by utilization of cells alone [3-15] or by cultivation of cardiac construct *in vitro* that can be surgically attached to the myocardium [16-30]. While cell injection can be pursued as a treatment option for small scale injuries, improved cell localization achieved by tissue engineering can potentially be utilized to repair large scale injuries and congenital malformations. In addition, engineered cardiac tissue can be utilized as a model system for study of normal and pathological cardiac function *in vitro*.

Most of the current tissue engineering approaches are limited by diffusional supply of oxygen from the surface of the construct to the interior resulting in a non-uniform cell distribution with the shell of functional tissue on the outside and an empty interior. Construct cultivation in perfused cartridges markedly improved the uniformity of cell distribution but the overall cell density remained low, due to the oxygen diffusional limitations associated with cell seeding.

In standard culture systems (dishes, flasks, rotating vessels), cardiomyocytes did not align in parallel as in the native heart and they remained poorly differentiated due to the lack of orderly excitation-contraction coupling [17, 18]. Application of contraction alone via cyclic mechanical stretch significantly improved the level of cell differentiation and force of contraction, but some hallmarks of cardiac differentiation were still missing (M bands, IC discs) [29]. In addition, the distribution and frequency of gap junctions, critical for electrical signal propagation in the tissue, remained unclear. Notably, excitation-contraction coupling, which is crucial for the development and function of native myocardium [31], has not been established in any of these culture systems. The main objective of this thesis was to develop the tissue culture approach that would remedy the problems associated with the conventional culture.

We hypothesized that functional, clinically sized (1-5 mm thick), compact cardiac constructs with physiologic cell densities can be engineered *in vitro* by mimicking cell microenvironment present in the native myocardium *in vivo*. The key parameters in the cell microenvironment

include: high cell density with multiple cell types, convective diffusive oxygen transport through a capillary network and orderly excitation contraction coupling (**Table1.1**) During the course of this PhD thesis each of the factors present in the Table 1.1 was tested independently. The obtained results are summarized in six manuscripts, whose abstracts are included as Chapters 3-8.

Table 1.1 **Factors governing cardiac tissue development *in vitro* and *in vivo*.**

	In vivo	*In vitro*
Cells	High density $5 \cdot 10^8$ cells/cm^3 Multiple cell types (myocytes, endothelial cells, fibroblasts)	$0.5 - 1 \cdot 10^8$ cells/cm^3 Multiple cell types (myocytes, Fibroblasts)
Oxygen and nutrient supply	Convection and diffusion	Convection and diffusion in perfusion bioreactor
Geometry	Capillary network (diameter 10μm, spacing 20μm)	Parallel channel array in the scaffold
Oxygen carrier	Hemoglobin	PFC Emulsion (Oxygent®)
Excitation-contraction coupling	Electrical signal propagation Ventricle contraction	Electrical stimulation Construct contraction

The organization of this thesis is as follows:

Chapter 2 described basicis of cardiac muscle structure and function and provides the overview of tissue culture methods up to date.

Chapter 3 address oxygen diffusional limitations during seeding by providing a method that enables uniform cell seeding at high initial densities (108cells/cm3) while maintaining viability. Seeding of cardiomyocytes at high initial densities is essential for cultivation of dense compact tissue since cardiomyocytes have limited ability to proliferate. The seeding method consists of two steps: rapid inoculation of gel/cell suspension onto collagen sponges followed by the application of alternating medium flow for convective oxygen supply.

Chapter 4 describes cultivation of cardiac constructs in the presence of convective-diffusive oxygen transport in perfusion bioreactors. Medium perfusion maintained aerobic cell metabolism, high viability and uniform distribution of cells expressing cardiac markers and superior contractile properties compared to the dish grown controls.

Chapter 5 describes establishment of orderly excitation-contraction coupling of engineered cardiac constructs during *in vitro* culture. Synchronous construct contractions were induced by suprathreshold electrical field stimulation using a commercial cardiac stimulator. Electrical stimulation enabled formation of tissue with elongated cells aligned in parallel and with organized ultrastructure remarkably similar to the one present in the native heart.

Chapter 6 investigates the effect of multiple cell types on the properties of engineered cardiac tissue. Cardiac fibroblasts and cardiac myocytes were cultivated synchronously, separately or serially (pretreatment of scaffolds with fibroblasts followed by the addition of myocytes). Presence of fibroblasts remarkably improved contractile response of the engineered cardiac constructs with the superior biochemical and morphological properties in the pretreated group.

Chapter 7 describes co-culture of cardiac fibroblasts and myocytes on an elastic scaffold with capillary-like channel array perfused with culture medium supplemented with synthetic oxygen carrier (PFC emulsion). Presence of PFC emulsion resulted in significantly higher cell density and improved contractile properties compared to the constructs cultivated in the culture medium alone, presumably by increasing total oxygen content.

Chapter 8 describes a mathemactical model of oxygen distribution in the channeled cardiac construct perfused with oxygen carrier supplemented culture medium. The release of oxygen from PFC particles was estimated not to be rate limiting.

Chapter 9 summarizes the results of this thesis and identifies problems that need to be addressed in the future work.

REFERENCES:

1. Association, A.H., *Heart Disease and Stroke Statistics-2004 Update.* 2004.
2. Reinlib, L. and L. Field, *Cell transplantation as future therapy for cardiovascular disease?: A workshop of the National Heart, Lung, and Blood Institute.* Circulation, 2000. **101**: p. e182-e187.
3. Koh, G.Y., et al., *Differentiation and long-term survival od C2C12 myoblast grafts in heart.* Journal of Clinical Investigation, 1993. **92**(3): p. 1115-1116.
4. Soonpaa, M.H., et al., *Formation of nascent intercalated disks between grafted fetal cardiomyocytes and host myocardium.* Science, 1994. **264**: p. 98-101.
5. Li, R.K., et al., *Cardiomyocyte transplantation improved heart function.* Annals of Thoracic Surgery, 1996. **62**: p. 654-660.
6. Taylor, D.A., et al., *Regenerating functional myocardium: improved performance after skeletal myoblast transplantation.* Nature Medicine, 1998. **4**: p. 929-933.
7. Reinecke, H., et al., *Survival, integration, and differentiation of cardiomyocyte grafts: a study in normal and injured rat hearts.* Circulation, 1999. **100**(2): p. 193-202.
8. Sakai, T., et al., *Fetal cell transplantation: a comparison of three cell types.* Journal of Thoracic and Cardiovascular Surgery, 1999. **118**(4): p. 715-724.
9. Condorelli, G., et al., *Cardiomyocytes induce endothelial cells to trans-differentiate into cardiac muscle: implications for myocardium regeneration.* Proceedings of the National Academy of Sciences USA, 2001. **98**(19): p. 10733-10738.
10. Etzion, S., et al., *Influence of embryonic cardiomyocyte transplantation on the progression of heart failure in a rat model of extensive myocardial infarction.* Journal of Molecular and Cellular Cardiology, 2001. **33**(7): p. 1321-1330.

11. Orlic, D., et al., *Bone marrow cells regenerate infarcted myocardium.* Nature, 2001. **410**(5): p. 701-705.
12. Menasche, P., et al., *Myoblast transplantation for heart failure.* Lancet, 2001. **357**(9252): p. 279-280.
13. Muller-Ehmsen, J., et al., *Rebuilding a damaged heart: long-term survival of transplanted neonatal rat cardiomyocytes after myocardial infarction and effect on cardiac function.* Circulation, 2002. **105**(14): p. 1720-1726.
14. Muller-Ehmsen, J., et al., *Survival and development of neonatal rat cardiomyocytes transplanted into adult myocardium.* Journal of Molecular Cellular Cardiology, 2002. **34**(2): p. 107-116.
15. Roell, W., et al., *Cellular cardiomyoplasty improves survival after myocardial injury.* Circulation, 2002. **105**(20): p. 2435-2441.
16. Akins, R.E., et al., *Cardiac organogenesis in vitro: Reestablishment of three-dimensional tissue architecture by dissociated neonatal rat ventricular cells.* Tissue Engineering, 1999. **5**(2): p. 103-118.
17. Bursac, N., et al., *Cardiac muscle tissue engineering: toward an in vitro model for electrophysiological studies.* American Journal of Physiology: Heart and Circulatory Physiology, 1999. **277**(46): p. H433-H444.
18. Carrier, R.L., et al., *Cardiac tissue engineering: cell seeding, cultivation parameters and tissue construct characterization.* Biotechnology and Bioengineering, 1999. **64**: p. 580-589.
19. Eschenhagen, T., et al., *Three-dimensional reconstitution of embryonic cardiomyocytes in a collagen matrix: a new heart model system.* FASEB Journal, 1997. **11**: p. 683-694.
20. Fink, C., et al., *Chronic stretch of engineered heart tissue induces hypertrophy and functional improvement.* FASEB Journal, 2000. **14**: p. 669-679.
21. Leor, J., et al., *Bioengineerred cardiac grafts: A new approach to repair the infarcted myocardium?* Circulation, 2000. **102**(suppl III): p. III56-III61.
22. Kofidis, T., et al., *In vitro engineering of heart muscle: Artificial myocardial tissue.* Journal of Thoracic and Cardiovascular Surgery, 2002. **124**(1): p. 63-69.
23. Li, R.-K., et al., *Survival and function of bioengineered cardiac grafts.* Circulation, 1999. **100**(Suppl II): p. II63-II69.
24. Li, R.-K., et al., *Construction of a bioengineered cardiac graft.* Journal of Thoracic and Cardiovascular Surgery, 2000. **119**: p. 368-375.
25. Papadaki, M., et al., *Tissue engineering of functional cardiac muscle: molecular, structural and electrophysiological studies.* American Journal of Physiology: Heart and Circulatory Physiology, 2001. **280**(Heart Circ. Physiol. 44): p. H168-H178.
26. Radisic, M., et al., *High density seeding of myocyte cells for tissue engineering.* Biotechnology and Bioengineering, 2003. **82**(4): p. 403-414.
27. Radisic, M., et al., *Medium perfusion enables engineering of compact and contractile cardiac tissue.* American Journal of Physiology: Heart and Circulatory Physiology, 2004. **286**: p. H507-H516.
28. Shimizu, T., et al., *Fabrication of pulsatile cardiac tissue grafts using a novel 3-dimensional cell sheet manipulation technique and temperature- responsive cell culture surfaces.* Circulation Research, 2002. **90**(3): p. e40-e48.
29. Zimmermann, W.H., et al., *Tissue engineering of a differentiated cardiac muscle construct.* Circulation Research, 2002. **90**(2): p. 223-230.
30. Zimmermann, W.H., et al., *Cardiac grafting of engineered heart tissue in syngenic rats.* Circulation, 2002. **106**(12 Suppl 1): p. I151-I157.
31. Severs, N.J., *The cardiac muscle cell.* Bioessays, 2000. **22**(2): p. 188-199.

2. BACKGROUND[1]

Overview

A variety of exciting new strategies have emerged over the past decade to address the clinical problem of tissue failure. Tissue engineering is particularly significant because it can provide biological substitutes of compromised native tissues. As compared to the transplantation of cells alone, engineered tissues have the potential advantage of *immediate functionality*. As compared to transplantation of native tissues, engineered tissues can alleviate the scarcity of suitable tissue transplants, as well as donor-recipient compatibility and disease transmission (for allografts), and donor site morbidity (for autografts). Engineered tissues can also serve as physiologically relevant models for *controlled studies of cells and tissues* under normal and pathological conditions. Ideally, a lost or damaged tissue could be replaced by an engineered graft that can re-establish appropriate structure, composition, cell signalling and function of the native tissue. In light of this paradigm, the clinical utility of tissue engineering will likely depend on our ability to replicate the *site-specific* properties of the particular tissue across different *size scales*. In engineered constructs, the cells should conform to a specific *differentiated phenotype*, while the *composition and architectural organization* of the extracellular matrix (ECM) should provide the necessary *functional properties* inherent to the tissue being replaced. Ideally, an engineered graft should provide *regeneration*, rather than *repair*, and undergo *remodelling* in response to environmental factors.

In general, the tissue engineering requirements can be summarized as follows. To begin with, it is necessary to generate a graft of a desired size and shape to repair a specific defect. Next, the grafts should have the biochemical composition, histomorphology and ultrastructure mimicking those of the native tissue being replaced. Furthermore, it is often necessary for a graft to provide immediate functionality at some minimal level. For load-bearing tissues for example, mechanical competence of the engineered tissue can critically determine if the graft will survive implantation. An engineered graft should also have the capacity to fully integrate (structurally and functionally) with the adjacent host tissues. Additional requirements include specific structural and functional

[1] Significant part of this chapter has been described in Obradovic B, Radisic M, Vunjak-Novakovic G "Tissue Engineering of Cartilage and Myocardium "In: Cell Immobilization Biotechnology: Applications (V. Nedovic and R. Willaert, eds.) Kluwer Academic Publishers (*in press*)

properties such as compressive stiffness for cartilage, contractile function for myocardium, and vascularization for most tissues.

Cells, biomaterial scaffolds, biochemical and physical regulatory signals have been utilized in a variety of ways to engineer tissues, *in vitro* and *in vivo*. Tissue engineering generally involves the presence of reparative cells, a structural template, facilitated transport of nutrients and metabolites, and a provision of molecular and mechanical regulatory factors.

Tissue Engineering Model System

One envisioned scenario of clinically relevant tissue engineering involves the use of *autologous cells*, a *biodegradable scaffold* (designed to serve as a structural and logistic template for tissue development), and a *bioreactor* (designed to enable environmental control and support cell differentiation and functional assembly into an engineered tissue) (**Figure 2.1**). Cells are generally isolated from a small tissue sample, expanded in culture under conditions selected to yield sufficient number for seeding a clinically sized scaffold and in some cases transfected to (over)express a gene of interest. Scaffolds should be made of biocompatible materials, preferentially those already approved for clinical use. Scaffold structure determines the transport of nutrients, metabolites and regulatory molecules to and from the cells, whereas the scaffold chemistry may have an important role in cell attachment and differentiation. The scaffold should biodegrade at the same rate as the rate of tissue assembly and without toxic or inhibitory products. Mechanical properties of the scaffold should ideally match those of the native tissue being replaced, and the mechanical integrity should be maintained as long as necessary for the new tissue to mature and integrate.

In this approach, a bioreactor should ideally provide all necessary conditions in *in vitro* environment for rapid and orderly tissue development by cells cultured on a scaffold. In general, a bioreactor is designed to perform one or more of the following functions: (*i*) establish a desired spatially uniform cell concentration within the scaffold during cell seeding, (*ii*) maintain controlled conditions in culture medium (e.g., temperature, pH, osmolality, levels of oxygen, nutrients, metabolites, regulatory molecules), (*iii*) facilitate mass transfer, and (*iv*) provide physiologically relevant physical signals (e.g., interstitial fluid flow, shear, pressure, compression) during cultivation of cell-polymer constructs.

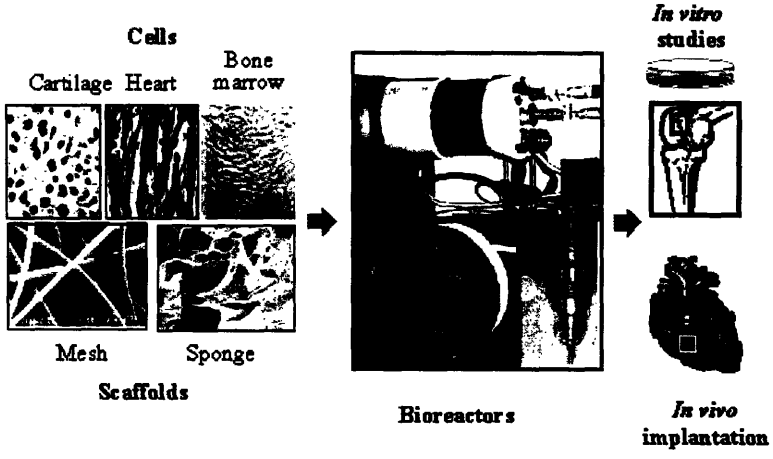

Figure 2.1. Tissue engineering based on cell cultivation on biomaterial scaffolds in bioreactors. Cells (e.g., from cartilage, heart or bone marrow) are cultured on a scaffold (e.g., highly porous, biodegradable mesh or a sponge) in a bioreactor (e.g., rotating bioreactor or perfused cartridge [1]). The resulting constructs are used for controlled in vitro studies or implanted in vivo (e.g., to repair an osteochondral defect [2] or injured myocardium [3]).

Three representative culture vessels that are frequently used for tissue engineering are compared in **Figure 2.2**. All culture vessels are operated in an incubator (to maintain the temperature and pH) with continuous gas exchange and periodic medium replacement.

Flasks contain constructs that are fixed in place by threading onto needles and cultured either statically or with magnetic stirring, with gas exchange through loosened side arm caps. Rotating vessels contain constructs that are freely suspended in culture medium between two concentric cylinders the inner of which serves as a gas exchange membrane. The vessel rotation rate is adjusted to maintain each construct settling at a stationary point within the vessel. This experimental set-up thus enables the evaluation of the effects of flow and mass transfer on engineered tissues and the selection of suitable culture environments to be further explored and optimised.

a)

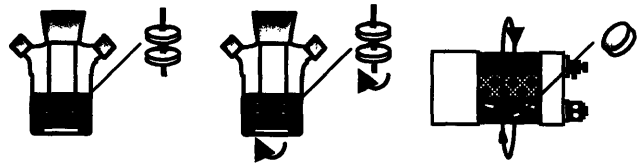

b) Cultivation parameter	Static flask	Mixed flask	Rotating vessel
Vessel diameter (cm)	6.5	6.5	14.6/5.1
Medium volume (cm^3)	120	120	110
Tissue construct or explant[1]	Fixed in place n = 12 per vessel	Fixed in place n = 12 per vessel	Freely settling n = 12 per vessel
Medium exchange (3 cm^3 per tissue per day)	Batch-wise	Batch-wise	Batch-wise
Gas exchange	Continuous via surface aeration	Continuous via surface aeration	Continuous via an internal membrane
Stirring/rotation rate (s^{-1})	0	0.83 – 1.25	0.25 – 0.67
Flow conditions	Static fluid	Turbulent[2]	Laminar[3]
Mixing mechanism	None	Magnetic stirring	Settling in rotational flow
Mass transfer in bulk medium	Molecular diffusion	Convection (due to medium stirring)	Convection (due to tissue settling)
Fluid shear at tissue surfaces	None	Steady, turbulent	Dynamic, laminar
Reference	9-13	9-13	9–11, 14-19

[1] 5 mm diameter x 2 mm thick discs
[2] The smallest turbulent eddies had a diameter of 250 μm and velocity of 0.4 cm/s [4]
[3] Tissues were settling in a laminar tumble-slide regimen in a rotational field [5]

Figure 2.2. Representative bioreactors. a) Schematic presentation of tissue cultivation in static flasks, mixed flasks and rotating vessels b) Overview of the operating conditions for each vessel type [based on 6, 7, 8].

Myocardium (cardiac muscle).

The myocardium (cardiac muscle) is a highly differentiated tissue composed of cardiac myocytes and fibroblasts with a dense supporting vasculature and collagen-based extracellular matrix. The myocytes form a three-dimensional syncytium that enables propagation of electrical signals across specialized intracellular junctions to produce coordinated mechanical contractions that pump blood forward. Only 20-40% of the cells in the heart are cardiac myocytes but they

occupy 80-90% of the heart volume. The average cell density in the native rat myocardium is on the order of $5x10^8$ cells/cm^3. Morphologically, intact cardiac myocytes have an elongated, rod shaped appearance. Contractile apparatus of cardiac myocytes consists of sarcomeres arranged in parallel myofibrils. High metabolic activity is supported by the high density of mitochondria and electrical signal propagation is provided by specialized intercellular connections, gap junctions [9, 10].

The control of heart contractions is almost entirely self-contained. Groups of specialized cardiac myocytes (pace makers), fastest of which are located in the sinoatrial node, drive periodic contractions of the heart. Majority of the cells in the myocardium are non-pace maker cells and they respond to the electrical stimuli generated by pace maker cells. Excitation of each cardiac myocyte is followed by the increase in the amount of cytoplasmic calcium which triggers mechanical contraction. The propagation of the electrical excitation through the tissue by ion currents in the extracellular and in the intercellular space results in synchronous contraction, that enables expulsion of the blood from the heart.

Clinical need

Cardiovascular disease is responsible for a preponderance of health problems in the developed countries, as well as in many developing countries. Heart disease and stroke, the principal components of cardiovascular disease, are the first and the third leading cause of death in the U.S., accounting for nearly 40% of all deaths. Congenital heart defects, which occur in nearly 14 of every 1000 newborn children [11] year of life [12]. Cardiovascular diseases result in substantial disability and loss of productivity, and largely contribute to the escalating costs of health care. About 61 million Americans (almost one-fourth of the population) live with cardiovascular diseases, such as coronary heart disease, congenital cardiovascular defects, and congestive heart failure, and 298.2 billion dollars were spent in 2001 to treat these diseases [13]. The economic impact of cardiovascular disease on the U.S. health care system is expected to grow further as the population ages.

Once damaged, the heart is unable to regenerate. Heart failure affects over five million Americans [14], and is the leading cause of morbidity and mortality in developed countries [15]. Currently, the only definitive treatment for end stage heart failure is cardiac transplantation. However, the limited availability of organs for transplantation has led to prolonged waiting periods that are often not survivable [16]. Repair of myocardial injuries has been attempted by injection of myogenic cells into scarred myocardium [17] and the replacement of scarred tissue with engineered grafts [18].

Tissue engineering of myocardium

Tissue engineering has emerged over the last decade as an interdisciplinary field with tremendous potential. Tissue engineering offers a possibility of creating tissue constructs to be used for repair of larger injuries or congenital malformations. In addition cardiac tissue constructs may be utilized for studies of normal and pathological tissue function *in vitro*. Substantial progress has been made in areas of biopolymers [19], cell-material interactions [20] and bio-mimetic culture devices [21]. In addition, functional tissues have been developed and implanted *in vivo,* including (but not limited to) cartilage [22], bone [23], bladder [24] and blood vessels [25,Niklason, 1999 #343]. However, fundamental and all-encompassing problems remain. One of the most important ones is mass transfer into the tissues that are greater than 100-200 μm in thickness, both during the *in vitro* cultivation and following implantation *in vivo*. This explains why tissue engineering has been most successful with tissues that are either thin (e.g., bladder) or have low oxygen requirements (e.g., cartilage). There are multiple challenges to be overcome to produce viable, functional cardiac tissue (**Table 2.1**).

Table 2.1 Key challenges of cardiac tissue engineering

• Development of appropriate biodegradable and biocompatible scaffolds that can provide adequate mass transfer, vascularization, and transduction of mechanical and electrical signals
• Development of bio-mimetic culture systems that promote differentiated function and excitation - contraction coupling of cardiac cells
• Development of functional vascular networks embedded into the cardiac muscle tissue to promote nutrient and oxygen transfer, angiogenesis and integration with the host vasculature.

In current approaches, fetal or neonatal rat cardiomyocytes are seeded onto scaffolds (collagen sponges, polyglycolic acid meshes) or cast in collagen gels, and cultivated immersed in the culture medium in static or mixed dishes, spinner flasks or rotating vessels [26, 27]. The metabolism and viability of the resulting constructs are assessed during culture by monitoring levels of glucose consumed, lactate produced and the release of lactate dehydrogenase from the samples of culture medium. Cell distribution, morphology and construct structure are assed by histology. Expression of cardiac specific markers is assessed by immunohistochemistry and confirmed by Western blots. Gene expression is assessed by RT-PCR. Cardiac specific ultrastructural features are detected by transmission electron microscopy. Functional assessment

of engineered constructs has been based on electrophysiological studies [28, 29], monitoring of synchronous contractions in response to electrical stimuli [30, 31] and measurement of force of contraction in paced [32] or spontaneously contracting constructs [33].

Cells. Three dimensional cardiac tissue constructs were successfully cultivated in dishes using variety of scaffolds and cell sources. Fetal rat ventricular cardiac myocytes were expanded after isolation, inoculated into collagen sponges and cultivated in static dishes for up to 4 weeks [3]. The cells proliferated with time in culture and expressed multiple sarcomeres. Adult human ventricular cells were used in a similar system, although they exhibited no proliferation [34]. Fetal cardiac cells were also cultivated on alginate scaffolds in static 96-well plates. After 4 days in culture the cells formed spontaneously beating aggregates in the scaffold pores [35]. Cell seeding densities of the order of 10^8cells/cm^3 were achieved in the alginate scaffolds using centrifugal forces during seeding [36]. Neonatal rat cardiac myocytes formed spontaneously contracting constructs when inoculated in collagen sponges within 36 hr [33] and maintained their activity for up to 12 weeks. The contractile force increased upon addition of Ca^{2+} and epinephrine.

Two-week constructs based on neonatal rat cardomyocytes exhibited spontaneously beating areas, whereas constructs based on embryonic chick myocytes exhibited no contractions and reduced in size by 60%. Immunohistochemistry, revealed presence of large number of non-myocytes in the constructs based on embryonic chick hear cells, while constructs based on neonatal rat cells consisted mostly of elongated cardiomyocytes [26].

Constructs based on the cardiomyocytes enriched by preplating exhibited lower excitation threshold (ET), higher conduction velocity, higher maximum capture rate (MCR), and higher maximum and average amplitude [37].

Scaffolds. The scaffolds utilized for cardiac tissue engineering include collagen fibers [38], collagen sponges [3, 33, 34] and polyglycolic acid meshes [26, 27, 37]. The main advantage of a synthetic scaffold such as PGA is that it provides mechanical stability, while scaffolds based on natural cell polymers such as collagen enable rapid cell attachment.

The scaffold free approaches include casting the cells in collagen gels followed by mechanical stimulation [39-41] and stacking of confluent cardiac cell monolayers [42]. The main advantage of scaffold free approaches is higher active force generated by such tissues. However, the main disadvantage remains tailoring the shape and dimensions of the scaffold free engineered tissues.

As an alternative, gels (Matrigel) were combined with scaffolds (collagen sponge) to achieve rapid cell inoculation and attachment along with the possibility of tailoring tissue shape and dimensions through the use of scaffolds [30].

Bioreactor hydrodynamics. The representative bioreactors utilized for tissue engineering of the myocardium include static or mixed dishes, static or mixed flasks and rotating vessels (**Figure 2.1** and **2.2**). These bioreactors offer three distinct flow conditions (static, turbulent, and laminar) and therefore differ significantly in the rate of oxygen supply to the surface of the tissue construct. Oxygen transport is a key factor for myocardial tissue engineering due to the high cell density, very limited cell proliferation and low tolerance of cardiac myocytes for hypoxia In all configurations oxygen is supplied only by diffusion from the surface to the interior of the tissue construct.

Static dishes remain the most widely used set-up for cardiac tissue engineering (**Table 2.2**). In static dishes, oxygen and nutrients are supplied mainly by diffusion, which is capable of satisfying oxygen demand of only ~100 μm thick surface layer of compact tissue, whereas the construct interior remained mostly acellular [43]. In contrast, cartilage has been successfully grown in static dishes to millimeter thicknesses. In *orbitally mixed dishes*, the rate of delivery of oxygen and nutrients to construct surfaces can be increased, but diffusion remains the main mechanism of mass transport within the tissue. Diffusional transport of oxygen to cardiac myocytes within dish-grown constructs resulted in prevalently anaerobic glucose metabolism [31]. Additional limitation of the culture in static or mixed dishes is that the bottom surface of the construct (the surface closest to the bottom of the dish) often lacks proper oxygenation and nutrients yielding asymmetric cell distribution with compact tissue mostly on the top surface.

To improve cell survival and assembly on all surfaces of the engineered tissue, cardiac constructs were cultivated suspended in the *spinner flasks* (**Table 2.2**). Cultivation in spinner flasks (at stirring rates of up to 90 rpm) improved construct properties [26], presumably due to enhanced mass transport at construct surfaces (**Figure2.2**). After 2 weeks of culture, constructs from mixed flasks had significantly higher cellularity index (~20μgDNA/construct) and metabolic activity (~150MTTunits/mg DNA) than those from static flasks (~5μgDNA/construct and ~50 MTT units/mg DNA). Mixing maintained medium gas and pH levels within the physiological range yielding a more aerobic glucose metabolism (L/G~1.5) in mixed flasks as compared to static flaks (L/G>2) [26]. Constructs contained a peripheral tissue-like region (50-70μm thick) in which cells stained positive for tropomyosin and organized in multiple layers in a

3-D configuration [37] Electrophysiological studies conducted using a linear array of extracellular electrodes showed that the peripheral layer of the constructs sustained macroscopically continuous impulse propagation on a centimeter-size scale [37]. However, construct interiors remained empty due to the diffusional limitations of the oxygen transport within the bulk tissue, and the density of viable myocytes was orders of magnitude lower than that in the neonatal rat ventricles [37]. Additional drawback of the cultivation in spinner flasks is that turbulent flow conditions may induce cell damage and dedifferentiation and result in the formation of a fibrous capsule at construct surfaces.

Table 2.2 Overview of cardiac tissue engineering studies

BIOREACTOR TYPE	CELL SOURCE	SCAFFOLD TYPE	CONSTRUCT SIZE	INITIAL CELL NUMBER	REF.
Static dish (96 well plate)	Fetal rat CM	Alginate	6 mm diameter x 1mm thick	$3 \cdot 10^5$	[35]
Static dish (5 ml culture medium)	Fetal rat CM	Bovine collagen (Gelfoam)	5 x 5 x 1 mm	$\sim 10^4$	[3]
Static dish (4 ml culture medium)	Neonatal rat CM	Bovine collagen (Tissue Fleece)	20 x 15 x 2.5 mm	$2 \cdot 10^6$	[33]
Static dish	Neonatal rat CM	Bovine collagen	5 x 5 x 3 mm	$0.5 \cdot 10^6$	[44]
Mixed dish (20rpm, 4ml culture medium)	Neonatal rat CM	Bovine collagen (Ultrafoam)	10 mm diameter x 1.5 mm thick	$6\text{-}12 \cdot 10^6$	[31]
Spinner flask (0, 50, 90 rpm, 120 ml culture medium)	Embryonic chick CM Neonatal rat CM	PGA	5 mm diameter x 2 mm thick	$1.3\text{-}8 \cdot 10^6$	[26]
Spinner flask (50 rpm, 120 ml culture medium)	Neonatal rat CM	PGA, sPGA	5 mm diameter x 2 mm thick	$8 \cdot 10^6$	[27, 37]
Rotating vessels (11 rpm, 100 ml culture medium)	Neonatal rat CM	PGA, sPGA, lPGA	5 mm diameter x 2 mm thick	$8 \cdot 10^6$	[26, 27, 37]
Rotating vessel	Neonatal rat CM	Bovine collagen	5 x 5 x 3 mm	$0.5 \cdot 10^6$	[44]
Perfused cartridge (0.2-3 ml/min)	Neonatal rat CM	PGA	11 mm diameter x 2 mm thick	$24 \cdot 10^6$	[43, 45]
Cyclic stretch (1.5-2 Hz, 1-20 % strain)	Embryonic chick CM Neonatal rat CM	Collagen gel		$1\text{-}2.5 \cdot 10^6$	[18, 32, 40]
Cyclic stretch (1.3 Hz)	Human heart cells	Bovine collagen (Gelfoam)	30 x 20 x 3 mm 20 x 20 x 3 mm	$3\text{-}30 \cdot 10^6$	[46]

Laminar conditions of flow in rotating vessels (**Table 2.2**) enabled the maintenance of oxygen concentration in medium and pH within the physiological range, and resulted in mostly aerobic cell metabolism (L/G~1) [26]. The metabolic activity of cells within constructs increased into the range of values measured for neonatal rat ventricles (~250 units MTT/mg DNA) and was significantly higher than in mixed flasks (~150 units MTT/mg DNA). The index of cell hyperthrophy was also comparable to the neonatal tissue (18mg protein/mg DNA). However, the construct cellularity remained 2-6 times lower than in native heart ventricles. In the best experimental group (heart cells enriched for cardiac myocytes by pre-plating, laminin-coated PGA scaffolds, low serum concentration) the outer layer of viable tissue was up to 160 μm thick [27]. Cells expressed cardiac-specific markers (e.g., tropomyosin, gap junction protein connexin, creatin kinase-MM, sarcomeric myosin heavy chain) at levels that were lower than in neonatal rat ventricles but higher than in constructs cultured in spinner flasks [27]. Electrophysiological properties were also improved, as evidenced by the prolonged action potential duration (APD, a measure of electrophysiological functionality of cell membrane), higher maximum capture rates (a measure of construct response to electrical pacing), and more physiological response to drugs. In particular, pharmacological studies done with 4-aminopyridine indicated that a decrease in transient outward potassium current may be responsible for the observed differences in APD and MCR [29]. Overall, dynamic laminar flow of rotating bioreactors improved properties of the peripheral tissue layer, but the limitations of the diffusional transport of oxygen to the construct interior were not overcome and constructs remained largely acellular.

Interstitial flow. In an attempt to enhance mass transport within cultured constructs, a perfusion bioreactors was developed that provides interstitial medium flow through the cultured construct at velocities similar to those found in native myocardium (~400–500 μm/s, [47]). In such a system oxygen and nutrients are supplied to the construct interior by both diffusion and convection.

In early studies, constructs were prepared by seeding cardiac myocytes onto PGA scaffolds in mixed flasks, a method that has been successfully used to seed chondrocytes. After 3 days, constructs were transferred into a perfusion cartridge and pulsatile flow of medium through the construct was provided by a peristaltic pump (0.2 - 3 ml/min) (**Table 2.2**). Gas exchange between culture medium and incubator air occurred in an external coil of silicone tubing within the medium recirculation loop. Perfusion during construct cultivation improved cell distribution, viability and differentiation. However, the overall cell density remained low due to the limitations of oxygen transport to the cells inside constructs during scaffold seeding in mixed flasks [43, 45].

Mechanical stimulation. To provide appropriate mechanical stimulation neonatal rat cardiac myocytes were reconstituted in collagen gel and cultivated in the presence of cyclic stretch (**Table 2.2**). In one set-up neonatal rat ventricular myocytes were suspended in a gel consisting of collagen I and Matrigel [40]. For each piece of tissue, 0.7 ml of the cell/gel mix was poured into a well (11 x 17 x 4 mm) made of silicone rubber containing one set of Velcro coated silicone tubes (7 mm length, 3mm OD 2mm ID). The mixture was allowed to gel at 37°C for 60 min before culture medium was added. After 4 days in culture, tissues were transferred for an additional 6 days into a motorized stretching device that applied either unidirectional and cyclic stretch (1.5 Hz, strain rate of up to 20%). Mechanical stimulation enhanced the alignment of cardiac myocytes, and resulted in higher mitochondrial density and longer myofilaments. As compared to the non-stimulated controls, stimulation markedly increased the RNA/DNA ratio (by 100 %) and protein/cell ratio (by 50 %). The force of contraction was also higher in stretched constructs, both under basal conditions and after stimulation with isoprenaline [40].

In an improved set-up, neonatal rat cardiac cells were suspended in the collagen/Matrigel mix and cast into circular molds [32]. After 7 days in culture, the strips of cardiac tissue were placed around two rods each fixed to a stretching bar of a custom made mechanical stretcher and subjected to unidirectional and cyclic stretch at 10% strain rate and 2 Hz. Mechanical stimulation improved the formation of interconnected and aligned cardiac muscle bundles with morphological features resembling adult rather than immature native tissue. Fibroblasts and macrophages were found through the constructs, and the capillary structures positive for CD31 were also noted. Cardiomyocytes exhibited well developed ultrastructural features: sarcomeres arranged in myofibrils, with well developed Z, I, A H and M bands, gap and adherence junctions, T tubules, and well developed basement membrane. The constructs exhibited contractile properties similar to the native tissue with high ratio of twitch to resting tension and strong β-adrenegenic response. Action potentials characteristic of rat ventricular myocytes were recorded.

Using another system for mechanical stimulation, cyclic mechanical stretch (1.33Hz) was applied to the constructs based on collagen scaffold and human heart cells (isolated from children undergoing repair of Tetralogy of Fallot) [46]. A rectangular piece of tissue was fixed at one end to the bottom of a square dish; the other end is attached to a steel rod the cyclic movement of which is induced by dynamically changing magnetic filed. Constructs subjected to chronic stretch had improved cell distribution and collagen matrix formation.

Summary

Tissue engineering can provide functional cell-based grafts to restore normal function of a compromised native tissue and to serve as physiologically relevant models for biological research. One approach to functional tissue engineering involves the *in vitro* cultivation of immature but functional tissue constructs by using: (i) cells isolated from a small tissue harvest and expanded *in vitro*, (ii) a biodegradable scaffold designed to serve as a structural and logistic template for tissue development, and (iii) a bioreactor designed to provide environmental conditions necessary for the cells to regenerate a functional tissue structure.

REFERENCES:

1. Freed, L.E. and G. Vunjak-Novakovic, *Tissue engineering bioreactors*, in *Principles of Tissue Engineering*, R.P. Lanza, R. Langer, and J. Vacanti, Editors. 2000, Academic Press: San Diego. p. 143-156.
2. Schaefer, D., et al., *Tissue engineered composites for the repair of large osteochondral defects.* Transactions of the Orthopaedic Research Society, 2000. **25**: p. 619.
3. Li, R.-K., et al., *Survival and function of bioengineered cardiac grafts.* Circulation, 1999. **100**(Suppl II): p. II63-II69.
4. Vunjak-Novakovic, G., et al., *Effects of mixing on the composition and morphology of tissue-engineered cartilage.* AIChE Journal, 1996. **42**(3): p. 850-860.
5. Freed, L.E. and G. Vunjak-Novakovic, *Tissue engineering of cartilage*, in *Biomedical Engineering Handbook*, J.D. Bronzino, Editor. 1995, CRC Press: Boca Raton. p. 1788-1807.
6. Freed, L.E., I. Martin, and G. Vunjak-Novakovic, *Frontiers in tissue engineering: in vitro modulation of chondrogenesis.* Clinical Orthopaedics and Related Research, 1999. **367S**: p. S46-S58.
7. Freed, L.E. and G. Vunjak-Novakovic, *Tissue engineering of cartilage*, in *The Biomedical Engineering Handbook*, J.D. Bronzino, Editor. 2000, CRC Press: Boca Raton. p. 124-1-124-26.
8. Vunjak-Novakovic, G., *Fundamentals of tissue engineering: scaffolds and bioreactors*, in *Tissue Engineering of Cartilage and Bone*, A.I. Caplan, Editor. 2003, John Wiley: London. p. 34-51.
9. MacKenna, D.A., et al., *Contribution of collagen matrix to passive left ventricular mechanics in isolated rat heart.* American Journal of Physiology, 1994. **266**: p. H1007-H1018.
10. Brilla, C.G., et al., *Pharmacological modulation of cardiac fibroblast function.* Herz, 1995. **20**: p. 127-135.
11. Gillum, R.F., *Epidemiology of congenital heart disease in the United States.* American Heart Journal, 1994. **127**(4 Pt 1): p. 919-927.
12. Hoffman, J.I., *Incidence of congenital heart disease: I. Postnatal incidence.* Pediatric Cardiology, 1995. **16**(3): p. 103-113.
13. Lysaght, M.J. and J. Reyes, *The growth of tissue engineering.* Tissue Engineering, 2001. **7**: p. 485-493.

14. Rich, M., *Epidemiology, pathophysiology, and etiology of congestive heart failure in older adults.* Journal of the American Geriatrics Society, 1997. **45**: p. 968-974.
15. Dominguez, L., et al., *Trends of congestive heart failure: epidemiology contrast with clinical trial results.* Cardiologia, 1999. **44**: p. 801-808.
16. Evans, R.W., *Economic impact of mechanical cardiac assistance.* Progress in Cardiovascular Diseases, 2000. **43**: p. 81-94.
17. Soonpaa, M.H., et al., *Formation of nascent intercalated disks between grafted fetal cardiomyocytes and host myocardium.* Science, 1994. **264**: p. 98-101.
18. Zimmermann, W.H., et al., *Cardiac grafting of engineered heart tissue in syngenic rats.* Circulation, 2002. **106**(12 Suppl 1): p. I151-I157.
19. Wang, Y., et al., *A tough biodegradable elastomer.* Nature Biotechnology, 2002. **20**: p. 602-606.
20. Hubbell, J.A., *Bioactive biomaterials.* Current Opinion in Biotechnology, 1999. **10**: p. 123-129.
21. Niklason, L.E., et al., *Functional arteries grown in vitro.* Science, 1999. **284**(5413): p. 489-493.
22. Freed, L.E., et al., *Chondrogenesis in a cell-polymer-bioreactor system.* Experimental Cell Research, 1998. **240**: p. 58-65.
23. Niklason, L.E., *Engineering of bone grafts.* Nature Biotechnology, 2000. **18**: p. 929-930.
24. Oberpenning, F., et al., *De novo reconstitution of a functional mammalian urinary bladder by tissue engineering.* Nature Biotechnology, 1999. **17**: p. 149-155.
25. L'Heureux, N., et al., *A completely biological tissue-engineered human blood vessel.* FASEB Journal, 1998. **12**: p. 47-56.
26. Carrier, R.L., et al., *Cardiac tissue engineering: cell seeding, cultivation parameters and tissue construct characterization.* Biotechnology and Bioengineering, 1999. **64**: p. 580-589.
27. Papadaki, M., et al., *Tissue engineering of functional cardiac muscle: molecular, structural and electrophysiological studies.* American Journal of Physiology: Heart and Circulatory Physiology, 2001. **280**(Heart Circ. Physiol. 44): p. H168-H178.
28. Bursac, N., et al. *Cardiac tissue engineering: an electrophysiological study.* in *Annual Meeting of the BMES.* 1998. Cleveland, OH.
29. Bursac, N., et al., *Cultivation in rotating bioreactors promotes maintenance of cardiac myocyte electrophysiology and molecular properties.* Tissue Engineering, 2003. **9**(6): p. 1243-1253.
30. Radisic, M., et al., *High density seeding of myocyte cells for tissue engineering.* Biotechnology and Bioengineering, 2003. **82**(4): p. 403-414.
31. Radisic, M., et al., *Medium perfusion enables engineering of compact and contractile cardiac tissue.* American Journal of Physiology: Heart and Circulatory Physiology, 2004. **286**: p. H507-H516.
32. Zimmermann, W.H., et al., *Tissue engineering of a differentiated cardiac muscle construct.* Circulation Research, 2002. **90**(2): p. 223-230.
33. Kofidis, T., et al., *In vitro engineering of heart muscle: Artificial myocardial tissue.* Journal of Thoracic and Cardiovascular Surgery, 2002. **124**(1): p. 63-69.
34. Li, R.-K., et al., *Construction of a bioengineered cardiac graft.* Journal of Thoracic and Cardiovascular Surgery, 2000. **119**: p. 368-375.
35. Leor, J., et al., *Bioengineerred cardiac grafts: A new approach to repair the infarcted myocardium?* Circulation, 2000. **102**(suppl III): p. III56-III61.
36. Dar, A., et al., *Cardiac tissue engineering Optimization of cardiac cell seeding and distribution in 3D porous alginate scaffolds.* Biotechnology and Bioengineering, 2002. **80**(3): p. 305-312.

37. Bursac, N., et al., *Cardiac muscle tissue engineering: toward an in vitro model for electrophysiological studies.* American Journal of Physiology: Heart and Circulatory Physiology, 1999. **277**(46): p. H433-H444.
38. Akins, R.E., et al., *Cardiac organogenesis in vitro: Reestablishment of three-dimensional tissue architecture by dissociated neonatal rat ventricular cells.* Tissue Engineering, 1999. **5**(2): p. 103-118.
39. Eschenhagen, T., et al., *Three-dimensional reconstitution of embryonic cardiomyocytes in a collagen matrix: a new heart model system.* FASEB Journal, 1997. **11**: p. 683-694.
40. Fink, C., et al., *Chronic stretch of engineered heart tissue induces hypertrophy and functional improvement.* FASEB Journal, 2000. **14**: p. 669-679.
41. Zimmermann, W.H., et al., *Three-dimensional engineered heart tissue from neonatal rat cardiac myocytes.* Biotechnology and Bioengineering, 2000. **68**: p. 106-114.
42. Shimizu, T., et al., *Fabrication of pulsatile cardiac tissue grafts using a novel 3-dimensional cell sheet manipulation technique and temperature- responsive cell culture surfaces.* Circulation Research, 2002. **90**(3): p. e40-e48.
43. Carrier, R.L., et al., *Perfusion improves tissue architecture of engineered cardiac muscle.* Tissue Engineering, 2002. **8**(2): p. 175-188.
44. van Luyn, M.J.A., et al., *Cardiac tissue engineering: characteristics of in unison contracting two- and three-dimensional neonatal rat ventricle cell (co)-cultures.* Biomaterials, 2002. **23**(24): p. 4793-4801.
45. Carrier, R.L., et al., *Effects of oxygen on engineered cardiac muscle.* Biotechnology and Bioengineering, 2002. **78**: p. 617-625.
46. Akhyari, P., et al., *Mechanical stretch regimen enhances the formation of bioengineered autologous cardiac muscle grafts.* Circulation, 2002. **106**(12 Suppl 1): p. I137-I142.
47. Fournier, R.L., *Basic Transport Phenomena in Biomedical Engineering.* 1998, Philadelphia: Taylor & Francis.

3. HIGH DENSITY SEEDING OF MYOCYTE CELLS FOR CARDIAC TISSUE ENGINEERING[2]

INTRODUCTION

Due to the limited ability of cardiac myocytes to regenerate [1] attempts have been made to repair myocardial injuries by injecting myogenic cells into the scarred myocardium [2-4], or in the case of large injuries to replace scarred tissue with engineered grafts [5, 6]. Three dimensional tissue constructs that express structural and physiological features characteristic of native cardiac muscle have been engineered using collagen gels [7-9], collagen fibers [10], collagen sponges [6, 11] and polyglycolic acid meshes [12-14], in conjunction with fetal or neonatal rat cardiac myocytes. In all cases, cells were seeded on scaffolds and cultivated immersed in culture medium in dishes [5, 6, 12, 14], spinner flasks [12-14] or rotating vessels [10, 12, 14]. Oxygen dissolved in medium was transported to the cells by molecular diffusion, which provided enough oxygen for an approximately 100 μm thick outer layer of functional tissue but not to the construct interior which remained relatively acellular [8, 12-14].

We previously developed a perfused bioreactor system in an attempt to enhance mass transport between culture medium and cells within cultured constructs [15]. Cells were seeded onto scaffolds in tissue culture dishes for 48 hours and subsequently cultured for 7 days with direct perfusion of culture medium. The transport of oxygen from the medium to the cells occurred via diffusion during cell seeding, and by a combination of diffusion and convection during cultivation. During cultivation, the flow of medium redistributed the cells evenly across the entire volume of the construct, but the cell density remained low due to the limitations in oxygen transport during cell seeding.

We hypothesized that rapid gel inoculation of hypoxia-sensitive cells in conjunction with direct medium perfusion through the seeded scaffold would result in high rate, yield, viability and uniformity of cell seeding. We report a new seeding strategy that enables the seeding of tissue engineering scaffolds at the initial cell densities comparable to those in adult rat myocardium (~10^8 cells/cm^3, [16]), and was developed by combining the methods for rapid cell inoculation using a gel [17] and scaffold seeding with cell suspension in perfusion systems [18]. Medium perfusion through the cell-polymer construct is established immediately, in order to maintain the viability of inoculated cells during cell attachment to scaffolds and subsequent construct

[2] Most of this chapter has been published in: Milica Radisic, Michelle Euloth, Liming Yang, Robert Langer, Lisa E. Freed and Gordana Vunjak-Novakovic:"High density seeding of myocytes cells for cardiac tissue engineering" Biotechnology and Bioengineering 82: 403-414, 2003

cultivation. The feasibility of the proposed seeding method was first evaluated in seeding and cultivation studies with neonatal cardiac myocytes. Subsequently, the effects of three system parameters (initial cell number, seeding time, seeding set-up) were systematically studied using C2C12 mouse muscle myoblast cell line. C2C12 cells were chosen as a model system due to their availability, ease of handling and evidence that they differentiate and express cardiac specific proteins [19-21] when grafted into the rat or mouse myocardium.

MATERIALS AND METHODS

Materials Dulbecco's modified Eagle Medium (DMEM), fetal bovine serum (FBS), N-2-Hydroxyethylpiperazine-N'-2-Ethane-Sulfonic Acid (HEPES), calcium and magnesium free phosphate buffered saline (PBS), 1x trypsin-EDTA solution in PBS, Hank's Balanced Salt Solution (HBSS) and penicillin were all from Gibco (Grand Island, NY). Collagenase Type II was from Worthington (Freehold, NJ). Trypsin was from U.S. Biochemicals (Cleveland, OH). Matrigel® and dispase were from Becton-Dickinson (Two Oak Park, Bedford, MA). The C2C12 mouse muscle myoblast cell line was from the American Type Culture Collection (Manassas, VA). Tissue culture dishes and T175 flasks were from Costar (Cambridge, MA). 10% Formalin buffer was from Sigma Diagnostic (St. Louis, MO). Ethidium monoazide bromide (EMA) was from Molecular Probes (Eugene, OR). The flow cytometer (model FACScan) was from Becton-Dickinson (Bedford, MA). Orbital shaker was from Bellco, (type BTB, Vineland, NJ) and the Push/Pull PHD2000 syringe pump was from Harvard Apparatus (Holliston, MA). Polycarbonate perfusion cartridges were kindly donated by the Advanced Tissue Sciences (LaJolla, CA). Platinum cured silicone tubing and the multichannel peristaltic pump (L/S^{tm} Masterflex) were from Cole-Parmer (Vernon Hills, IL). Reservoir bag was 32 ml gas permeable VueLife^{tm} bag (American Fluoroseal Corporation, Gaithersburg, MD). Syringes were from Becton Dickinson (Two Oak Park, Bedford, MA) and three-way stop-cocks from Baxter Healthcare (Irvin, CA). Heating tape was from VWR (Bridgeport, Connecticut). The temperature controller was from Barnstead/Thermolyne (Dubuque, Iowa). The programmable cardiac stimulator was from Nihon Kohden (type SEC-3102). The electrodes (1cm x 0.5cm) were custom made by coating 500 μm thick silicon wafers with 3000 Å of silicon nitride, 100 Å of Ti, and 1000 Å of gold.

C2C12 cells, a cell line derived from murine myoblasts, were subcultured in T-75 flasks (P4 to P9) in Dulbecco's Modified Eagle Medium (DMEM) containing 4.5 g/L glucose, supplemented with 10% fetal bovine serum (FBS), 10 mM N-2-hydroxyethylpiperazine N'-2-ethanesulfonic acid (HEPES), 2 mM L-glutamine and 100 units/ml penicillin. In order to prepare

constructs, C2C12 cells at passage numbers ranging from 4 to 9 were dissociated with trypsin and counted using a hemocytometer.

Cardiomyocytes were obtained from 1 to 2 day old neonatal Sprague Dawley rats using a protocol approved by the Institute's Committee on Animal Care. In brief, ventricles were quartered, incubated overnight at 4°C in a 0.06 % (w/v) solution of trypsin in Hank's Balanced Salt Solution (HBSS), washed in culture medium, and subjected to a series of digestions (3 min, 37°C, 150 rpm) in 0.1 % (w/v) solution of collagenase type II in HBSS. The first digestate was discarded, and the cell suspensions from the subsequent 4 - 6 digestions were centrifuged (750 rpm, 4 min), resuspended in HBSS each, pooled, and resuspended in DMEM containing 4.5 g/L glucose supplemented with 10% FBS, 10 mM HEPES, 2 mM L-glutamine and 100 units/ml penicillin. Cells were pre-plated for one 60 min period to enrich for cardiomyocytes (i.e. cells that remained unattached were used to prepare constructs). Cell number and viability were determined by hemocytometer and either trypan blue exclusion or fluorescence activated cell sorting (FACS) described below. Approximately 20 hearts from two different rat litters were used.

Scaffolds were discs punched from sheets of Ultrafoam® collagen hemostat (Davol Inc., Cranston, RI), a water-insoluble, partial HCl salt of purified bovine dermal (corium) collagen formed as a sponge with interconnected pores. Discs had dry dimensions of 1.33 cm diameter x 0.3 cm thick, and dimensions of 1.1 cm diameter x 0.15 cm thick following hydration in culture medium for 1 hr in a 37 °C incubator.

Gel inoculation Scaffolds were inoculated with cells at the density of $0.68 \cdot 10^8$ or $1.35 \cdot 10^8$ cells/cm^3 as follows. Ultrafoam™ discs were preweted with culture medium and placed into the 37°C 5%CO2 humidified incubator (Napco, Winchester, VA) for one hour before inoculation. Cells were pelleted by centrifugation (1000 rpm, 10 min) and resuspended in Matrigel®, a basement membrane preparation extracted from the Engelbreth-Holm-Swarm mouse sarcoma and solubilized in DMEM at the concentration of 7.458 mg/ml. Cells (6 or $12 \cdot 10^6$ per scaffold) were resuspended using 5 µl of liquid Matrigel® per one million cells, while working on ice to prevent premature gelation (Matrigel® is liquid at 2-8 °C and it gels rapidly at 22-35°C). Pre-wetted scaffolds were gently blotted dry and the Matrigel®/cell suspension was delivered evenly to the top surface of each scaffold using an automatic pipette. Gelation was achieved within 10 min of the transfer of inoculated scaffolds into either orbitally mixed dishes or perfused cartridges as described below.

Seeding and cultivation *Orbitally Mixed Dishes*: Six-well tissue culture dishes containing one gel-cell inoculated scaffold and 8 ml of culture medium per well were placed on a 25 rpm orbital shaker and incubated at 37°C/5%CO_2 in a humidified incubator to serve as

controls. ***Perfused cartridges***: All components (cartridges, screens, gaskets, tubing) were steam sterilized for 30 min. Two seeding loops, each containing one perfused cartridge, were placed onto a Push/Pull syringe pump as shown in **Figure 3. 1.** Each cartridge was connected to two 80 cm long coils of 1.6mm ID, 3.2mm OD platinum cured silicone tubing serving as gas exchangers, and two 10 mL syringes serving as medium reservoirs, sampling ports and for de-bubbling. Cartridges were completely filled with culture medium, with the use of a pair of 3 mL syringes, one full and one empty, connected to the circuit at the inlet and outlet of the cartridge via 3-way stopcocks. The total volume of medium in the cartridge, tubing and reservoir syringes was 8 mL (1.5 mL in the cartridge, 4 mL in the tubing, 2.5 mL in one syringe; the other syringe was empty).

Gel-cell inoculated scaffolds were placed between two stainless steel screens and two silicone gaskets, and transferred into 1.5 ml polycarbonate perfusion cartridges (one scaffold per cartridge). The screens (85% open area) provided mechanical support during perfusion and the gaskets (1 mm thick, 10 mm OD, 5 mm ID) routed the culture medium directly through the construct. Any air bubbles were displaced by culture medium injected from the de-bubbling syringe (Syringe 2, **Figure 3.1**) into the downstream syringe (Syringe 4, **Figure 3.1**). The seeding set-up was placed in a 37°C/5%CO_2 incubator, and the pump was programmed to the set flow rate, with the reversal of flow direction after 2.5ml was perfused in a given direction.

The cartridges containing constructs seeded with neonatal cardiac myocytes were transferred into perfusion loops consisting of a reservoir bag, a gas exchanger (a coil of silicone tubing, 3m long) and a multichannel peristaltic pump. Each loop was primed with 32 ml of culture medium, unidirectional medium flow was established, and the flow rate was set at 0.5ml/min and maintained throughout the cultivation. Constructs cultured in dishes (one constructs in 8 mL medium per well) placed on an orbital shaker (25 rpm) served as controls.

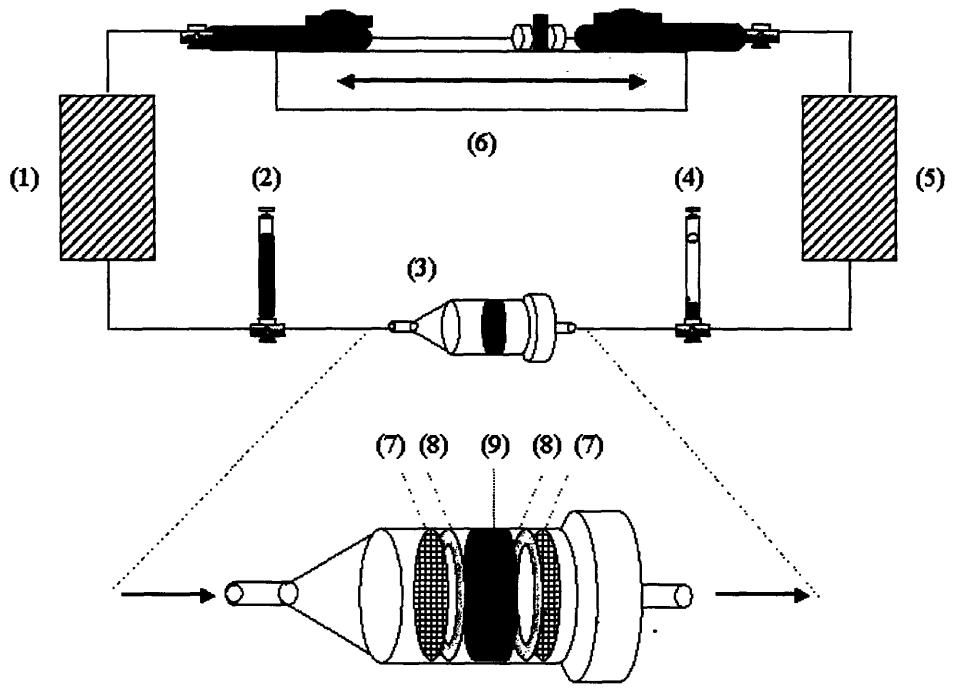

Figure 3.1 Seeding set-up for alternating flow perfusion: (1) and (5) gas exchangers; (2) and (4) reservoir syringes; (3) perfusion cartridge; (6) Push/Pull syringe pump. Construct (9) obtained by inoculating gel-cell suspension is placed into a cartridge (3) between two stainless steel support screens (7) and two silicone gaskets (8) and transferred into a cartridge (3).

Experimental design In feasibility studies, scaffolds were inoculated with 12 x 10^6 neonatal cardiac myocytes and seeded in perfusion or orbitally mixed dish for 1.5 hr as described above. After seeding constructs were cultured for 7 days either with direct perfusion of culture medium; orbitally mixed dishes served as controls. Constructs were evaluated at the end of cultivation with respect to cell number, viability and metabolic activity, expression of sarcomeric α-actin, and contractile responses to electrical stimulation as described below.

For systematical seeding studies with C2C12 cells a randomized factorial experimental design was used with three factors: seeding time T (two levels: 1.5 and 4.5 hr), initial cell number C (two levels: 6 x 10^6 and 12 x 10^6 cells/scaffold), and seeding set-up S (three levels: dishes on an orbital shaker set to 25 rpm; perfusion at 0.5 mL/min and perfusion at 1.5 mL/min). Three independent seeding experiments were performed (n = 3 for all measurements) for each combination of the three factors.

This experimental design was selected in order to assess the individual effects of the three seeding factors (T, S, C), three possible two-factor interactions (T*C, T*S, C*S) and one possible three-factor interaction (T*S*C). The seeding time was set to 1.5 hr (low) and 4.5 hr (high), based on the attachment times of 1-4 hrs reported for cardiomycoytes seeded on surfaces coated with collagen IV, laminin and fetal bovine serum [22-24], and attachment times of 1-5 hrs reported for C2C12 cells seeded on untreated glass surfaces (Acarturk et al., 1998) or laminin and collagen covered glass (unpublished data from our laboratory). Since Matrigel ® contains both laminin and collagen type IV and the Ultrafoam contains collagens type I and II, it was expected that most cells would attach within 1.5 h.

The cell numbers (6 and $12 \cdot 10^6$ cells per scaffold disc) corresponded to the cell densities of $0.68 \cdot 10^8$ and $1.35 \cdot 10^8$ cells/cm^3 that were on the same order as those measured for the adult rat myocardium ($5 \cdot 10^8$ cells/cm^3, [16]). The minimum flow rate in perfused cartridges was determined from the mass balance of oxygen supply by culture medium and consumption by the cells for the high cell density:

$$F(C_{in}-C_{out})=RN \qquad (1)$$

where F (cm^3/min) is the flow rate of culture medium, C_{in}=220 μmol/L and C_{out}=0 μmol/L are inlet and outlet oxygen concentrations in culture medium, respectively, R=3.62 nmol/min/10^6 is the oxygen consumption rate of C2C12 cells at normoxic conditions [25] and $N=12 \cdot 10^6$ is the higher of the two total cell numbers. In order to assure a margin of safety, the low value of flow rate was set to 0.5 ml/min (Level II of the factor set-up) and the high value was set to 1.5 ml/min (Level III of the factor set-up).

Analytical methods Constructs were sampled after 10 min of gelation, at the end of the 1.5 or 4.5 hr seeding period, and after 7 days of cultivation and evaluated with respect to the cell number, viability, metabolism and spatial distribution. Glucose and lactate concentrations were assessed in culture medium sampled at the end of 1.5-hr or 4.5-hr seeding period from the perfuion loop or Petri dishes, using glucose and L-lactate analyzer Model 2300 STAT Plus (Yellow Springs Instruments, Yellow Springs, OH). For histological evaluation, constructs were fixed in 10% formalin buffer for 24 hr, dehydrated, embedded in paraffin, sectioned (5μm thick) in cross-section through the center and stained with Haematoxylin and Eosin (H&E). Cardiac myocyte constructs were immunostained with monoclonal anti α-actin (sarcomeric, mouse IgM isotype) as described previously (Carrier et al., 1999).

The seeding cell yield and cell viability were assessed prior to seeding, after 10 min of gelation, and after 1.5 hr or 4.5 hr of scaffold seeding. Initial cell populations (trypsinized C2C12 cells, freshly isolated neonatal rat cardiomyocytes) were aliquoted into Petri dish wells and EMA

was added (10 µl of 50 µg/ml solution per 1 x 10^6 cells suspended in 100 µl PBS). Constructs were diced into approximately 2 mm x 2 mm cubes in a Petri dish and 100µl of PBS and 10 µl of EMA solution (50 µg/ml) per 1 x 10^6 cells seeded were added. The dishes were placed on ice under fluorescent light at the distance of 18 cm for 10 min to allow for EMA to cross link to DNA of non-viable cells. To obtain single cell suspensions for cell count and fluorescence activated cells sorting (FACS), the EMA labeled constructs were digested with collagenase and dispase (10 ml of solution containing 0.6 mg/ml collagenase type II with 282 units/mg and 1.2 units/ml of dispase in culture medium per construct) for 30 min at 37°C, and 30 min on ice, with periodic pipetting to dissociate cell aggregates. EMA-labeled dissociated cells were rinsed with culture medium and counted using a hemocytometer (VWR, Bridgeport, NJ). Cells were separated by centrifugation (1000rpm, 10 min), resuspended in PBS at the concentration of 10^6cells/ml and subjected to FACS.

The following parameters were calculated for triplicate samples: (i) *total seeding yield*, defined as the ratio of the number of cells harvested from the construct and the number of cells initially seeded onto the scaffold, (ii) *change in cell viability*, defined as the difference between the viability of cells in the initial cell population (i.e. prior to scaffold seeding) and that of the cells harvested from constructs, and (iii) *live cell yield*, defined as the ratio of the numbers of live cells harvested from the construct and initially seeded onto the scaffold.

The electrophysiological function of engineered cardiac constructs was evaluated by monitoring contractile activity upon electrical stimulation. Each constructs was placed between two gold electrodes connected to a cardiac stimulator, in a 100 mm Petri dish filled with 120 ml Tyrode's solution (140 mM NaCl, 5.4 mM KCl, 0.33mMNaH_2PO_4, 1.8mM $CaCl_2$, 1mM $MgCl_2$, 5mM HEPES, 5.5mM D-glucose). The pH of the Tyrode's solution was adjusted to 7.4 and the temperature was maintained at 37°C using a heating tape fixed to the bottom of the Petri dish and connected to a temperature controller. The entire set-up was placed on an optical microscope. Contractile responses to electrical stimuli (monophasic pulses, 2ms duration) were monitored using a 10x magnification . The stimulation was applied at a rate of 1 Hz starting at an amplitude of 1 V. The amplitude was gradually increased until the excitation threshold was reached and the entire construct started to beat synchronously. Discs cored out of perfusion constructs were compared to dish constructs and full thickness slices of left ventricles of 2 day old neonatal Sprague-Dawley rats (sections obtained by bisecting ventricle parallel to the base apex line).

Statistical Analysis The individual effects and interactions between seeding factors were determined by three factor analysis of variance (Multiway ANOVA) using SAS 8.0 for Unix

(SAS Institute Inc., Cary, NC) [26, 27]. $P<0.05$ was considered significant. The proportion of variance explained by each factor or interaction ω^2 was calculated as described in Lindman [27]:

$$\omega^2=\sigma^2_{effect}/\sigma^2_{total} \quad (2)$$

where σ^2_{effect} is the estimate of variance explained by the given effect and σ^2_{total} is the estimate of total data variance. Pairwise comparisons between certain experimental groups were performed by Student's t-test.

RESULTS

Feasibility studies. Feasibility of the proposed method was assessed by inoculating scaffolds (1.1 mm diameter x 1.5 mm thick discs following hydration) with neonatal rat cardiac myocytes ($12 \cdot 10^6$ per scaffold) and placing the resulting constructs either in perfused cartridges (0.5 ml/min) or in orbitally mixed dishes (25 rpm) for a period of 1.5 h. Total seeding yield was slightly but not significantly lower in the perfusion group than in the dishes (**Table 3.1**). The decrease in cell viability during seeding was markedly lower in perfusion than in dishes. The molar ratio of lactate produced to glucose consumed, an index of cell aerobicity, was also significantly lower in perfusion than in dishes.

To asses the impact of seeding procedure in the long term culture, scaffolds inoculated with $12 \cdot 10^6$ neonatal cardiac myocytes and seeded in perfusion (0.5 ml/min) or orbitally mixed dishes (25 rpm) for 1.5hr were cultivated for additional 7 days in perfusion (0.5 ml/min) or orbitally mixed dish (25 rpm), respectively. Perfusion was associated with (a) negligible decrease in cell viability, presumably due to the maintenance of aerobic cell metabolism as evidenced by a relatively low lactate-to-glucose ratio, and (b) decrease in the total seeding yield, presumably due to the wash-out of unattached cells (**Table 3.1**). In contrast, cell viability markedly decreased in dishes, a result consistent with more anaerobic cell metabolism evidenced by a relatively high lactate-to-glucose ratio (**Table 3.1**). Cell patches expressing sarcomeric α–actin were relatively uniformly distributed throughout constructs cultivated in perfusion, and confined within only a 200-300μm thick top layer of constructs cultivated in dishes (**Figure 3. 2a**).

Spontaneous construct beating was not observed in either group after 7 days of cultivation, suggesting that cells were functionally assembled into tissue-like structures. Consistently, in response to electrical stimulation (e.g., at 5V and 1 Hz) constructs from both groups were reproducibly induced to contract synchronously (please see the **video clip**). However, the constructs cultured in perfusion maintained constant frequency of contractions, whereas the constructs cultivated in orbitally mixed dishes spontaneously increased beating frequencies and every 1 – 2 min exhibited episodes resembling arrhythmia. The excitation

threshold of the constructs cultivated in perfusion was lower but not significantly than that measured for constructs cultured in dishes, and both excitation thresholds were significantly higher then those measured for neonatal rat ventricles (**Figure 3. 2b**).

Table 3.1. Seeding and cultivation of cardiomyocytes in perfused cartridges. Cell numbers, viability and metabolic activity measured for constructs inoculated with $12 \cdot 10^6$ neonatal cardiac myocytes and seeded (1.5 hr) and cultured (7 days) in perfused cartridges (0.5 ml/min) or in orbitally mixed dishes (25 rpm). Data are Average ± SD (n = 3).

Time	*Seeding set-up*	*Total cell yield*	*Change in viability [%] ($viab_{in}$-$viab_{out}$)*	*Live cell yield*	*L/G [mol/mol]*	*Glucose consumption rate [μmol/hr]*
1.5 hr	Dishes (25 rpm)	1.03 ± 0.11	25.79 ± 1.24	0.70 ± 0.09	1.04 ± 0.08	2.47 ± 0.21
	Perfusion (0.5 ml/min)	0.89 ± 0.12	11.59 ± 9.05	0.76 ± 0.05	0.81 ± 0.09*	2.22 ± 0.37
7 days	Dishes (25 rpm)	0.59 ± 0.09	33.03 ± 9.39	0.35± 0.05	2.26 ± 0.30	0.42 ± 0.09
	Perfusion (0.5 ml/min)	0.48 ± 0.04*	-1.16 ± 5.35*	0.50 ± 0.09	1.18 ± 0.49*	0.49 ± 0.30

* significantly different than dish ($p < 0.05$)

Detailed studies of seeding parameters. The effects of seeding set-up (S; three levels), seeding time (T; two levels) and initial cell number (C; two levels) were systematically assessed by inoculating scaffolds with C2C12 cells. After 10 min of gelation, scaffolds inoculated with 6 and $12 \cdot 10^6$ cells had total cell yields of 101 ± 12 % and 102 ± 15 %, respectively, and decreases in cell viability of 0.29 ± 2.03 % and 5.78 ± 2.31 %, respectively.

Total cell yield. Total seeding yields were consistently high in all groups (**Figure 3. 3 a, d**). The differences between groups were not statistically significant, except for slightly but significantly lower yield in the high flow rate (1.5 ml/min) perfusion group, presumably due to washout of unattached cells. The total yield depended on the individual effects of the seeding set-up ($p = 0.0081$), and seeding time ($p = 0.0075$), but not on the initial cell number (**Table 3.2**). The fractions of the observed variance that could be attributed to seeding set-up and time were $\omega^2 = 0.15$ and $\omega^2 = 0.12$, respectively.

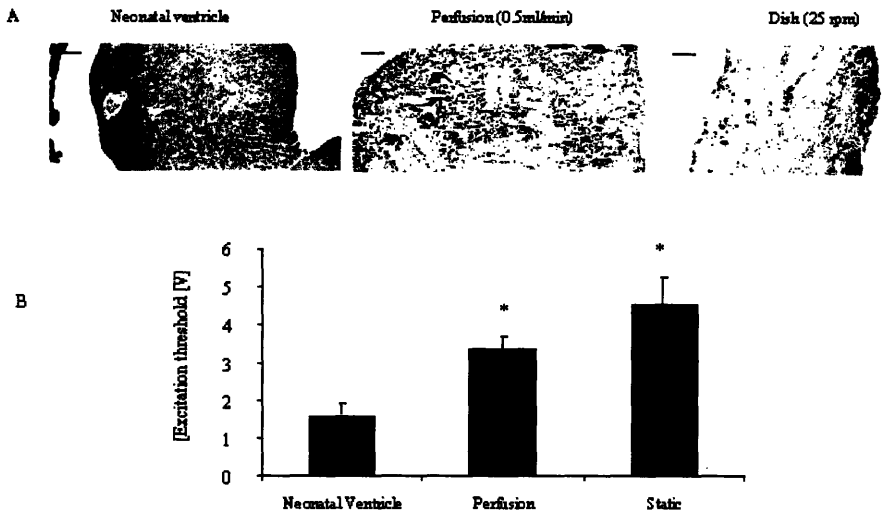

*Figure 3.2. Morphology and contractile responses of cardiac myocyte constructs (a) Expression of sarcomeric α-actin in neonatal rat ventricle and in constructs inoculated with 12 million cells, seeded for 1.5 hr in alternating flow perfusion (0.5 ml/min) or orbitally mixed dish (25 rpm) cultivated for 7 days in perfusion (0.5 ml/min) or in orbitally mixed dish (25 rpm) respectively. Cross-sections. Scale bar 100μm. (b) Excitation threshold of a neonatal rat ventricle and corresponding tissue constructs. * significantly different then neonatal rat ventricle*

Change in cell viability. For constructs seeded in dishes, cell viability markedly decreased with both the duration of seeding (1.5 vs. 4.5 hr, **Figure 3.3 b, e**) and initial cell number (6 vs. 12 million, **Figure 3.3 b, e**), such that constructs seeded with 12 million cells for 4.5 h contained more than 50 % non-viable cells (**Figure 3.3e**). For constructs that were perfused at low flow rate (0.5 ml/min), the same trend was less pronounced, such that constructs seeded with 12 million cells contained approximately 20% non-viable cells at 4.5 h post-seedign (**Figure 2 e**). Importantly, for constructs perfused at high flow rate (1.5 ml/min), neither the duration of seeding nor the initial cell number had any significant effect on cell viability (**Figure 3.3 b, e**). Overall, the decrease in cell viability in constructs seeded in dishes was an order of magnitude higher than that in either perfusion group, and the effects of the seeding method (dish vs. perfusion) were most pronounced for high initial cell number ($12 \cdot 10^6$) and longer seeding time (4.5hr).

The change in cell viability was influenced by all seeding parameters, both individually and interactively (**Table 3.2**). The most significant effects were seeding set-up, S ($p < 0.0001$),

initial cell number, C ($p < 0.0001$) and the interaction between the seeding time and set-up, T*S ($p < 0.0001$). The highest fraction of the observed variance, 0.56, could be attributed to the seeding set-up alone; an additional fraction of 0.17 could be attributed to the interactive effects of seeding set up and seeding time (**Table 3.2**).

Table 3.2. The effects of seeding parameters. The individual effects of the initial cell number (**C**), seeding time (**T**), and seeding set-up (**S**) and their interactions (**T*S, T*C, S*C, T*S*C**) were assessed by multi-way ANOVA.

	Total yield		**Change in cell viability (%)**		**Live cell yield**		**Lactate/Glucose (mol/mol)**		**Glucose Consumption (mg/hr)**	
	p	***ω²***	***p***	***ω²***	***p***	***ω²***	***p***	***ω²***	***p***	***ω²***
C	NS	0.01	<.0001	0.15	0.0054	0.07	NS	0.00	<.0001	0.27
T	0.0075	0.12	<.0001	0.06	<.0001	0.27	0.0048	0.12	<.0001	0.33
S	0.0081	0.15	<.0001	0.56	0.0002	0.20	0.0035	0.17	0.0028	0.09
T*S	NS	0.01	<.0001	0.17	0.0082	0.09	NS	0.00	NS	0.01
T*C	NS	0.00	0.0009	0.01	NS	0.00	NS	0.01	NS	0.01
S*C	NS	0.00	<.0001	0.03	NS	0.03	0.0022	0.20	NS	0.02
T*S*C	NS	0.07	0.0083	0.01	NS	0.02	NS	0.02	NS	0.01

p denotes the probability for each effect, individual or interactive; effect was considered significant if $p < 0.05$.
ω² denotes the fraction of variance that can be attributed to a specific effect.
NS-not significantly different.

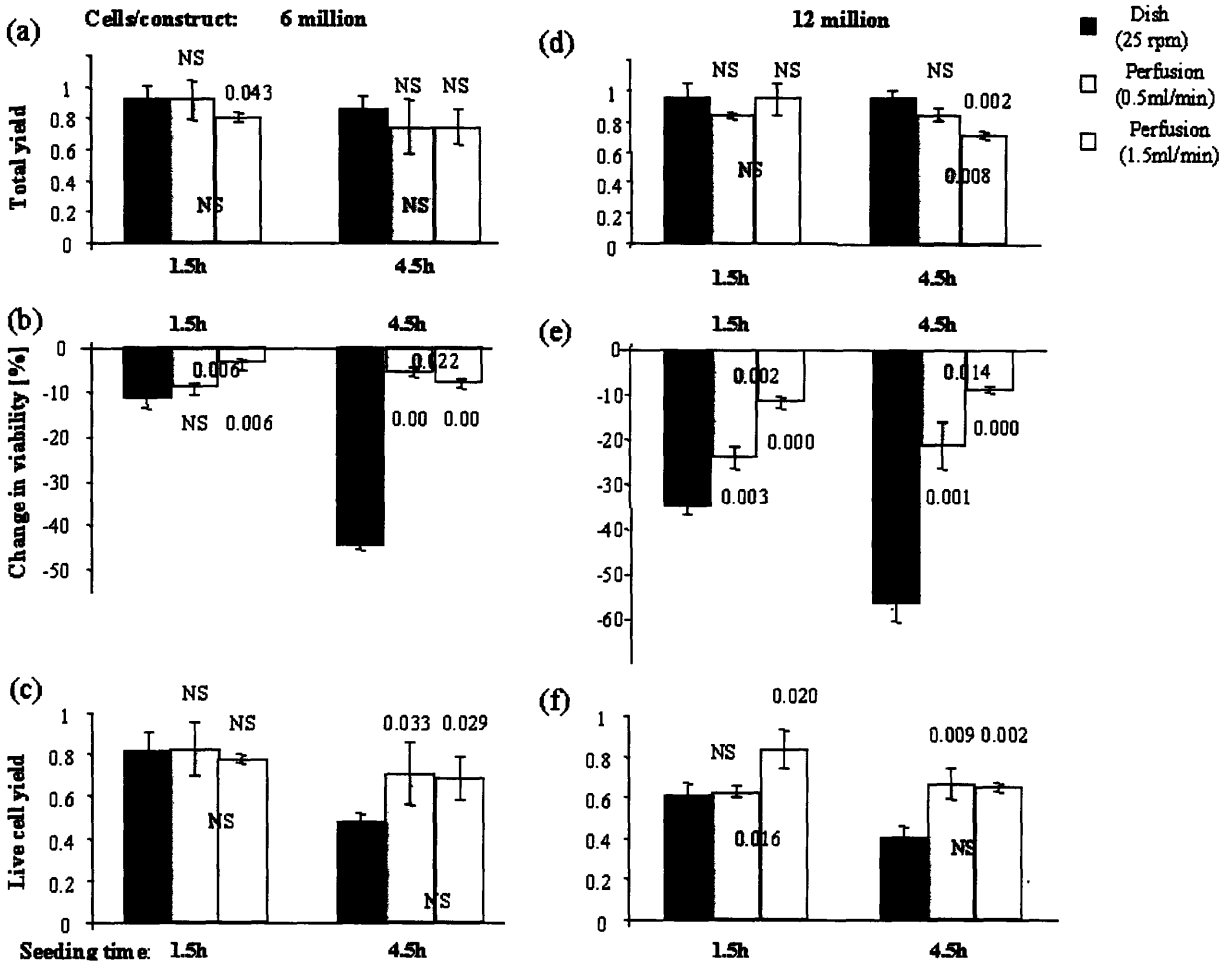

Figure3 3. Seeding parameters. Effects of seeding set-up, seeding time (1.5 and 4.5 h) and initial cell number (6 and 12 million) on (a, d): Total yield; (b, e): Change in cell viability; (c, f):Live cell yield. Data represent average ± standard deviation (n = 3). Numbers above bars are the p values of pairwise comparisons between the dish and perfusion groups; numbers in the bars are the p values of pairwise comparison between the two perfusion groups. Differences are considered significant if $p < 0.05$. NS = not significant.

Live cell yield. There was no significant effect of the seeding set-up on the yield of live cells at the low initial cell number (6 million cells) or for the short seeding period (1.5 h) (**Fig 3.3c, f**). However, as either the initial cell number or the seeding time was increased, perfusion at either flow rate yielded significantly more live cells (up to 50%) than dishes. The live cell yield was influenced by the seeding set-up S ($p = 0.0002$), seeding time T ($p < 0.0001$), and initial cell number C ($p = 0.005$) as well as interactions between the seeding set-up and time T*S ($p = 0.008$). The highest fractions of the observed variance could be attributed to the seeding set-up (0.20) and time (0.27).

To further characterize the kinetics of change in the live cell numbers, cell viability was measured at the beginning of seeding ($t = 0$), after 10 min (i.e., after Matrigel® gelation), and after 1.5 h and 4.5 h of seeding in either dishes or perfusion. The number of live cells on the scaffold decreased exponentially with time according to the first order kinetic model. (**Table 3.3**) The correlation coefficient was high ($0.88 \leq r^2 < 0.998$) in all groups except for one ($12 \cdot 10^6$ cells seeded in perfusion at 0.5 ml/min, $r^2 = 0.56$). The exponential decay time constant, τ, was approximately twice as high in perfusion as compared to dishes. Perfusion at the low flow rate yielded slightly but not significantly higher time constant than perfusion at the high flow rate. The initial cell number had no significant effect on τ.

Table 3.3. Kinetics of change in live cell numbers. The number of live cells on the scaffold was presented as a function of time following cell inoculation using a first order exponential fit of measured data, to obtain the initial cell number N_0 and the time constant τ.

Initial cell number (cells per scaffold)						
	6×10^6			12×10^6		
	Model parameters $N=N_0e^{(-t/\tau)}$					
	$N_0 [10^6]$	τ [h]	r^2	$N_0 [10^6]$	τ [h]	r^2
Dish (25 rpm)	6.1	15	0.998	11..3	12	0.95
Perfusion (0.5 ml/min)	5.9	30	0.94	10.8	28	0.56
Perfusion (1.5 ml/min)	5.8	29	0.88	11.7	25	0.99

Metabolic indices. The molar ratio of lactate produced to glucose consumed (L/G) was used as an index of aerobicity; ideally L/G=1 for completely aerobic metabolism and L/G= 2 for a completely anaerobic metabolism. The following trends were observed (**Table 3.4**): L/G was lower in perfusion than in dishes; L/G increased as the seeding time increased; L/G was lower in perfusion at the high than the low flow rate. Seeding time T ($p = 0.005$) and type of set-up S ($p = 0.003$) significantly influenced L/G (**Table 3.2**). Although the initial cell number C alone had no effect on L/G, an interactive effect between seeding time and set-up T*C was observed ($p = 0.002$), that accounted for the highest fraction of data variance ($\omega^2 = 0.20$), whereas independent effects of T and S accounted for $\omega^2 = 0.17$ and $\omega^2 = 0.12$, respectively.

The glucose consumption rate (G, mg/h), was used as a measure of the total metabolic activity of attached cells. G was lowest for constructs seeded in dishes, intermediate for those perfused at 0.5 ml/min and the highest for those perfused at 1.5 ml/min; the differences were statistically significant for constructs seeded with 6 million cells for 4.5 h. G increased as the initial cell number increased and decreased with an increase in seeding time. Consistent with these observations were the results of multiway-ANOVA (**Table 3.2**) showing that G depended on the individual effects of set-up S ($p = 0.003$), time T ($p < 0.0001$) and initial cell number C ($p < 0.0001$). The variances that could be attributed to S, T and C were $\omega^2 = 0.09$, $\omega^2 = 0.33$ and $\omega^2 = 0.27$, respectively.

Table 3.4. Metabolic indices for 12 different seeding conditions. Ratio of actate produced per unit glucose consumed (mol/mol, **bold**) and glucose consumption rate (μmol/hr, in parentheses).

	Initial cell number (cells per scaffold)			
	6×10^6		12×10^6	
	Seeding time [hr]			
Seeding set-up	1.5	4.5	1.5	4.5
Dishes (25 rpm)	**1.84 ± 0.83** (3.06 ± 1.97)	**2.4 ± 0.08** (1.55 ± 0.06)	**1.45 ± 0.36** (6.06 ± 1.20)	**1.37 ± 0.18** (3.72 ±0.46)
Perfusion (0.5 ml/min)	**1.03 ± 0.41** (4.64 ± 0.45)	**1.72 ± 0.12*** (1.94 ± 0.15)*	**1.81 ± 0.31** (5.73 ± 1.63)	**1.88 ± 0.12*** (3.62 ± 0.60)
Perfusion (1.5 ml/min)	**1.08 ± 0.38** (4.84 ± 1.52)	**1.41 ± 0.33*** (2.57 ± 0.43)*	**0.87 ± 0.27&** (9.58 ± 2.14)	**1.53 ± 0.29** (4.41 ± 0.60)

* significantly different between dish and perfusion ($p < 0.05$)
& significantly different between perfusions at 0.5 ml/min and 1.5 ml/min ($p < 0.05$)

Cell distribution. Cell distribution was evaluated from the full cross sections cut through the centers of the constructs, by comparing cell densities in the top, center and bottom areas of a 0.65 μm wide strip extending from one construct surface to the other. Constructs seeded in dishes generally exhibited non uniform cell distributions with most cells located in the 100-200 μm thick layer at the top surface of the construct, and smaller number of cells that penetrated the entire construct depth (**Figure 3.4**). Constructs seeded in perfusion exhibited spatially uniform distributions of high cell density regions throughout the perfused volume of the construct (**Figure 3.4**), except the regions at outer edge of the construct which were shielded from the fluid flow by silicone gaskets (**Fig. 3.1**). There was no significant difference in the appearance of constructs seeded at 0.5 ml/min and 1.5 ml/min (data not shown).

DISCUSSION

We report that gel-cell inoculation into a scaffold followed immediately by the establishment of perfusion of culture medium through the construct can be utilized to generate tissue engineered constructs with high initial densities of viable myocytic cells. The work was motivated by the need to optimize seeding of 3D scaffolds with hypoxia-sensitive cells at physiological densities. General seeding requirements for 3-D scaffolds include (a) high yield, to maximize the utilization of donor cells, (b) high kinetic rate, to minimize time in suspension for anchorage dependent cells, (c) spatially uniform distribution of attached cells, to provide basis for uniform tissue regeneration (d) high initial construct cellularity to enhance the rate of tissue development and (e) appropriate nutrient and oxygen supply to maintain cell viability during the seeding procedure.

Polymer scaffolds for cardiac tissue engineering have been seeded using a variety of techniques: adding of a concentrated cell suspension onto the scaffold [6, 11], seeding in well mixed suspension of cardiomyocytes in orbitally mixed dishes [12], spinner flasks [12, 13] or rotating vessels [14], and a combination of the two approaches [14]. All of these methods resulted in constructs with viable cells concentrated at the construct surfaces, most likely due to the diffusional limitations of oxygen supply to the construct interior. Perfusion through the constructs that were prepared by seeding scaffolds with cell suspension in mixed flasks resulted in redistribution of the cells throughout the entire volume of the construct [15, 28]. However, cell density remained low, presumably due to the 1-3 day long seeding in flasks which limited the total cell number. Therefore, in order to engineer tissue constructs with high and spatially uniform

cell concentrations it is necessary to overcome oxygen diffusional limitations throughout both steps: scaffold seeding and construct cultivation.

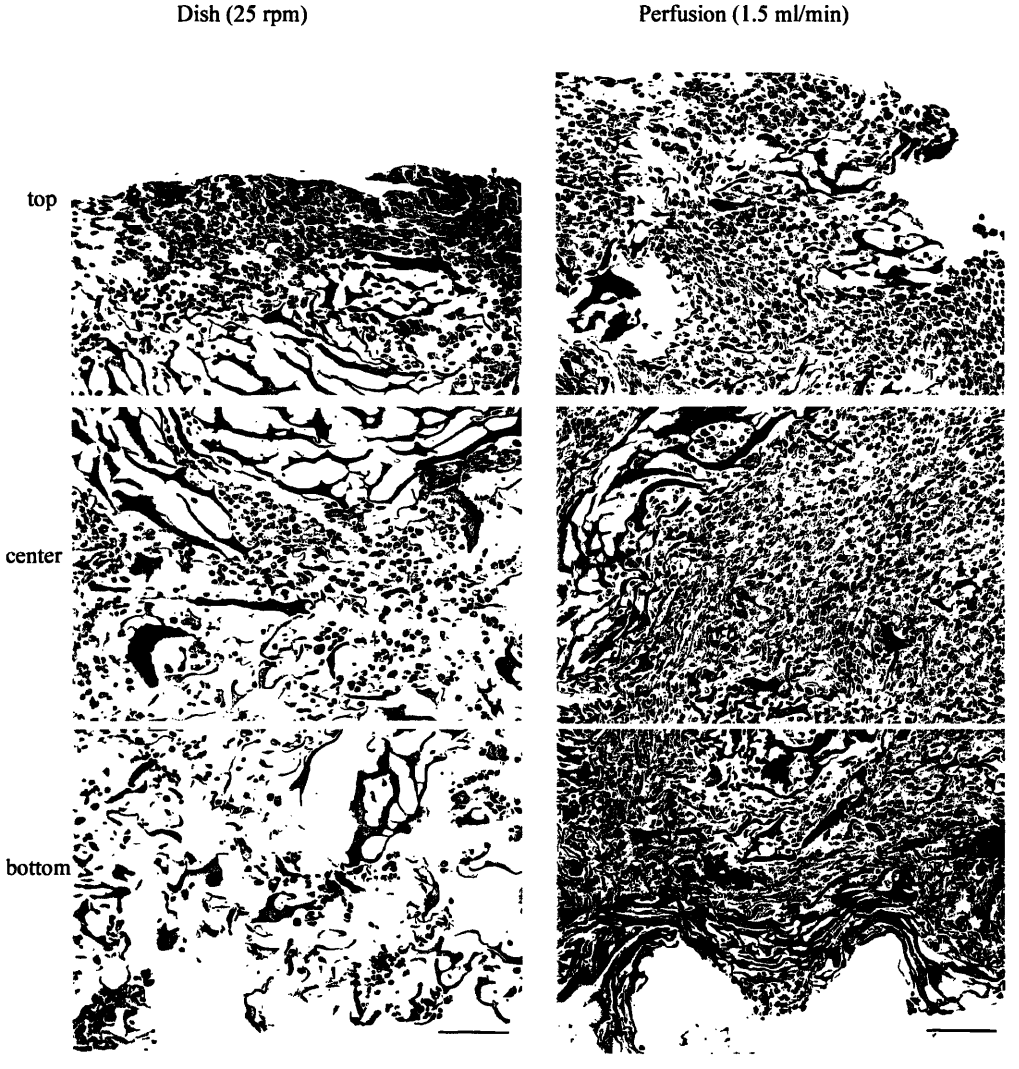

Figure 3.4. Cell distributions. *Cross-sections of constructs inoculated with 12 million cells and then transferred for a period of 4.5 hr either into dishes (25 rpm, left) or into perfused cartridges (1.5 ml/min, right). The top, center and bottom areas of a 650 μm wide strip extending from one construct surface to the other are shown. Scale bar 100μm*

Rapid inoculation of large numbers of cells onto the scaffold (corresponding to the initial cell densities of 0.67 –1.35 10^8 cell/cm^3) using Matrigel® was combined with flow perfusion to enhance mass transport to and from the cells and thereby maintain cell viability. Alternating flow was utilized to minimize cell washout during attachment, and to maintain unrestricted flow through the scaffold pores. Matrigel ® was selected because it contains laminin and collagen IV known to promote surface attachment of cardiac myocytes [22-24]. Feasibility studies were carried out using neonatal rat cardiac myocytes, because these are the most frequently used cells in cardiac tissue engineering. Systematic studies were done using C2C12 myocyte cells because these cells are readily available, well characterized, and representative of hypoxia sensitive cells such as cardiomyocytes.

Medium perfusion maintained the viability of cardiac myocytes during both the seeding (1.5 or 4.5 h) and the cultivation (7 days), while the cell yield remained comparable for constructs cultured in perfusion and in dishes (**Table 3.1**). Direct perfusion of culture medium resulted in uniform cell distributions (**Figure 3.2a**) and substantially higher cell densities than in any of the previous studies done by ourselves or others (Carrier et al, 2002a; Carrier et al, 2002b). Perfusion also resulted in constructs that contracted synchronously in response to electrical stimulation. The maintenance of perfusion at all times during scaffold seeding and construct cultivation is thus essential for achieving physiological densities of viable cells.

The finding of high total yields for both cardiac myocytes (**Table 3.1**) and C2C12 cells (**Fig. 3.3a, d**), under all conditions tested and independent on the initial cell number or seeding set up (**Table 3.2**), implies that the cells were apparently "locked" into the scaffold during the 10 min gelation period. The slight decrease in the total yield between 1.5h and 4.5h (**Fig 3.3a, d**) is likely due to the detachment of dead or loosely bound cells and wash away by flow in perfusion. The gelation itself had no adverse effects on cell viability, which implied that all observed effects were due to other factors associated with cell seeding. Gel inoculation thus satisfies the requirement of high seeding yield that maximizes donor cell utilization, an essential feature for cells with limited proliferation potential such as cardiomyocytes.

Establishment of medium perfusion through the construct immediately after gelation was essential for the maintenance of cell viability, as suggested by Multiway-ANOVA analysis demonstrating that the change in cell viability was influenced the most by the type of seeding set-up used (**Table 3.2**, ω^2=0.56 for the seeding set-up, S). Accordingly, the change in viability was the smallest for cells seeded in perfusion at high flow rate and the largest for cells seeded in the orbital dishes. At longer times (4.5h), the decrease in viability was 3- or 9-fold higher for constructs seeded in dishes as compared to those seeded at low or high perfusion flow rate,

respectively (**Figure 3.2 b, e**). Such profound differences are most likely the result of insufficient diffusional supply of oxygen within constructs seeded in orbital dishes as compared to those seeded in perfusion where oxygen and nutrients are supplied by a combination of diffusion and convection. Relatively smaller decreases in viability in perfusion groups at longer seeding times (4.5 h) as compared to shorter seeding time (1.5 h) (**Fig 3.3a, d**) is consistent with the fact that damaged or dead cells are gradually washed away by flow leaving only healthy and viable cells on the scaffold. If not removed promptly from the tissue construct, the damaged cells could potenatially send apoptosis signals to the neighboring healthy cells or to release harmful intracellular compounds into the environment that can cause further damage.

The yield of the live cells is the parameter most likely to determine the success of any seeding procedure, and it depends on the total yield and change in viability. When seeding times are short enough for the cells to tolerate hypoxia, and the cell concentrations are relatively low to limit the metabolic needs, cell seeding in dishes can yield acceptable results (**Figure 3.3c**, data for 6 million cells per construct and 1.5 h seeding time). However, with an increase in time, cell number or both, hypoxia-induced cell damage increases and the advantages of seeding in perfusion become evident (**Figure 3.3f**, data for 12 million cells per construct and 4.5 h seeding time). Consistently, the molar ratio of the lactate produced to glucose consumed was influenced by the interaction between seeding set-up and initial cell number (**Table 3.2**, $\omega^2 = 0.20$ for the S*C interaction) In scaffolds seeded at low densities, cells maintained aerobic metabolism even in orbital dishes, whereas in scaffolds seeded at high densities, the limitations of oxygen diffusion became rather significant (**Table 3.4**).

The decrease in number of viable cells with time in culture was characterized by the first order exponential decay (**Table 3.3**). Regardless of the cell number, the time constant for both perfusion groups (~ 25 – 30 h) was approximately twice as that in dishes (12 -15 hr). Based on the time constants, a given cell number can be supported two times longer in perfusion then in the orbital shaker. The observed decrease in live cell number in perfusion is a result of a specific technique used for construct fixation between two gaskets that prevented fluid flow around the construct and shield the flow through the construct periphery. Medium did not perfuse the peripheral region of the construct, and the cells that are located between the two gaskets are experiencing at least partial oxygen and nutrient deprivation, a more anaerobic metabolism with increased L/G ratio, and eventually the loss of cell viability. However, this "necrotic edge" can be trimmed off before use, to obtain constructs with an essentially 100% cell viability.

Most of the cells in the constructs seeded in dishes were located in the 100 – 200 μm thick top layer. When the cell/gel suspension was applied to pre-wetted scaffolds, about half of it

penetrates the construct by capillary forces, and the rest forms a layer on the top surface. In contrast, flow helps distribute the high-density cell patches evenly across the central part of the constructs seeded in perfusion (**Figure 3.4**).

In summary, the present study demonstrated that gel/cell inoculation in conjunction with the immediate establishment of alternating-flow perfusion enabled rapid and spatially uniform seeding of myocytic cells at densities close to physiological while maintaining cell viability. The experiments of this kind could be extended to a variety of cell/scaffold systems of interest for tissue engineering. We anticipate that the benefits of gel-cell seeding with perfusion would be the most obvious in the high density seeding of hypoxia sensitive cells such as cardiomyocytes.

ACKNOWLEDGMENTS

This work was supported by the National Aeronautics & Space Administration (Grant NCC8-174). We would like to thank Sue Kangiser for her help with the manuscript preparation and Jan Boublik for help with cardiac myocyte isolation.

REFERENCES

1. Claycomb, W., *Proliferative potential of the mammalian ventricular cardiac muscle cells*, in *The development and regenerative potential of cardiac muscle*, J. Oberpriller, J. Oberpriller, and A. Mauro, Editors. 1991, Harwood Academic Publishers. p. 351-.
2. Scorsin, M., et al., *Can grafted cardiomyocytes colonize peri-infarct myocardial areas?* Circulation, 1996. **94**(9 Suppl): p. II337-II340.
3. Soonpaa, M.H., et al., *Formation of nascent intercalated disks between grafted fetal cardiomyocytes and host myocardium.* Science, 1994. **264**: p. 98-101.
4. Connold, A.L., et al., *The survival of embryonic cardiomyocytes transplanted into damaged host myocardium.* Journal of Muscle Research and Cell Motility, 1997. **18**: p. 63-70.
5. Leor, J., et al., *Bioengineerred cardiac grafts: A new approach to repair the infarcted myocardium?* Circulation, 2000. **102**(suppl III): p. III56-III61.
6. Li, R.-K., et al., *Survival and function of bioengineered cardiac grafts.* Circulation, 1999. **100**(Suppl II): p. II63-II69.
7. Eschenhagen, T., et al., *Three-dimensional reconstitution of embryonic cardiomyocytes in a collagen matrix: a new heart model system.* FASEB Journal, 1997. **11**: p. 683-694.
8. Zimmermann, W.H., et al., *Three-dimensional engineered heart tissue from neonatal rat cardiac myocytes.* Biotechnology and Bioengineering, 2000. **68**: p. 106-114.
9. Fink, C., et al., *Chronic stretch of engineered heart tissue induces hypertrophy and functional improvement.* FASEB Journal, 2000. **14**: p. 669-679.
10. Akins, R.E., et al., *Cardiac organogenesis in vitro: Reestablishment of three-dimensional tissue architecture by dissociated neonatal rat ventricular cells.* Tissue Engineering, 1999. **5**(2): p. 103-118.
11. Li, R.-K., et al., *Construction of a bioengineered cardiac graft.* Journal of Thoracic and Cardiovascular Surgery, 2000. **119**: p. 368-375.

12. Carrier, R.L., et al., *Cardiac tissue engineering: cell seeding, cultivation parameters and tissue construct characterization.* Biotechnology and Bioengineering, 1999. **64**: p. 580-589.
13. Bursac, N., et al., *Cardiac muscle tissue engineering: toward an in vitro model for electrophysiological studies.* American Journal of Physiology: Heart and Circulatory Physiology, 1999. **277**(46): p. H433-H444.
14. Papadaki, M., et al., *Tissue engineering of functional cardiac muscle: molecular, structural and electrophysiological studies.* American Journal of Physiology: Heart and Circulatory Physiology, 2001. **280**(Heart Circ. Physiol. 44): p. H168-H178.
15. Carrier, R.L., et al., *Perfusion improves tissue architecture of engineered cardiac muscle.* Tissue Engineering, 2002. **8**(2): p. 175-188.
16. Mandarim-de-Lacerda, C.A. and L.M.M. Pereira, *Numerical density of cardiomyocytes in chronic nitric oxide synthesis inhibition.* Pathobiology, 2000. **68**: p. 36-42.
17. Ameer, G.A., T.A. Mahmood, and R. Langer, *A biodegradable composite scaffold for cell transplantation.* Journal of Orthopaedic Research, 2002. **20**(1): p. 16-19.
18. Kim, S.S., et al., *Dynamic seeding and in vitro culture of hepatocytes in a flow perfusion system.* Tissue Engineering, 2000. **6**(1): p. 39-44.
19. Reinecke, H. and C.E. Murry, *Transmural replacement of myocardium after skeletal myoblast grafting into the heart: Too much of a good thing?* Cardiovascular Pathology, 2000. **9**(6): p. 337-344.
20. Koh, G.Y., et al., *Differentiation and long-term survival od C2C12 myoblast grafts in heart.* Journal of Clinical Investigation, 1993. **92**(3): p. 1115-1116.
21. Robinson, S.W., et al., *Arterial delivery of genetically labeled skeletal myoblasts to the murine heart: long-term survival and phenotypic modification of implanted myoblasts.* Cell Transplantation, 1996. **5**(1): p. 77-91.
22. Lundgren, E., et al., *Extracellular matrix components influence the survival of adult cardiac myocytes in vitro.* Experimental Cell Research, 1985. **158**(2): p. 371-381.
23. Piper, H.M., S.L. Jacobson, and P. Schwartz, *Determinants of cardiomyocyte development in long-term primary culture.* Journal of Molecular and Cellular Cardiology, 1988. **20**(9): p. 825-835.
24. Borg, T.K., et al., *Recognition of extracellular matrix components by neonatal and adult cardiac myocytes.* Developmental Biology, 1984. **104**: p. 86-96.
25. Arthur, P.G., J.J. Gles, and C.M. Wakeford, *Protein synthesis during oxygen conformance and severe hypoxia in the mouse muscle cell line C2C12.* Biochimica et Biophysica Acta, 2000. **1475**: p. 83-89.
26. Montgomery, D.C., *Design and Analysis of Experiments.* 4th ed. 1997, New York: John Wiley & Sons Inc.
27. Lindman, H.R., *Analysis of Variance in Experimental Design.* 1992, New York: Springer-Verlag.
28. Carrier, R.L., et al., *Effects of oxygen on engineered cardiac muscle.* Biotechnology and Bioengineering, 2002. **78**: p. 617-625.

4. MEDIUM PERFUSION ENABLES ENGINEERING OF COMPACT AND CONTRACTILE CARDIAC TISSUE [3]

INTRODUCTION

The limited ability of cardiac muscle to regenerate after myocardial infarction motivates studies aimed at curative treatment options. Engineered cardiac constructs may serve as grafts for myocardial repair, but only if they are thick and compact, contain a high density of metabolically active cardiomyocytes, and contract synchronously in response to electrical stimulation.

Cardiac constructs that expressed distinct structural and functional features characteristic of differentiated myocardium have been engineered *in vitro* starting from cardiac myocytes in conjunction with collagen gels [1-4], collagen fibers [5], collagen sponges [6-10], and polyglycolic acid meshes [11-13], or by stacking confluent cell monolayers into thin pulsatile sheets [14]. In some cases, *in vitro* cultivation involved the use of bioreactors [11-13] or the application of mechanical stretch [1, 15, 16]. In all cases, oxygen transport through the tissue was largely governed by molecular diffusion, which can support only a thin (100 – 200 μm) surface layer of functional tissue, and leaves construct interior relatively acellular [4, 11].

Construct cultivation in perfused cartridges markedly improved the uniformity of cell distribution, but the overall cell density remained low due to the limitations of diffusional oxygen supply during scaffold seeding [17, 18]. In a recent study, we showed that gel inoculation, in conjunction with interstitial flow of culture medium, enables rapid seeding of hypoxia-sensitive cells (C2C12 cell line) at high and spatially uniform initial densities, and evaluated the feasibility of the proposed method for seeding and cultivation of cardiomyocytes. Seeding in perfusion yielded spatially uniform physiologic cell density, whereas dish-seeded constructs contained viable cells only within a thin (100-200 μm) surface layer [10].

Based on these previous studies, we hypothesized that thick, compact and functional cardiac constructs could be engineered *in vitro* by providing convective-diffusive oxygen transport similar to that present *in vivo* between the capillary network and the cells within native myocardium. To test this hypothesis, we established a culture system that maintained efficient oxygen supply to the cells at all times during scaffold seeding and construct cultivation, and

---

[3] Most of this chapter has been published in Milica Radisic, Liming Yang, Jan Boublik, Richard J. Cohen, Robert Langer, Lisa E. Freed and Gordana Vunjak-Novakovic "Medium perfusion enables engineering of compact and contractile cardiac tissue" ", American Journal of Physiology-Heart and Circulatory Physiology 286: H507-516, 2004

characterized in detail construct metabolism, structure and function. Neonatal rat cardiomyocytes were suspended in Matrigel®, inoculated into collagen sponges at a physiologic cell density, and cultured for 7 days. Medium perfusion through cell-seeded scaffolds was established within 10 min of cell inoculation and maintained throughout the duration of construct cultivation at an interstitial velocity of 500 μm/s corresponding to the average blood velocity within native myocardium [19].

MATERIALS AND METHODS

Tissue culture. Cardiomyocytes were obtained from 1 - 2 day old neonatal Sprague Dawley (Charles River) rats according to procedures approved by the Institute's Committee on Animal Care, as previously described [11]. Porous collagen scaffolds (Ultrafoam®, Davol Inc.) formed as 11 mm diameter x 1.5 mm thick discs were inoculated at the density of $1.35 \cdot 10^8$ cells/cm^3 scaffold volume. Cells were suspended in Matrigel® (Becton Dickinson) using 12 10^6 cells in 60 μL Matrigel®, delivered into scaffolds and transferred immediately following gelation into either orbitally mixed dishes or perfused cartridges as previously described [10].

In the perfused group, constructs were placed between two stainless steel screens and two silicone gaskets, and transferred into 1.5 ml polycarbonate perfusion cartridges (kindly donated by the Advanced Tissue Sciences, La Jolla, CA; one scaffold per cartridge). The screens (85% open area) provided mechanical support during perfusion and the gaskets (1 mm thick, 10 mm OD, 5 mm ID) routed the culture medium through the central area of the construct. Constructs were subjected to alternating flow perfusion at 0.5 mL/min for the first 1.5 h to prevent washout of cardiomyocytes before they attach to the scaffold (**Figure 4.1A**) and then to unidirectional perfusion for the duration of culture (an additional 7 days) (**Figure 4.1B**). Control constructs were cultivated in orbitally mixed dishes (25 rpm).

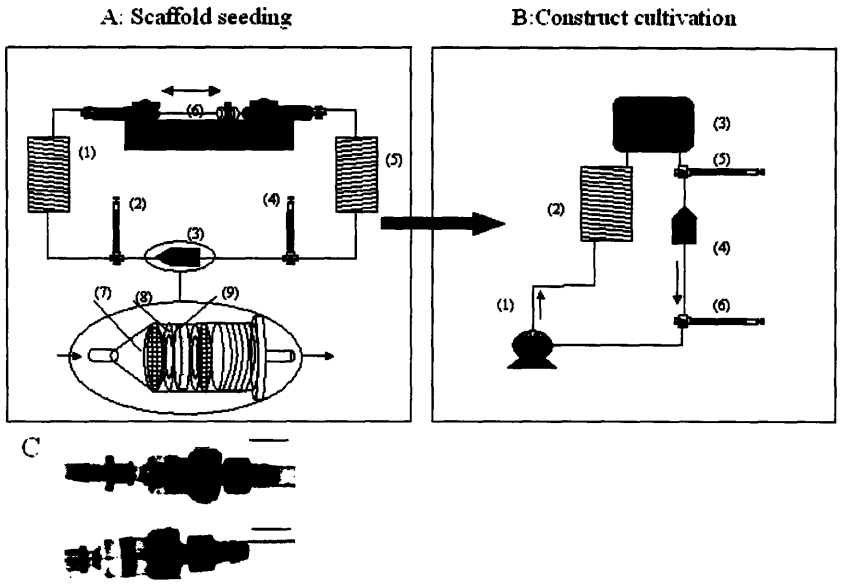

Figure4. 1. Perfused cartridges with interstitial flow of culture medium. (A) Scaffold seeding. *Gel-cell inoculated scaffolds were placed between two stainless steel screens (7) and two silicone gaskets (8), and transferred into cartridges (3, one scaffold per cartridge). The screens (85% open area) provided mechanical support during perfusion and the gaskets (1 mm thick, 10 mm OD, 5 mm ID) routed the culture medium directly through the construct. Air bubbles were displaced by culture medium injected from the de-bubbling syringe (4) into the downstream syringe (2). Each cartridge was placed in a perfusion loop consisting of a push-pull pump (6), two gas exchangers (1, 5) and two syringes (2, 4). The total volume of medium was 8 mL. For a period of 1.5 h, the pump was programmed to the flow rate of 0.5 ml/min, with the reversal of flow direction after 2.5 ml was perfused in a given direction.* ***(B) Construct cultivation.*** *Each cartridge with a seeded construct (4) was transferred into a perfusion loop consisting of one channel of a multi-channel peristaltic pump (1), gas exchanger (a coil of thin silicone tubing, 3m long) (2), reservoir bag (3) and two syringes (5, 6). The total volume of medium in each loop was 32 mL. The flow rate was set at 0.5ml/min and maintained throughout the 7 day cultivation. Constructs seeded and cultivated in orbitally mixed dishes (35 mm well, 8 mL medium, 25 rpm) served as controls.* ***(C) Flow visualization.*** *top: bulk flow through the construct center, bottom: stream of tracer dye. Scale bar: 10 mm.*

Culture medium was Dulbecco's Modified Eagle Medium (DMEM, 4.5 g/L glucose) supplemented with 10% Fetal Bovine Serum (FBS), 10 mM hydroxyethylpiperazine-N'-2-ethane-sulfonic acid (HEPES), 2 mM L-glutamine and 100 units/ml penicillin (all from Gibco).

Flow visualization. Fluid flow in the perfused cartridge fitted with Ultrafoam® scaffold was evaluated by introducing a pulse of methylene blue tracer dye (Sigma) into the inlet flow of distilled water. The flow rate was set to 0.5 ml/min. In separate studies, a thin stream of red flow tracer dye (VWR) was injected isokinetically 3 mm upflow of the scaffold, to evaluate any dissipation of fluid flow across the cartridge. High resolution inages were taken using a digital camera (Nikon Coolpix 900).

Analytical methods Constructs and culture medium were sampled immediately post-seeding and after 1.5 hr, 1 day and 7 days of culture. Cell number, viability, metabolism (lactate yield on glucose) and cell cycle were assessed at all time points; cell distribution, presence of contractile proteins and contractile function were assessed at 7 days. A total of 26 rat litters (~260 heart ventricles) was used in 10 independent experiments, with n = 2 - 8 constructs per data point.

Cell number and *cell viability* were assessed using ethidium monoazide bromide (EMA) in conjunction with fluorescence activated cells sorting (FACS) as previously described [10]. In brief, EMA was added to aliquots of freshly isolated neonatal rat cardiomyocytes or constructs (10 µl of 50 µg/ml solution per 1 x 10^6 cells suspended in 100 µl PBS) in 6-well dishes that were placed on ice under fluorescent light for 10 min to allow for EMA to cross link to DNA of non-viable cells. EMA labeled constructs were digested with collagenase and dispase (10 ml of solution containing 0.6 mg/ml collagenase type II with 282 units/mg and 1.2 units/ml of dispase in culture medium per construct) for 30 min at 37°C, and 30 min on ice, with periodic pipetting to dissociate cell aggregates. EMA-labeled dissociated cells were rinsed with culture medium and counted using a hemocytometer (VWR, Bridgeport, NJ). Cells were resuspended in PBS at the concentration of 10^6cells/ml and subjected to FACS (FACScan, Becton-Dickinson). The change in cell viability was calculated as the difference between the measured viabilities of freshly isolated cells and cells harvested from digested constructs. As an independent measure of cell damage and death, Lactate Dehydrogenase (LDH) assay was performed on samples of culture medium after 1, 3 and 7 days of culture using a commercial kit (Chiron Diagnostics, East Walpole MA), as described previously [11].

Cell metabolism was assessed from the molar ratio of lactate produced to glucose consumed (ideally, 1 mol/mol for aerobic and 2 mol/mol for anaerobic metabolism). Glucose and lactate concentrations were measured in culture medium sampled at timed intervals using glucose and L-lactate analyzer Model 2300 STAT Plus (Yellow Springs Instruments, Yellow Springs, OH).

For *cell cycle analysis*, constructs were digested and cells were permeabilized in 70% ethanol (1 ml/10^6 cells) for 30min at 4°C. After centrifugation (10 min, 1000 rpm) the pellet was resuspended in solution of 50 µg/ml RNase A and 0.1% Triton X in PBS (0.5 ml/10^6 cells) to digest double-stranded RNA that might interfere with staining. Propidium iodide was added (50 µg/ml) and the cell suspension was subjected to FACS (FACScan, Becton-Dickinson) to determine the fraction of cells in Go/G1, S and G2/M phases. Peak deconvolution was performed using ModFit LT V2.0 for Macintosh.

For *histological evaluation*, constructs were paraffin embedded, bisected and cross-sectioned (5 µm thick) and either stained with hematoxylin and eosin or immunostained as previously

described [11] with monoclonal antibodies for sarcomeric α actin (diluted 1:500, Sigma), cardiac troponin I (diluted 1:150, Biodesign) or sarcomeric tropomyosin (diluted 1:100, Sigma).

The *contractile function* of engineered cardiac constructs was evaluated by monitoring contractile activity upon electrical stimulation at 10X magnification using a microscope (Nikon Diaphot). Each constructs was placed in a 100 mm Petri dish containing of 120 ml Tyrode's solution (140 mM NaCl, 5.4 mM KCl, 0.33 mM NaH_2PO_4, 1.8 mM $CaCl_2$, 1 mM $MgCl_2$, 5 mM HEPES, 5.5 mM D-glucose, pH 7.4) between two custom made gold electrodes connected to a cardiac stimulator (Nihon Kohden). The temperature was maintained at 37°C using a heating tape (VWR) attached to the bottom of the Petri dish. The stimuli (square pulses, 2 ms duration) were applied at a rate of 60 bpm starting at an amplitude of 1 V that was gradually increased at 0.1 V increments until the excitation threshold (ET) was reached and the entire construct was observed to beat synchronously.

The maximum capture rate (MCR) was defined as the maximum pacing frequency (bpm) for a synchronous stimulus-response of the constructs. To measure MCR, the stimulation frequency was increased (from 60 to 600 bpm, in 20 bpm increments) at a constant voltage (equal to either 150% or 200% of the ET). The construct response was measured at each frequency and the frequency was increased until the contractions became asynchronous, irregular or completely ceased. The maximum frequency for synchronous contractions was recorded as the MCR. The value of ET, which was different from one construct to another due to the differences in their structures, served as a baseline voltage for the measurement of MCR. One example of the recording sequence is shown in Radisic_video_3 (supplemental information).

Constructs cultured in perfused cartridges were compared to constructs cultured in mixed dishes and to neonatal rat ventricles (full thickness slices obtained by bisecting the left ventricle parallel to the base apex line). The effect of palmitoleic acid (PA), a gap-junction blocker [20], was investigated by incubating constructs or slices of native ventricles in PA (8.3 mM in Tyrode's solution) for 20 min at 37 °C and then determining ET and MCR as described above. To test if the effect of PA was reversible, constructs were transferred to Tyrode's solution and re-tested after an additional 20 min at 37°C.

Statistical analysis: Individual and interactive effects of culture system and time were determined using the two-way ANOVA (SgimaStat). Culture system was investigated at two levels (orbital shaker at 25 rpm; perfusion 0.5 ml/min), the effect of time was investigated at three levels (1.5 hr, 1 day and 7 days) in respect to live cell number, cell viability, glucose consumption rate and molar ratio of lactate produced to glucose consumed. For cell cycle fractions, the effect of time was investigated at two levels (1 day and 7 days). All experimental data passed normality

and equal variance tests. For pairwise comparisons we chose the most conservative Tukey's post hoc test with $P < 0.05$ considered as significant.

RESULTS

Cell number and viability Cell survival was consistent with the conditions of flow in each experimental group. Flow visualization demonstrated that the central 5 mm diameter region of the perfused constructs had uniform interstitial flow, whereas the outer-edge ring between the two gaskets was shielded from flow (**Figure 4. 1**). In orbitally mixed dishes, fluid flow was generated at construct surfaces, but not in their interiors.

The effects of culture system and time of culture on cell survival and function are shown in **Figure 4.2**; the corresponding statistical data are shown in **Table 4.1**.

Table 4. 1. P values for the individual and interactive effects of culture time (T) and culture system (S) on cell viability and metabolism

	LIVE CELL NUMBER	CELL VIABILITY [%]	L/G [MOL/MOL]	GLUCOSE CONSUMPTION [MOL/HR PER10^6 CELLS]	LDH [U]
T	< 0.001	0.002	< 0.001	< 0.001	NS
S	< 0.001	< 0.001	0.003	0.035	<0.001
T*S	NS	0.035	0.038	NS	NS

Determined by a two-way ANOVA in conjunction with Tukey's post-hoc test; $p < 0.05$ was considered significant.

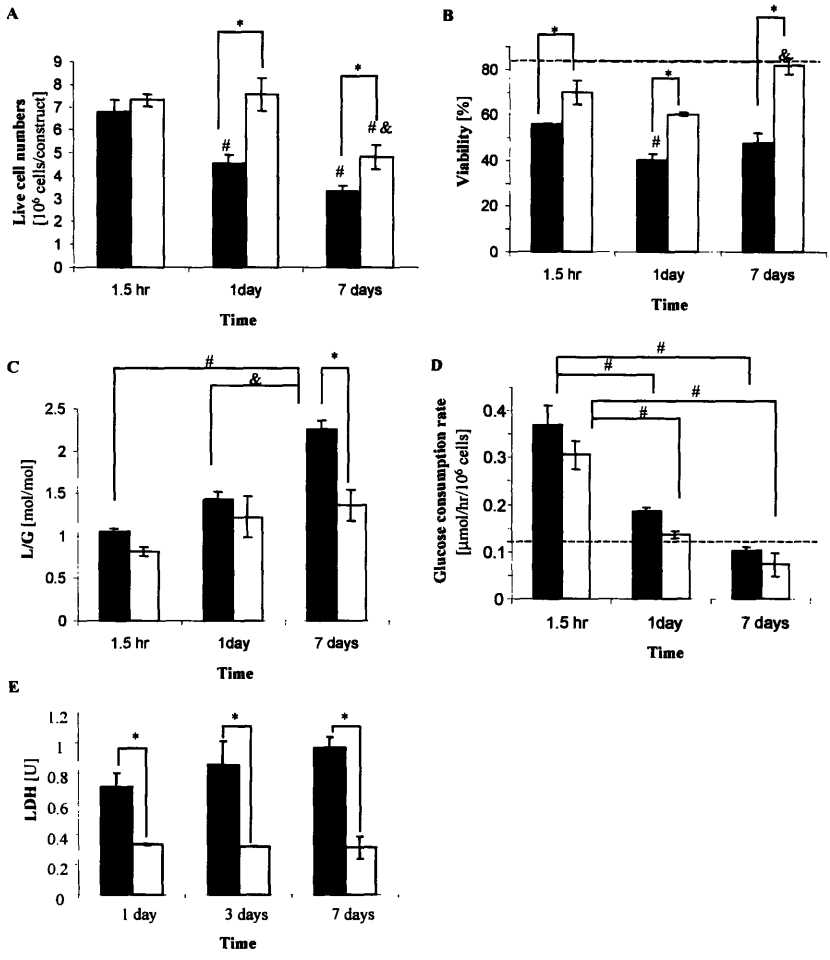

Figure 4 2. Cell viability and metabolism. (A) Live cell number per construct, (B) Viability of cells on the construct. Dashed line represents viability of freshly isolated cells: 83.8 ± 2.0 (n=6) (C) Molar ratio of lactate produced to glucose consumed. (D) Glucose consumption rate in µmol/hr/10^6 cells. Dashed line represents reported [21] values of glucose consumption rate. (E) Lactate Dehydrogenase (LDH) content (U) in culture medium. Open bars represent perfused constructs; filled bars represent dish-grown controls. Data are expressed as average ± standard error; p values were calculated by one-way ANOVA in conjunction with Tukey's test for pair-wise multiple comparisons (n = 3 – 9 samples per data point). Differences were considered significant if p < 0.05. (*) significant difference between perfused and dish-grown constructs. (#) significant difference between 1 or 7-day and 1.5 hr constructs; (&) significant difference between 7-day and 1 day constructs.

In seeded constructs (1.5 h time point), the live cell numbers were comparable for perfused and control constructs (approximately 7 million cells per construct in both groups, **Figure 4.2A**). Throughout the cultivation (1 day and 7 day time points), the number of live cells in perfused constructs was significantly higher than in dish-grown constructs (**Figure 4.2A**). Notably, the number of live cells in dish-grown constructs decreased rapidly during the first day of culture and

continued to decrease relatively slowly between day 1 nd day 7. In contrast, live cell numbers in perfused constructs did not change from 1.5 h to day 1 and decreased slowly over the time of culture. The volume fraction of the construct that was adequately perfused corresponds roughly to the fraction of cells that remained viable over 7 days of culture (**Figure 4.2 A**). Cell viability was significantly higher in perfused than in dish-grown constructs at all time points (**Figure 4.2B**). Importantly, the final cell viability in perfused constructs (81.6 ± 3.7%, **Figure 4.2 B**) was not significantly different than the viability of the freshly isolated cells (83.8 ± 2.0) and it was markedly and significantly higher than the cell viability in dish-grown constructs (47.4 ± 7.8 %, **Figure 4.2 B**). The overall level of cell damage and death was assessed by monitoring the levels of LDH activity in the culture medium. At all time points tested (1,3 7 days) the levels of LDH were significantly lower in perfusion compared to the orbitally mixed dish (**Figure 4.2E**) indicating less cell damage and death.

Cell Metabolism The oxygen tension in culture medium (pO_2) was significantly higher at the inlet of perfusion cartridges than in orbitally mixed dishes (145 ± 1 vs. 135 ± 1 mm Hg,, $p < 0.05$ n = 5-8). The measured decrease in oxygen tension across the perfused cartridge was only 8 mm Hg, suggesting that culture medium rich in oxygen was available to the cells throughout the construct volume. In contrast, culture medium rich in oxygen was available only to the cells at surfaces of dish-grown constructs. The molar ratio of lactate produced to glucose consumed (L/G) was ~ 1 for perfused constructs throughout the duration of culture, indicating aerobic cell metabolism (**Figure 4.2C**). In contrast, L/G increased progressively from 1 to ~ 2 with time of culture for dish-grown constructs, indicating a transient to anaerobic cell metabolism. (**Figure 4.2C**). The increase in L/G with time in dish cultures was statistically significant ($p < 0.001$). The consumption rate of glucose, the primary energy source in our system, per unit live cells was not significantly different between the groups at any time point. It decreased after seeding to the values that were comparable at 1 day and 7 days of cultivation and consistent with previously published data [21] (**Figure 4.2D**).

Individual and interactive effects of culture system and culture time on cell viability and metabolic function. Importantly, both the culture system (perfusion or orbital dish) and the time of culture (1.5 h; 1 day; 7 days) had statistically significant individual effects on the cell survival parameters shown in **Figure 4.2** (live cell number, cell viability, L/G, glucose consumption). Culture system alone had significant effect on the levels of LDH in culture medium. For cell viability and L/G, we detected additional interactive effects of culture system and culture time (**Table 4.1**).

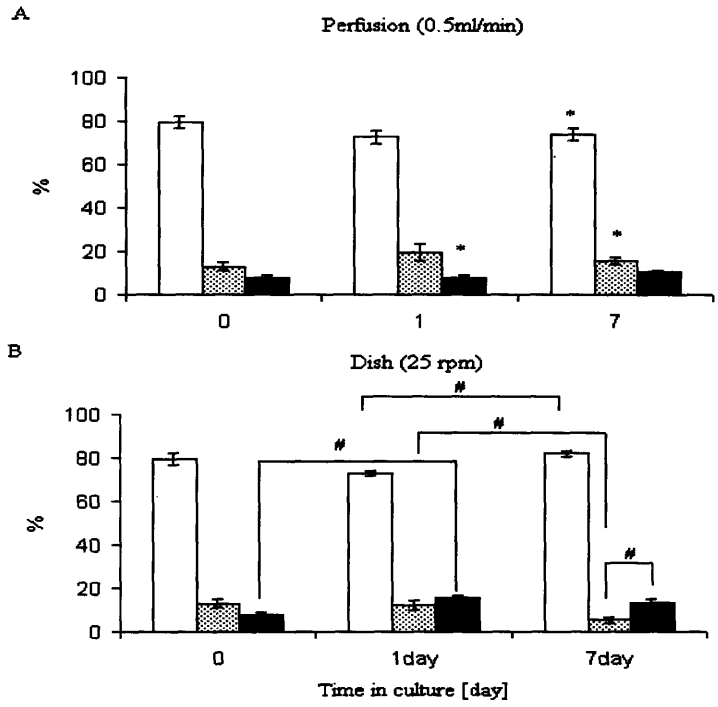

Figure 4.3. Fractions of cells in the G0/G1, S and G2/M phases of the cell cycle. (A) Perfused constructs. (B) Dish-grown constructs. Engineered cardiac constructs were digested with collagenase II/dispase at timed intervals, collected cells were permeabilized and labeled with propidium iodide, and DNA was determined using fluorescence activated cell sorting (FACS). Time 0 denotes freshly isolated neonatal cardiac myocytes. Open bars represent the percentage of cells in G0/G1 cycle; light gray bars represent the fraction of cells in S cycle; dark grey bars represent the fraction of cells in G2/M cycle. Data are expressed as average +- standard error; p values were calculated by one-way ANOVA in conjunction with Tukey's test for pair-wise multiple comparisons (n = 2 – 4 samples per data point). Differences were considered statistically significant if p < 0.05. (#) significant difference between the fractions of cells within orbital dish group; (*) significant difference between the corresponding perfused and dish-grown constructs.

Cell cycle Cell cycle analysis of the mononucleated cell fraction indicated that there was a proliferative cell compartment both in perfused and dish-grown constructs (**Figure 4.3**). The relative fractions of cells in G0/G1, S and G2/M cycle determined for the initial cell population (time 0 in **Figure 4.3 A** and **B**) were maintained throughout the duration of culture in perfused but not in dish-grown constructs. Cells isolated from perfused constructs and freshly isolated cardiomyocytes had more cells in the S phase than in the G2/M phases, whereas cells isolated from dish-grown constructs appeared unable to complete the cell cycle and accumulated in the

G2/M phase. After 7 days of culture, the percentage of cells in the S phase was significantly higher in perfused than in dish-grown constructs (**Figure 4.3**). Statistical analysis demonstrated significant effects of culture system on fractions of cells in the S phase ($p = 0.005$) and G2/M phase ($p = 0.01$), and culture time on the fraction of cells in the G0/G1 phase ($p = 0.018$).

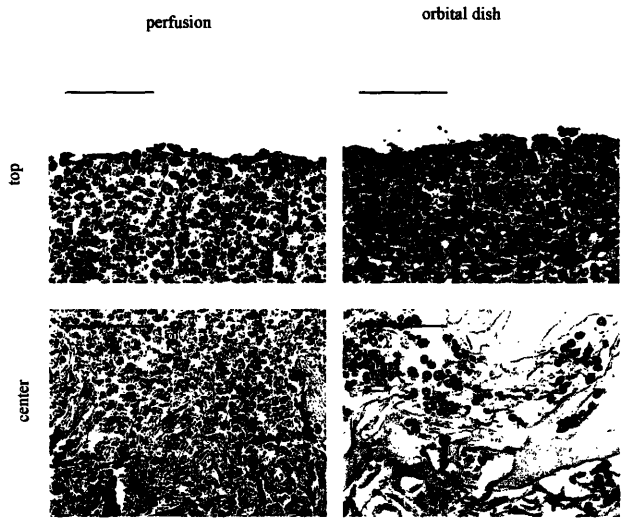

Figure 4. 4. Cell distribution. Distribution of sarcomeric α-actin expressing cells at the periphery (a, b) and in the interiors (c, d) of constructs cultivated in perfusion (a, c) or in orbitally mixed dishes (b, d). Scale bar: 100 μm.

Tissue architecture. After 7 days of culture, the overall tissue architecture appeared markedly better for perfused than dish-grown constructs. The 100 – 200 μm thick peripheral layers of constructs from both groups consisted of tightly packed cells expressing cardiac differentiation markers, in contrast to construct interiors which were markedly different (**Figure 4.4**). Medium perfusion maintained high and spatially uniform cell density throughout the construct volume (except in the outer-edge regions shielded from fluid flow) (**Figure 4.4 A**), whereas molecular

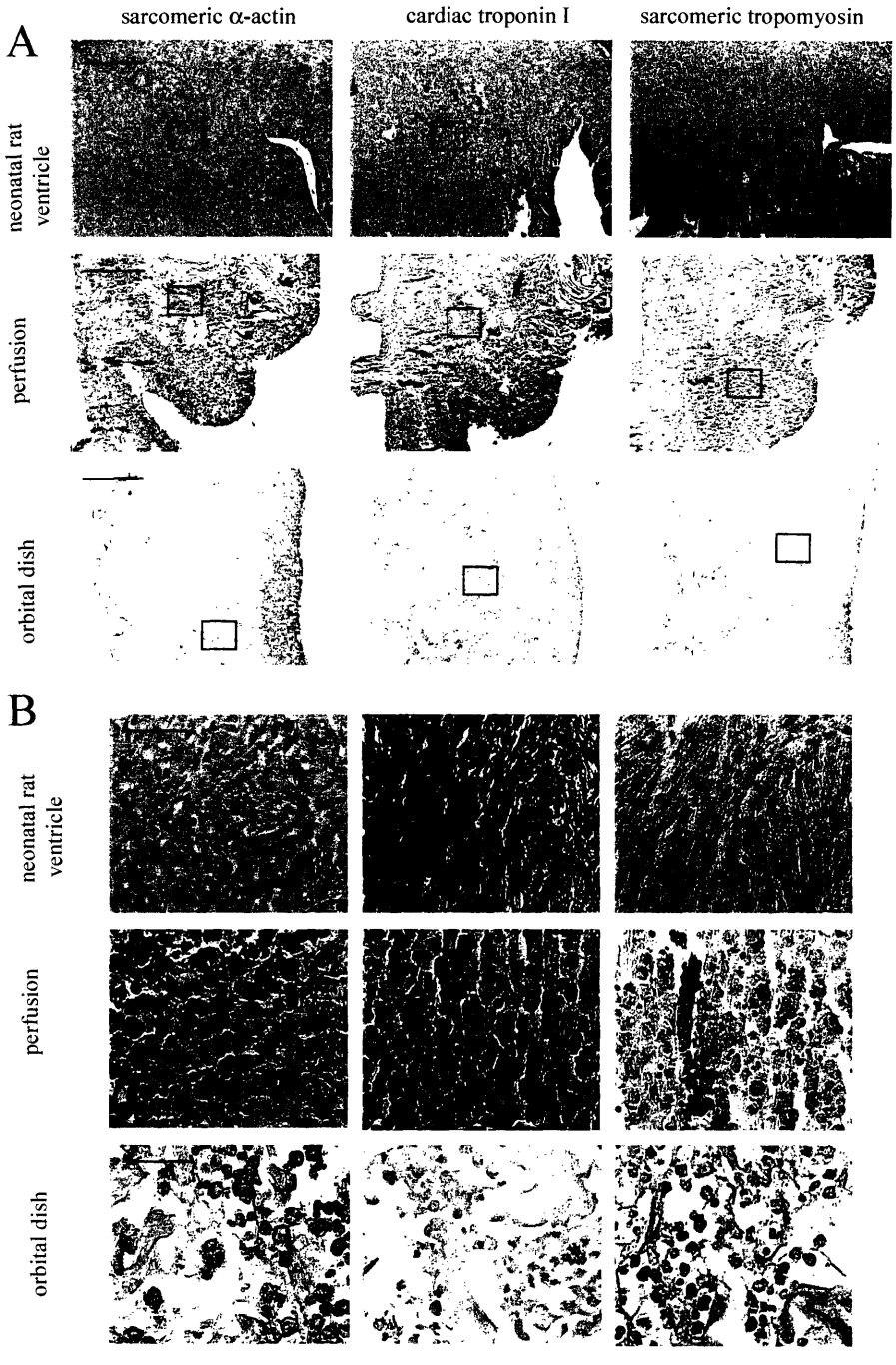

Figure 4. 5. Tissue architecture and cell differentiation. Immunohistochemical staining of three contractile proteins in native neonatal rat ventricles and 7-day constructs seeded and cultured either in perfusion or in orbitally mixed dishes. (A) Tissue architecture. Scale bar: 300 μm. (B) Cell differentiation. Higher magnification of the central regions of the three groups of tissues (boxes in panel A correspond to images shown in panel B). Scale bar: 50 μm.

diffusion in the interiors of dish-grown constructs supported only low density of scattered cells (**Figure 4.4 B**).

Sarcomeric α-actin, cardiac troponin I and sarcomeric tropomyosin were present throughout the perfused construct volume (**Figure 4.5 A, B**). In contrast, dish-grown constructs exhibited spatially non-uniform cell distributions, with most cells expressing contractile proteins located within a 100-300 μm thick surface layer, and only a small number of viable differentiated cells in the construct interior (**Figure 4.5A, B**). Constructs from both groups consisted mainly of mononucleated cells, and exhibited the lack of well established structural alignment of the contractile proteins that was observed in native tissue. The central perfused regions of the constructs (5 mm diameter x 1.5 mm thick) consisted of tightly packed cells expressing sarcomeric α-actin, cardiac troponin I and sarcomeric tropomyosin, similar to neonatal rat ventricles, and distinctly different from the tissue present in the centers of dish-grown constructs (5 mm dia x 1.5 mm thick) that contained only isolated and poorly differentiated cells (**Figure 4.5B**).

Contractile behavior Spontaneous contractions were observed in some constructs early in culture (dish-grown constructs 2 – 3 days after seeding), and ceased after approximately 5 days of cultivation. At the end of cultivation (day 7), spontaneous contractions were not observed in either group of constructs. In response to electrical stimulation (e.g., at 5V and 60 bpm), constructs from both groups were reproducibly induced to contract synchronously (please see Radisic_video_1 and Radisic_video_2). However, in perfused constructs the contraction frequency was constant, whereas in dish-grown constructs the contraction frequency spontaneously increased every 1 – 2 min and the contraction pattern appeared arrhythmic. The excitation threshold (ET) was significantly lower in perfused than in dish-grown constructs, and all construct ETs were significantly higher than those measured for neonatal rat ventricles. There was no significant difference in the maximum capture rates (MCR) measured for the two groups at supra-threshold stimulus amplitudes (150% and 200% of ET, **Table 4. 2**).

Table 4.2. Contractile properties of neonatal ventricles, 7-day perfused constructs and 7-day dish-grown constructs. Excitation threshold (ET) was measured at a stimulation frequency of 60 bpm. Maximum capture rate (MCR) was measured at voltages equivalent to 150% and 200% ET. Data were collected before the treatment with palmitoleic acid (before PA) and after the washout of palmitoleic acid (after PA). Constructs could not be induced to contract in the solution containing PA. Data are expressed as averages ± standard error. p values were calculated by one-way ANOVA in conjunction with Tukey's test for pair-wise multiple comparisons.(n = 2 - 6). Differences were considered statistically significant if $p < 0.05$.

	Neonatal rat ventricle	Perfused construct (7 days @ 0.5ml/min)	Dish-grown construct (7 days @ 25 rpm)
ET (V)			
Before PA[*]	1.6 ± 0.1	3.3 ± 0.2[*]	4.5 ± 0.4[*&]
After PA[**]	1.5 ± 0.1	3.5 ± 0.1[*]	4.4 ± 0.1[*&]
MCR at 150%ET (bpm)			
Before PA[*]	413 ± 7	420 ± 30	502 ± 32
After PA[**]	465 ± 15	415 ± 35	378 ± 31[§]
MCR at 200% ET (bpm)			
Before PA[*]	427 ± 40	415 ± 45	523 ± 14
After PA[**]	427 ± 58	435 ± 45	380 ± 31[§]

[*] significant difference between constructs and neonatal rat ventricles
[&] significant difference between perfused and dish-grown constructs
[§] significant difference before and after PA treatment

Upon incubation with palmitoleic acid (PA), a gap junctional blocker, synchronous construct contractions could not be induced even at 9.9 V. Contractile activity resumed following the washout of PA. The maximum capture rates (MCRs) of perfused constructs and neonatal ventricles were similar to those recorded before the PA treatment, suggesting that the effect of PA was completely reversible. However, the MCRs of dish-grown constructs failed to recover their baseline levels after PA wash-out (**Table 4.2**).

DISCUSSION

Tissue engineered grafts for the repair of impaired myocardium should ideally meet the following requirements: (a) sufficient size and thickness to allow for the repair of infarcted areas or congenital malformations, (b) spatially uniform and physiologic density of viable, metabolically active cells (~10^8cells/cm^3), (c) presence of contractile proteins and other cardiac

markers of cell differentiation, (d) functional coupling resulting in synchronous macroscopic contraction in response to stimuli, and (e) mechanical integrity to allow for surgical implantation. Previous studies of engineered cardiac tissue have demonstrated cell coupling and differentiation [13, 15], mechanical and electrophysiological function [12, 15]. Implantation of engineered constructs has been studied in small animal models [4, 6, 14, 22]. One overwhelming limitation of all previous studies, the small thickness of viable and functional engineered tissue (100 - 200 μm), was attributed to the diffusional transport limitations of oxygen supply [17, 18] and the need to utilize perfusion as a potential means to overcome this limitation has been recognized [4].

Medium perfusion was used in our previous studies to culture cardiac constructs seeded in orbitally mixed dishes [17, 18]. Perfusion resulted in spatially uniform cell distributions, but the constructs cell densities remained low due to diffusional limitations of oxygen supply during cell seeding [17, 18]. In particular, our previous seeding techniques required a 72-hr period during which only the cells in surface regions of the construct remained viable; perfusion during cultivation redistributed viable cells throughout the entire construct volume.

We subsequently showed that rapid cell inoculation using Matrigel® in combination with the immediate establishment of medium perfusion shortened the seeding period from 72 hr to 10 min. [10]. This technique helped overcome the diffusional limitations of oxygen transport to the cells during seeing and resulted in constructs with physiologic densities of viable cells [10].

We hypothesized that the formation of compact, contractile cardiac tissue can be achieved by providing convective-diffusive oxygen transport during construct cultivation. The flow configuration in perfused constructs (**Figure 4.1A, inset**) does not provide a separate compartment for medium flow that would correspond to the capillary space and may therefore induce hydrodynamic cell damage. However, the exchange of oxygen, nutrients and metabolites occurs by the combination of convection through the tissue phase and diffusion over short distances, in a manner resembling some aspects of mass transport *in vivo*. Using this approach, we cultivated cardiac constructs with a perfused central area (5 mm diameter x 1.5 mm thick) that was compact and consisted of highly viable (~85%) cells expressing sarcomeric α-actin, cardiac troponin I and sarcomeric tropomyosin (**Figure 4.4A**), and contracted synchronously at a constant frequency in response to electrical stimulation (**Table 4.2**). These perfused regions could potentially be utilized as a patch for myocardium repair or studies of tissue function *in vitro*.

One of the most important results of this study is that the culture system (S: perfusion or orbitally mixed dishes) and the time of culture (T: 1.5 hr; 1 day; 7 days) had statistically significant effects on the number of live cells (**Figure 4 .2A**), cell viability (**Figure 4.2B**), lactate yield on glucose (L/G) (**Figure 4.2C**), glucose consumption (**Figure 4.2D**) and medium LDH

(**Figure 4.2E**) in engineered constructs. S and T also affected in a statistically significant manner the number of cells in the S and G2/M phases of the cell cycle (**Figure 4.3**). Additional interactive effects of culture system and culture time on cell viability and L/G were also detected (**Table 4.1**). Notably, perfusion improved all parameters that determine cell survival and function in engineered constructs at all times during the cultivation (**Figures 4.2** and **4.3**), presumably due to the convective-diffusive transport of oxygen, as compared to oxygen diffusion within dish-grown constructs.

Although constructs cultivated in perfusion contained significantly more live cells after 1 and 7 days in culture (**Figure 4.2A**), the live cell numbers decreased with time in both systems. The initial decrease in live cell numbers observed 1.5 hr after seeding (**Figure 4.2A**) can be attributed to the insufficient oxygen supply to the cells in the peripheral region shielded from fluid flow in perfused constructs (**Figure 4.1A**, inset) and in the interior of dish-grown constructs. Poor oxygenation of the outer edge of the perfused constructs is consistent with the finding that the volume fraction of the construct that was adequately perfused corresponds roughly to the fraction of surviving cells (live cell number/seeded cell number) after 7 days of cultivation (**Figure 4.2A**). The perfused volume fraction (and thereby the fraction of surviving cells) would increase for thinner silicone gaskets and larger diameter scaffolds. Rather slow decrease of live cell numbers in perfused constructs between 1 and 7 days (**Figure 4.2A**), in conjunction with the maintenance of cell viability (**Figure. 4.2B**) and aerobic cell metabolism during the entire cultivation period (L/G ~ 1, **Figure 4.2C**), suggests that mechanisms other than diffusional limitations of oxygen supply are responsible for the decrease in live cell number in perfused constructs. Relatively low cell viability and live cell numbers in dish-grown constructs (**Figure 4.2B, Figure 4.2A**) are consistent with the prevalently anaerobic cell metabolism (**Figure 4.2C**) resulting from diffusional transport of oxygen. As a result, a "viable shell" formed at the construct surface within 1.5 h of cell seeding. Approximately constant cell viability in this shell is also consistent with the diffusional limitations of oxygen transport from the construct surface into the interior.

High cell viability is essential for the use of engineered constructs as tissue models for controlled *in vitro* studies (e.g., cell function, tissue development), as well as for the envisioned *in vivo* applications. Cell viability was significantly higher in perfusion than in orbitally mixed dishes at all time points (**Figure 4.2B**). A transient decrease in cell viability after 1 day in culture in perfusion is consistent with the washout of dead cells from the perfused constructs. If not removed promptly from the tissue construct, cells that die by necrosis swell and burst, releasing their intracellular contents, which can damage surrounding cells [23]. *In vivo,* the intracellular contents of the cells that die by apoptosis are cleared by phagocytosis of apoptotic bodies, the

process usually carried out by macrophages. In the lack of efficient clearance, the apoptotic bodies undergo a process called secondary apoptosis and release the lysosomal content into the environment. [24, 25]. In our *in vitro* system there are no efficient cellular means of clearing the apoptotic bodies. Even fibroblasts which have some phagocytic ability were demonstrated to undergo secondary apoptosis *in vitro* [26]. Importantly, improper removal of apoptotic cells *in vivo* had been associated with a number of pathological states e.g osteoarthritis [27], lupus erythematosus [28] and cystic fibrosis [29-31]. Therefore, the perfusion of medium provides means for the washout of apoptotic and necrotic cells, thereby minimizing the presence of their intracellular contents within the tissue constructs.

As an independent measure of the cell damage and death, we monitored the level of LDH in the culture medium in both systems, ensuring that both cells contained within the tissue construct and cells present in culture medium were accounted for in both groups. The LDH assay has been used to complement cell viability determined by membrane exclusion dyes (e.g propidium iodide [32, 33] or calcein AM [34]). Since LDH is an intracellular enzyme, its presence in the culture medium is indicative of irreversible cell damage and correlates with decreases in cell viability and live cell numbers. Significantly lower levels of LDH in perfusion compared to the orbitally mixed dishes at all time points thus indicated that perfusion reduced the level of cell damage. The slow increase in the LDH levels (**Figure 4.2E**) in orbital dishes parallels the increase in L/G (**Figure 4.2C**), while the constant levels of LDH in perfusion parallel relatively constant L/G, a relationship that has previously been demonstrated for the LDH and lactate output [35, 36].

There was no apparent difference in the rate of glucose consumption per unit live cells between dish-grown and perfused constructs, although the live cell numbers differed by a factor of two (**Figure 4.2D**), a result consistent with the fact that anaerobic metabolism yields twice as much lactate per unit glucose as aerobic metabolism. The rate of glucose consumption exhibited a transiently high value 1.5 hr after seeding, and then decreased to a constant value consistent with the reported data for glucose consumption in the absence of fatty acids [21].

The maintenance of the relative fractions of cells in the various phases of the cell cycle at levels determined for the initial cell population in perfused but not in dish-grown constructs is likely to be due to the better control of cellular environment. Cell cycle analysis revealed a proliferative compartment in both groups of constructs (**Figure 4.3**), indicating that the measured live cell number resulted from a balance of cell death and proliferation in the population of cardiomyocytes and fibroblasts used to seed the scaffolds. The higher number of live cells in perfused than dish-grown constructs (**Figure 4.2A**) is consistent with the higher fraction of cells

in the S phase. Importantly, the presence of fibroblasts can improve mechanical properties of engineered cardiac tissue [15].

The spatial uniformity of sarcomeric α actin, cardiac troponin I and tropomyosin that was highest in neonatal rat ventricles and higher in the perfused than in dish-grown constructs (**Figure 4.4 and 4.5**) was consistent with the respective differences in the modes of oxygen transport *in vivo* and *in vitro*. In a native rat heart, oxygen is supplied through the capillary network and the total oxygen content is increased by the carrier protein hemoglobin, supporting cell respiration in a thick compact tissue. In perfused cartridges, culture medium flows through the constructs at an average velocity comparable to that found in the native capillary network (~ 500 μm/s), and thereby supports a high density of viable cells throughout the entire volume of the construct. In dishes, the absence of fluid flow within the constructs leads to formation of a 100 - 200 μm thick outer layer of tissue that receives oxygen by diffusion from the construct surfaces.

The level of structural alignment of contractile proteins, that was subnormal in both groups of engineered constructs, can potentially be improved by utilization of physical forces (e.g mechanical stimulation, [15]. Therefore, the perfusion system that maintains cell viability, aerobic metabolism and uniform distribution, could be further improved by addition of defined physical forces. An ideal system would likely include the interstitial medium flow through the construct along with mechanical and/or electrical signals.

The excitation threshold for synchronous macroscopic contractions, which was the lowest for neonatal rat ventricle and the highest for constructs cultivated in orbitally mixed dishes, is consistent with observed differences in tissue architecture. In perfused constructs, with regions of densely packed cells distributed throughout the construct volume, ETs were lower than in dish-grown constructs where densely packed cells were present only at construct surfaces. MCR was measured at 150 and 200% ET in order to take into account cell regions that were poorly connected to the cell network and may have higher ET. Comparable MCRs measured at 150% and 200% of ET indicate that the cell network was established in both groups without large unconnected regions, at least in the surface region. However, the measured electrical properties are not necessarily a predictor of wave propagation in engineered constructs. Wave propagation studies will be needed to further characterize the spatial homogeneity of functional cell coupling.

As expected, the addition of PA resulted in cessation of contractile activity, indicating that signal propagation through the gap junctions was crucial for synchronous macroscopic contractions. The effect of gap-junctional blocker on ET and MCR was completely reversible in neonatal rat ventricles and perfused constructs, but not in dish-grown constructs (**Table 4.1**),

suggesting that the level of organization of the tissue architecture and the robustness of cell response were different in the two groups.

Tissue constructs cultivated in perfusion may be utilized for *in vitro* testing to optimize the methods of cultivation and generate constructs capable of implantation. Although perfused constructs meet most of the requirements necessary for the *in vivo* implantation (e.g size, cell uniformity, viability, contractility and metabolic activity) some requirements are yet to be achieved (e.g modulation of cell morphology). Several previous studies have shown the feasibility of implanting polymers seeded with cardiac or stem cells (15, 16, 20, 22). Cell survival following implantation likely depends on oxygen supply into the construct interior throughout the period needed for the development of functional capillary network and construct integration with the host myocardium. We therefore envision the use of constructs with an array of channels that will be implanted parallel to the epicardial surface (to reduce diffusional distances for mass transport and provide space for in-growth of new blood vessels). To further enhance angiogenesis and vasculogenesis, constructs can be implanted under a membrane containing a vehicle for VEGF release. Together, the use of channeled constructs and transplantation techniques that promote oxygen supply to the cells and the in-growth of new blood vessels are expected to result in improved cell survival and implant function as compared to previously published methods.

In conclusion, interstitial flow of culture medium yielded thick, compact and contractile cardiac constructs containing physiologic densities of metabolically active and viable cells expressing cardiac markers. The maintenance of oxygen supply to the cells throughout the duration of *in vitro* cultivation was key for maintaining cell viability and function. These constructs might potentially be used for myocardium repair or studies of normal and pathological tissue function *in vitro*.

ACKNOWLEDGMENTS

This work was supported by the National Aeronautics & Space Administration (Grant NCC8-174). I would like to thank Sue Kangiser for her help with the manuscript preparation and Thanh-Nga Tran for kindly donating gold plated silicon.

REFERENCES

1. Eschenhagen, T., et al., *Three-dimensional reconstitution of embryonic cardiomyocytes in a collagen matrix: a new heart model system.* FASEB Journal, 1997. **11**: p. 683-694.
2. Zimmermann, W.H., et al., *Three-dimensional engineered heart tissue from neonatal rat cardiac myocytes.* Biotechnology and Bioengineering, 2000. **68**: p. 106-114.
3. Fink, C., et al., *Chronic stretch of engineered heart tissue induces hypertrophy and functional improvement.* FASEB Journal, 2000. **14**: p. 669-679.
4. Zimmermann, W.H., et al., *Cardiac grafting of engineered heart tissue in syngenic rats.* Circulation, 2002. **106**(12 Suppl 1): p. I151-I157.
5. Akins, R.E., et al., *Cardiac organogenesis in vitro: Reestablishment of three-dimensional tissue architecture by dissociated neonatal rat ventricular cells.* Tissue Engineering, 1999. **5**(2): p. 103-118.
6. Li, R.-K., et al., *Survival and function of bioengineered cardiac grafts.* Circulation, 1999. **100**(Suppl II): p. II63-II69.
7. Li, R.-K., et al., *Construction of a bioengineered cardiac graft.* Journal of Thoracic and Cardiovascular Surgery, 2000. **119**: p. 368-375.
8. van Luyn, M.J.A., et al., *Cardiac tissue engineering: characteristics of in unison contracting two- and three-dimensional neonatal rat ventricle cell (co)-cultures.* Biomaterials, 2002. **23**(24): p. 4793-4801.
9. Kofidis, T., et al., *In vitro engineering of heart muscle: Artificial myocardial tissue.* Journal of Thoracic and Cardiovascular Surgery, 2002. **124**(1): p. 63-69.
10. Radisic, M., et al., *High density seeding of myocyte cells for tissue engineering.* Biotechnology and Bioengineering, 2003. **82**(4): p. 403-414.
11. Carrier, R.L., et al., *Cardiac tissue engineering: cell seeding, cultivation parameters and tissue construct characterization.* Biotechnology and Bioengineering, 1999. **64**: p. 580-589.
12. Bursac, N., et al., *Cardiac muscle tissue engineering: toward an in vitro model for electrophysiological studies.* American Journal of Physiology: Heart and Circulatory Physiology, 1999. **277**(46): p. H433-H444.
13. Papadaki, M., et al., *Tissue engineering of functional cardiac muscle: molecular, structural and electrophysiological studies.* American Journal of Physiology: Heart and Circulatory Physiology, 2001. **280**(Heart Circ. Physiol. 44): p. H168-H178.
14. Shimizu, T., et al., *Fabrication of pulsatile cardiac tissue grafts using a novel 3-dimensional cell sheet manipulation technique and temperature- responsive cell culture surfaces.* Circulation Research, 2002. **90**(3): p. e40-e48.
15. Zimmermann, W.H., et al., *Tissue engineering of a differentiated cardiac muscle construct.* Circulation Research, 2002. **90**(2): p. 223-230.
16. Akhyari, P., et al., *Mechanical stretch regimen enhances the formation of bioengineered autologous cardiac muscle grafts.* Circulation, 2002. **106**(12 Suppl 1): p. I137-I142.
17. Carrier, R.L., et al., *Effects of oxygen on engineered cardiac muscle.* Biotechnology and Bioengineering, 2002. **78**: p. 617-625.
18. Carrier, R.L., et al., *Perfusion improves tissue architecture of engineered cardiac muscle.* Tissue Engineering, 2002. **8**(2): p. 175-188.
19. Fournier, R.L., *Basic Transport Phenomena in Biomedical Engineering.* 1998, Philadelphia: Taylor & Francis. p. 24.
20. Burt, J.M., K.D. Massey, and B.N. Minnich, *Uncoupling of cardiac cells by fatty acids: Structure activity relationships.* American Journal of Physiology: Cell Physiology, 1991. **260**: p. C439-C448.
21. Casey, T.M. and P.G. Arthur, *Hibernation in noncontracting mammalian cardiomyocytes.* Circulation, 2000. **102**(25): p. 3124-3129.

22. Leor, J., et al., *Bioengineerred cardiac grafts: A new approach to repair the infarcted myocardium?* Circulation, 2000. **102**(suppl III): p. III56-III61.
23. Lodish, H., et al., *Molecular Cell Biology.* 4th edition ed. 1999: W.H Freeman and Company. p. 1045.
24. Laubner, K., et al., *Apoptotic cells induce migration of phagocytes via caspacse-3-mediated release of a lipid attraction signal.* Cell, 2003. **113**: p. 717-730.
25. Vivers, S., I. Dransfield, and S.P. Hart, *Role f macrophage CD44 in the disposal of the inflammatory cell corpses.* Clinical Science, 2002. **103**: p. 441-449.
26. Terman, A., N. Abrahamsson, and U.T. Brunk, *Ceriod/Lipofuscin-loaded hunman fibroblasts show increased susceptibility to oxidative stress.* Experimental Gerontology, 1999. **34**: p. 755-770.
27. Lotz, M., S. Hashimoto, and K. Kuhn, *Mechanisms of chondrocyte apoptosis.* Osteoarthritis and Cartilage, 1999. **7**: p. 389-391.
28. Herrmann, M., et al., *Impaired phagocytosis of apoptotic cell material by monocyte-derived macrophages from patients with systemic lupus erythematosus.* Arthritis and Rheumatism, 1998. **41**(7): p. 1241-1250.
29. Vandivier, R.W., et al., *Impaired clearance of apoptotic cells from cystic fibrosis airways.* Chest, 2002. **121**(3 Suppl): p. 89S.
30. Vandivier, R.W., et al., *Elastase-mediated phosphatidylserine receptor cleavage impairs apoptotic cell clearance in cyctic fibrosis and bronchiectasis.* Journal of Clinical Investigation, 2002. **109**: p. 661-670.
31. Hu, B., et al., *Deficient in vitro and in vivo phagocytosis of apoptotic T cells by resident murine alveolar macrophages.* Journal of Immunology, 2000. **165**: p. 2124-2133.
32. Vanden Hoek, T.L., et al., *Reperfusion injury in cardiac myocytes after simulated ischemia.* American Journal of Physiology: Heart and Circulatory Physiology, 1996. **270**(39): p. H1334-H1341.
33. Vitadello, M., et al., *Overexpression of the stress protein Grp94 reduces cardiomyocyte necrosis due to calcium overload and simulated ischemia.* FASEB Journal, 2003. **17**: p. 923-925.
34. Nakano, M., D.L. Mann, and A.A. Knowlton, *Blocking the endogeneous increase in HSP 72 increase susceptibility to hypoxia and reoxygenation in isolated adult feline cardiocytes.* Circulation, 1997. **95**: p. 1523-1531.
35. Fantini, E., et al., *Oxygen and substrate deprivation on isolated rat cardiac myocytes: temporal relationship between electromechanical and biochemical consequences.* Canadian Journal of Physiology and Pharmacology, 1990. **68**: p. 1148-1156.
36. Kolodgie, F.D., et al., *Myocardial protection of contractile function after global ischemica by phusiologic estrogen replacment by physiologic estrogen replacement in the ovariectomized rat.* Molecular and Cellular Cardiology, 1997. **29**: p. 2403-2414.

5.THE ROLE OF ELECTRICAL STIMULATION OF CONTRACTILITY IN FUNCTIONAL ASSEMBLY OF MYOCARDIUM *IN VITRO*

INTRODUCTION:

Nearly 8 million people in the United States alone have suffered from myocardial infarction, with 800,000 new cases occurring each year [1]. Conventional therapies are limited by the inability of myocardium to regenerate after injury [2] and the shortage of organs available for transplantation. Cell based therapies have been considered as a novel and potentially curative treatment option [3], either by utilization of cells alone [4-16]or by tissue engineering of cardiac grafts *in vitro* that can be surgically attached to the myocardium [17-31].

In standard culture systems (dishes, flasks, rotating vessels), cardiomyocytes did not align in parallel as in the native heart and they remained poorly differentiated most likely due to the lack of orderly externally imposed excitation-contraction coupling [18, 19]. Application of contraction alone via cyclic mechanical stretch significantly improved the level of cell differentiation and force of contraction, but some hallmarks of cardiac differentiation were still missing (M bands, IC discs) [30]. In addition, the distribution and frequency of gap junctions, critical for electrical signal propagation in the tissue, remained unclear. Notably, orderly coupling between electrical excitation and contractions, which is crucial for the development and function of native myocardium [32], has not been established in any of these culture systems.

We hypothesized that the excitation-contraction coupling of cardiac constructs cultured *in vitro* will enhance the level of differentiation and functional assembly of engineered tissue via physiologically relevant mechanisms. We report the development of a biomimetic system in which cardiac constructs are stimulated to contract synchronously during culture in response to a pulsatile electric field. The supra-threshold electrical signals resulted in concurrent development of conductive and contractile properties of engineered cardiac constructs in just 8 days of culture, with strong dependence on the initiation and duration of the applied stimulation.

MATERIALS AND METHODS:

Cell isolation: Cardiomyocytes were obtained from 1 - 2 day old neonatal Sprague Dawley (Charles River) rats according to procedures approved by the Institute's Committee on Animal Care, as previously described [18]. In brief, ventricles were quartered, incubated overnight at 4°C in a 0.06 % (w/v) solution of trypsin in Hank's Balanced Salt Solution (HBSS, Gibco), washed in culture medium, and subjected to a series of digestions (3 min, 37°C, 150 rpm) in a 0.1 % (w/v) solution of collagenase type II in HBSS. The first digestate was discarded, and

the cell suspensions from the subsequent 4 - 6 digestions were centrifuged (750 rpm, 4 min), resuspended in HBSS each, pooled, and resuspended in Dulbecco's Modified Eagle's Medium (DMEM, Gibco) containing 4.5 g/L glucose supplemented with 10% FBS, 10 mM HEPES, 2 mM L-glutamine and 100 units/ml penicillin. Cells were pre-plated for one 60 min period to enrich for cardiomyocytes (i.e. cells that remained unattached were used to prepare constructs).

Construct preparation: Ultrafoam™ (Davol) collagen sponge scaffolds (8 x 6 x 1.5mm) were preweted with culture medium and placed into the 37°C 5%CO2 humidified incubator (Napco, Winchester, VA) for one hour before inoculation. Cells ($6 \cdot 10^6$) were pelleted by centrifugation (1000 rpm, 10 min) and resuspended in Matrigel® (30µl, Becton-Dickinson), while working on ice to prevent premature gelation. Pre-wetted scaffolds were gently blotted dry, placed in six well plates (1/well) and the Matrigel®/cell suspension was delivered evenly to the top surface of each scaffold using an automatic pipette. Gelation was achieved within 15 min at 37°C. Subsequently, culture medium was added (4ml/well) and the plates were orbitally mixed (25 rpm) for 3 days.

Electrical stimulation: After 1, 3 or 5 days of cultivation without electrical stimulation, the constructs were transferred to a chamber consisting of a 100 mm glass dish fitted with two ¼" diameter carbon rods (Ladd Research Industries) placed at a distance of 1 cm and connected to a commercial cardiac stimulator (Nihon Kohden) via platinum wires (Ladd Research Industries). Silicone tubing (Cole-Parmer) spacers were used to create six wells between the two electrodes, enabling the cultivation of six constructs per dish. In one group (designated "stimulated"), the constructs were stimulated with square pulses, 2 ms in duration, supra-threshold amplitude of 5 V (field strength of 5V/cm), frequency of 1 Hz for the remainder of cultivation (up to 8 days). The stimulation voltage was adjusted to the minimum required to induce synchronous construct contractions (observable with optical microscope at 10x magnification). Construct placed in an identical chamber but without electrical stimulation served as control (designated "non-stimulated"). All chambers were orbitally mixed at 25 rpm. Experiments were performed in a 37°C / 5% CO_2 humidified incubator. Total of 130 constructs were prepared in 5 independent experiments that utilized a total of 10 rat litters.

Metabolic parameters: Medium samples were taken at days 3, 5 and 8 of tissue culture and evaluated for glucose, lactate using a glucose and L-lactate analyzer Model 2300 STAT plus (Yellow Spring Instrument) and for lactate dehydrogenase levels (LDH) using a commercially available kit (LDH-L, Chiron Diagnostics, [19]).

DNA and total protein: Samples for DNA and total protein were taken at the beginning of electrical stimulation (day 1, 3 or 5) and at the end of cultivation period (Day 8) and frozen in

liquid nitrogen. They were homogenized in a buffer (1N NH_4OH, 2% Triton X-100) by Mini-bead beater (Biospec Products) with 6 cycles 10s cycles at 25 rpm. After centrifugation for 10 minutes at 12,000 *g* at 4°C, the homogenates were stored at -80°C until further analysis. For DNA assay, the homogenate was incubated at 37°C for 10 min and then diluted with 10 mM Tris-1 mM EDTA buffer containing 100 mM NaCl (1:20). After centrifugation (2,500g for 30 min), the supernatant was collected to measure DNA content fluorometrically by Hoescht dye binding [19]. Total protein was measured by a commercially available kit (Bio-Rad) as previously described ([18, 19]).

Western blots: Samples for Western blot were taken as described above for biochemical assays. Construct homogenates were diluted (1:2) in Laemni buffer (Bio-Rad) containing 5% mercaptoethanol and 2% SDS and boiled for 5 minutes to denature proteins. They were separated on 12% Tris-glycine minigels (Bio-Rad) using kaleidoscope-prestained standards (Bio-Rad) at a constant voltage (100 V, 2 hours, room temperature). Three constructs from each group and time point were analyzed to compare the expression of the protein bands, and each lane was loaded with the same amount of protein (20 μg). Eluted proteins were electroblotted in 1x Tris/Glycine/SDS running buffer (Bio-Rad) onto polyvinylidene difluoride membranes (Bio-Rad) at 100 V for 60 minutes at room temperature in the Bio-Rad Trans-Blot cell. Blots were first incubated with 5% nonfat dry milk in 0.1 % Tween 20 in PBS (PBS-T) at room temperature for 1 hour to block non-specific binding and then, for an additional 1hr at 50rpm, with the appropriate primary antibody: (1) rabbit anti-connexin 43 (Cx-43) (Chemicon), diluted 1:10 in PBS-T; (2) goat anti-creatin kinase-MM (CK-MM) (Biodesign), diluted 1:3,000 in PBS-T; (3) mouse anti-troponin I (TnI) (Biodesign), diluted 1:3,000 in PBS-T; (4) mouse anti-α-myosin heavy chain(MHC) (ATCC hybridoma supernatant); and (5) mouse anti-β-MHC (Chemicon), diluted 1:50 in PBS-T. Blots were washed five times with PBS-T and incubated for 1 hour at room temperature with rabbit anti-goat, rabbit anti-mouse, or sheep anti-rabbit IgG antibodies (Sigma), respectively, all conjugated to horseradish peroxidase and diluted 1:10,000 in PBS-T. After five additional washes, the immunocomplexes were developed using enhanced horseradish peroxidase-luminol chemiluminescence (ECL Western blotting detection reagents, Amersham) and detected after exposure to photographic film (Hyperfilm-ECL) for 5-30 seconds. Band intensity was quantified by image analysis (Scion Image software).

RT-PCR: RNA from the constructs sampled (n=3 per group, at day 3 and day 8 of cultivation) was extracted using Trizol reagent (GibcoBRL) and RNeasy® mini kit (Qiagen) following manufacturer's instructions. Briefly, constructs in Trizol were disintegrated using a steel-ball bead beater (6 cycles of 10 seconds each at 25 rpm). The supernatant was collected after centrifugation at

14,000 rpm for 15 minutes. Total RNA was collected by RNA column chromatography using water as eluant. RNA concentration was determined by measuring the absorbance at 260 nm by a UV spectrophotometr.. One step RT-PCR was carried according to the manufacturer's protocol (Qiagen). Total RNA (0.5-0.05 . |g) was used with specific primers and the RT-PCR reactions were performed at 50°C for 30 minutes, 95°C for 15 minutes, 94°C for 1 minute (23 cycles), 60°C for 1 minute, 72°C for 1.5 minutes, and at 72°C for 10 minutes. The following primers were used in PCR reactions:

Forward α-MHC:	5'-GGAAGAGCGAGCGGCGCATCAAGG-3'
Reverse α-MHC:	5'-CTGCTGGACAGGTTATTCCTCA-3'
Forward β-MHC:	5'-GCCAACACCAACCTGTCCAAGTTC-3'
Reverse β -MHC:	5'-TCAAAGGCTCCAGGTCTCAGGGC-3'
Forward Cx-43:	5'-CATTGGGGGGAAGGCGTGAGG-3'
Reverse Cx-43:	5'-AGCGCACGTGAGAGATGGGGAAG-3'
Forward GAPDH:	5'-TGGAAAGCTGTGGCGTGATG-3'
Reverse GAPDH:	5'-TCCACCACCCTGTTGCTGTAGC-3'
Forward integrin β1:	5'-GCAGCAGCATCTTAGTCACAGTAGG-3'
Reverse integrin β1:	5'-TTTGATTCTGTTTAACTAGTCCTGG-3'
Forward cardiac actin:	5'-CAGATCTTCTCCATGTCG-3'
Reverse cardiac actin:	5'-GGCTGGCTTTGCGGGTGA-3'

Histology and immunohistochemistry: Constructs were sampled at day 3 and day 8, rinsed in PBS, and fixed in 10% neutral buffered formalin (Sigma-Aldrich) for 6-12 hrs. Samples were embedded in paraffin, sectioned at 5 μm, and stained with hematoxylin and eosin (H & E) for general evaluation. Staining for cardiac troponin I, sarcomeric α-actin, α-myosin heavy chain (α-MHC), β-myosin heavy chain (β-MHC) and connexin-43 in n=4-6 samples per group and time point was used to assess the distributions of cardiac myocytes and tissue organization.

For immunohistochemical staining, cardiac tissue sections were depariffinized and antigen was retrieved by heat treatment for 20 min at 95°C in declocking chamber (Biocare Medical). Subsequently, endogenous peroxidase activity was quenched by incubation in 0.3% hydrogen peroxide (VWR) for 30 min at room temperature, the sections were then blocked with 10% horse serum (Vector Laboratories) for 30 min at room temperature, then incubated for 1 hour at 37°C with mouse anti-cardiac troponin I (Biodesign) and mouse anti-sarcomeric α-actin (Sigma) monoclonal antibodies diluted 1:150 and 1:500, respectively in PBS containing 0.5%

Tween 20 (Sigma) and 1.5% horse serum. Subsequently, sections were incubated for 30 min at room temperature with a secondary antibody (horse anti-mouse IgG, Standard Elite ABC kit, Vector Laboratories), diluted 1:200, and then with an avidin-biotin complex agent for 30 min at room temperature and 3,3'-diaminobenzidine (Sigma) for 15 min at RT. A humidified chamber was used for all incubation steps. Sections were counterstained with Harris hematoxylin (Sigma-Aldrich) and cover-slipped using xylene-based mounting media (Cytoseal). Sections of neonatal rat heart ventricles and bovine tendons served as positive and negative controls, respectively. Controls were prepared using the same methods, and in the same batch with engineered constructs. Tissue architecture was assessed from stained tissue sections using videomicroscopy and Scion Image software.

For immunofluorescence, sections were deparaffinized and antigen was retrieved by heat treatment for 20 min at 95°C in decloacking chamber (Biocare Medical), blocked with 10% horse serum (Vector Laboratories) for 40 min at room temperature, then incubated for 1 hour at 37°C with primary antibodies: mouse anti-α-myosin heavy chain (hybridoma supernatant, ATCC, full strength), mouse anti-β-myosin heavy chain (Chemicon, full strength) and rabbit anti-Connexin-43 (Chemicon, 1:50) diluted in PBS containing 0.5% Tween 20 and 1.5% horse serum. Subsequently, the sections were incubated with the following secondary antibodies (all from Vector Laboratories) for 30 min at 37°C: Texas Red conjugated horse anti-mouse IgG (1:100) for α-MHC visualization, fluorescein conjugated anti-mouse IgG (1:100) for β-MHC visualization, and fluorescein conjugated goat anti-rabbit IgG (1:200) for Cx-43 visualization. The sections were counterstained with DAPI and cover-slipped (Vectorshield mounting medium with DAPI). Neonatal rat ventricles and bovine articulate cartilage served as positive control and negative control, respectively. Construct architecture and cell distribution were assessed from tissue sections using a fluorescent microscope (Axioplan, Zeiss) and Open Lab software.

Transmission Electron Microscopy: Constructs (n=6 per group and time point) were taken at day 3 and day 8 and fixed in Karnovsky's reagent (0.1 M sodium cacodylate with 2% paraformaldehyde and 2.5% gluteraldehyde, pH = 7.4), post-fixed in 1% osmium tetroxide in veronal-acetate buffer, dehydrated in graded ethanol in propylene oxide, and embedded in Epon 812 (Polysciences). Sections (70 nm thick) were prepared using a Leica Ultra Cut and a diamond knife, stained with lead citrate and uranyl acetate, and examined using a Philips EM410 transmission electron microscope operated at 80 kV (JEOL-100CX, JEOL).

***Morphometric analysis*:** Morphometric analysis was performed on 20-46 randomly taken transmission electron micrographs at magnification of 100,000. A test grid with uniform squares (0.26 cm x 0.26 cm) was superimposed onto the micrographs and the area covered by sarcomeres,

mithochondria, nuclei and the overall area of the cells were determined. The volume fraction of each organelle was determined as previously described {Loud, 1984 #2023. The frequency of intercalated discs and gap junctions (number per μm^2) was determined by counting. A total of 20 micrographs of non-stimulated constructs, 46 micrographs of stimulated constructs and 42 micrographs of neonatal heart ventricles were evaluated with respect to each structural parameters by two independent observers.

Contractile response: The contractile function of engineered cardiac constructs was evaluated by monitoring contractile activity upon electrical stimulation at 10X magnification using a microscope (Nikon Diaphot). Each construct that was evaluated was placed in a 100 mm Petri dish containing 120 ml of Tyrode's solution (140 mM NaCl, 5.4 mM KCl, 0.33 mM NaH_2PO_4, 1.8 mM $CaCl_2$, 1 mM $MgCl_2$, 5 mM HEPES, 5.5 mM D-glucose, pH 7.4) between two custom made gold electrodes connected to a cardiac stimulator (Nihon Kohden). The temperature was maintained at 37°C using a heating tape (VWR) attached to the bottom of the Petri dish. The stimuli (square pulses, 2 ms duration) were applied at a rate of 60 bpm starting at the amplitude of 1 V. The amplitude was increased in 0.1V increments, until the entire construct was observed to beat synchronously, a voltage defined as the excitation threshold (ET). Maximum capture rate (MCR) was determined at 200 % of ET by increasing the stimulation frequency in 50bpm increments, until the paced contractions became irregular or completely ceased. To measure the amplitude of contractions, video recorded beating sequences (1-5 min in duration) were digitized at the rate of 30 frames/s. The en-face area of each construct was measured as function of time using image analysis (Scion Image software). Amplitude of contraction was expressed as fractional area change.

Electrical activity: Electrical activity was recorded for stimulated constructs at the end of cultivation using a platinum electrode positioned ~ 2mm away from the pair of stimulating electrodes (carbon rods). Conventional cardiac stimulator (Nihon Kohden) was used to apply square biphasic pulses 2ms duration and 5V at 1 Hz.

Statistical analysis: Differences between the experimental groups were analyzed using Tukey's test followed by one way ANOVA for pairwise comparisons or Dunn's test; $p<0.05$ was considered significant. Unless otherwise noted, all data are expressed as average±standard error.

RESULTS:

Stimulated constructs had significantly stronger contractile responses to pacing as compared to non-stimulated controls (video clips). For constructs stimulated from day 3 to day 8 of culture,

the amplitude of synchronous contractions was 7-fold higher than for otherwise identical non-stimulated constructs (**Figure 5.1a**). Importantly, the contractile behavior progressively developed with time (**Figure 5.1b**).

Excitation threshold (ET), defined as the minimum stimulation voltage amplitude at 1 Hz for which the entire construct was observed to beat synchronously, decreased with time of culture toward values that were measured for native heart (**Figure 5.1c**). The maximum capture rate (MCR), defined as the maximum pacing frequency for synchronous construct contractions at 150 % ET, increased with the duration of electrical stimulation. Consistently, the MCR of stimulated 8-day constructs was markedly and significantly higher than the MCR of either non-stimulated or early (3-day) constructs (**Figure 5.1d**). The shape, amplitude (~100 mV) and duration (~200 ms) of trans-membrane potentials recorded for cells in constructs that were electrically stimulated during culture (**Figure 5.1e**) were similar to the action potentials reported for cells from constructs that were mechanically stimulated during culture {Zimmermann, 2002 #1125}.

Expression of genes for sarcomeric α-actin, α-MHC, β-MHC, connexin –43 and β-integrin was confirmed for all groups at all time points (**Figure 5.5**). Stimulated constructs exhibited higher levels of α-myosin heavy chain (MHC), connexin 43, creatin kinase-MM and troponin I relatively to either non-stimulated 8-day constructs or to early (3-day) constructs (**Figure 5.1f**). Comparable levels of mRNA in all groups (**Figure 5**), but different relative protein levels are consistent with translational regulation as reported [33]. The ratio of α-MHC (adult) and β-MHC (neonatal) isoforms (~1.5 in 3 day constructs), decreased to 1.4 in non-stimulated group at the end of cultivation period, and increased to 1.8 in the stimulated group, suggesting that electrical stimulation enhanced the differentiation and maturation of cardiomyocytes (**Figure 1g**).

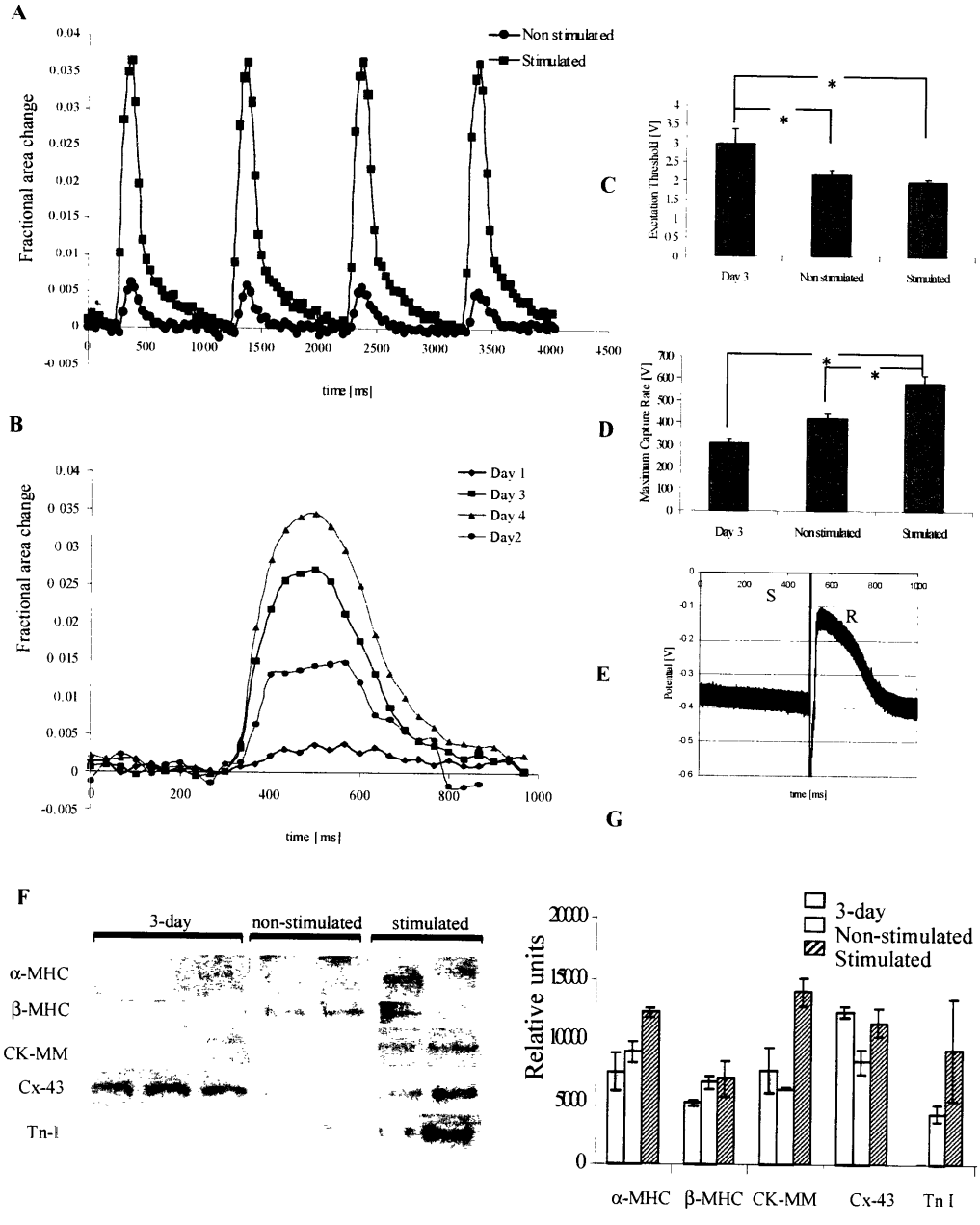

Figure 5.1. Functional properties of engineered cardiac constructs A) Contraction amplitude is about 7 times higher in stimulated constructs compared to non-stimulated constructs at the end of the cultivation period (8-day) B) Contraction amplitude increases with stimulation time in the stimulated group C)Excitation threshold is the lowest in stimulated constructs D) Maximum capture rate is significantly higher in stimulated group compared to the non-stimulated and Day 3 constructs Statistical analysis performed by Tukey's test with one way ANOVA (n=5-10). $P<0.05$ considered significant E) Electrical response to stimulation recorded in stimulated group. (F) Protein levels determined by Western blots (G) Relative protein amounts as determined from Western blots using integrated pixel density analysis n=(2-3).

Notably, improved contractile properties were not the result of differences in construct cellularity or cell metabolism (**Table 5.1**), but rather due to the improved cell morphology, alignment, and structural organization of the conductive and contractile apparatus. No significant differences were found between the non-stimulated and stimulated constructs with respect to glucose metabolism, cell damage (release of lactate dehydrogenase) and cellularity (mg DNA/g wet weight)(**Table 5.1**). The lack of pathological cell hypertrophy in electrically stimulated engineered cardiac tissue was evidenced by the lack of ANF expression and comparable contents of RNA and DNA per wet weight. (**Table 5.1**).

Table 5.1. Glucose metabolism and biochemical properties of stimulated and non stimulated constructs. Statistical analysis performed by Tukey's test in conjunction with one way ANOVA (n=2-6). *significantly different than day 3 group

	DAY 3	NON STIMULATED	STIMULATED
Glucose consumption rate [μmol/day/construct]	10.41 ± 0.67	4.41 ± 0.71*	5.07 ± 1.25*
Lactate/Glucose [mol/mol]	1.29 ± 0.09	1.14 ± 0.10	1.12 ± 0.15
Medium LDH [U/construct/day]	0.153 ± 0.006	0.030 ± 0.003*	0.048 ± 0.005*
Wet Weight [mg]	71 ± 12	50 ± 3	42 ± 11
Cellularity Index [mg DNA/g ww]	0.58 ± 0.11	0.53 ± 0.04	0.49 ± 0.06
RNA Index [mg RNA/g ww]	0.080 ± 0.008	0.097 ± 0.009	0.097 ± 0.014

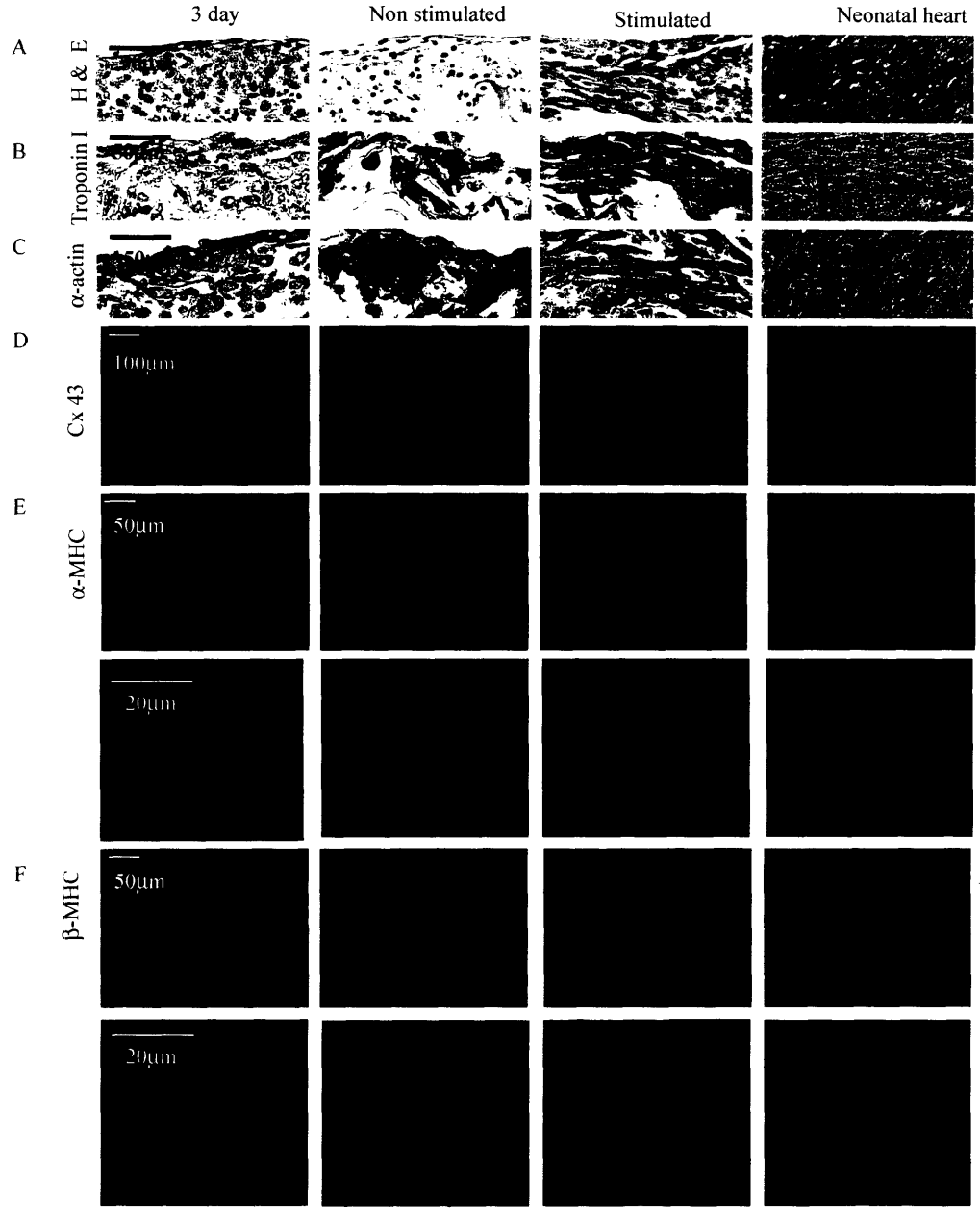

Figure 5.2. Tissue morphology and expression of cardiac markers: A) Hematoxylin and Eosin B) troponin I C)sarcomeric α-actin, D)Connexin-43, E) α-MHC, F) β-MHC . Central cross-sections

At the ultrastructural level, stimulated constructs demonstrated a remarkable level of differentiation, comparable to that of native myocardium. Cells were aligned and elongated, and contained centrally positioned elongated nuclei, similar to native myocardium and in contrast to the non-stimulated constructs that consisted of round, disorganized cells (**Figure 5.3a**) with high

nucleus to cytoplasm ratio. Cells in stimulated constructs and neonatal rat ventricles contained abundant mitochondria positioned between myofibrils; in non-stimulated constructs, mitochondria were scattered around the cytoplasm (**Figure 5.3b**). Morphometric analysis documented that the volume fractions occupied by nuclei and mitochondria decreased and increased, respectively, in a statistically significant manner from non-stimulated to stimulated constructs to neonatal heart ventricles (**Figure 5.3f**). In addition, substantially larger amounts of glycogen were present in stimulated constructs and neonatal rat ventricles than in non-stimulated constructs. Electrical stimulation of contractility induced the development of long, well aligned registers of sarcomeres containing compact and clearly visible M, Z lines, H, I and A bands closely resembling those in native myocardium (**Figure 5.3 b, c**). The development of in-register sarcomeres that resulted from the application of supra-threshold electrical stimulation is a hallmark of maturing cardiomyocytes [32].

The volume fraction of sarcomeres in stimulated 8-day constructs was comparable to that measured for a neonatal rat ventricle by us and others [34]in contrast to non-stimulated constructs that contained only scattered and poorly organized sarcomeres (**Figure 5.3h**). In stimulated samples, intercalated discs were positioned between aligned Z lines (**Figure 3d**) and were as frequent as in neonatal rat ventricles, in contrast to non-stimulated constructs where intercalated discs were rare. Gap junctions were also substantially better developed (**Figure 5.3e**) and more frequent (**Figure 5.3f**) in stimulated than in non-stimulated tissue constructs. The presence of T-tubules (**Figure 5.3e, inset**) was evident in all samples. Overall, electrical stimulation of contractility resulted in remarkably well-developed construct ultrastructure over only 8 days of *in vitro* cultivation.

The optimal time point for the initiation of electrical stimulation - 3 days post seeding - is coincident with the appearance of spontaneous sporadic contractions of the cardiac tissue constructs. If electrical stimulation was initiated too early (12 hr upon cell seeding on scaffolds, designated as day 1), constructs could not be induced to contract synchronously in response to the electric field stimulation, a finding consistent with the low degree of capture in monolayer cultures of cardiomyocytes that were stimulated sooner than 6 to 8 hrs after isolation [35]. Constructs that were stimulated too early developed only weak contractile responses and maintained a predominantly round cell morphology. The amount of cx-43 was substantially reduced as compared to either non-stimulated constructs or constructs stimulated at a later time of culture (**Figure 5.4 a**). Interestingly, the initiation of electrical stimulation late in culture (5 days following cell seeding on scaffolds) enabled the establishment of gap junctions, but failed to

enhance functional organization of the contractile apparatus and cell morphology in response to electrical stimulation (**Figure 5.4 a**).

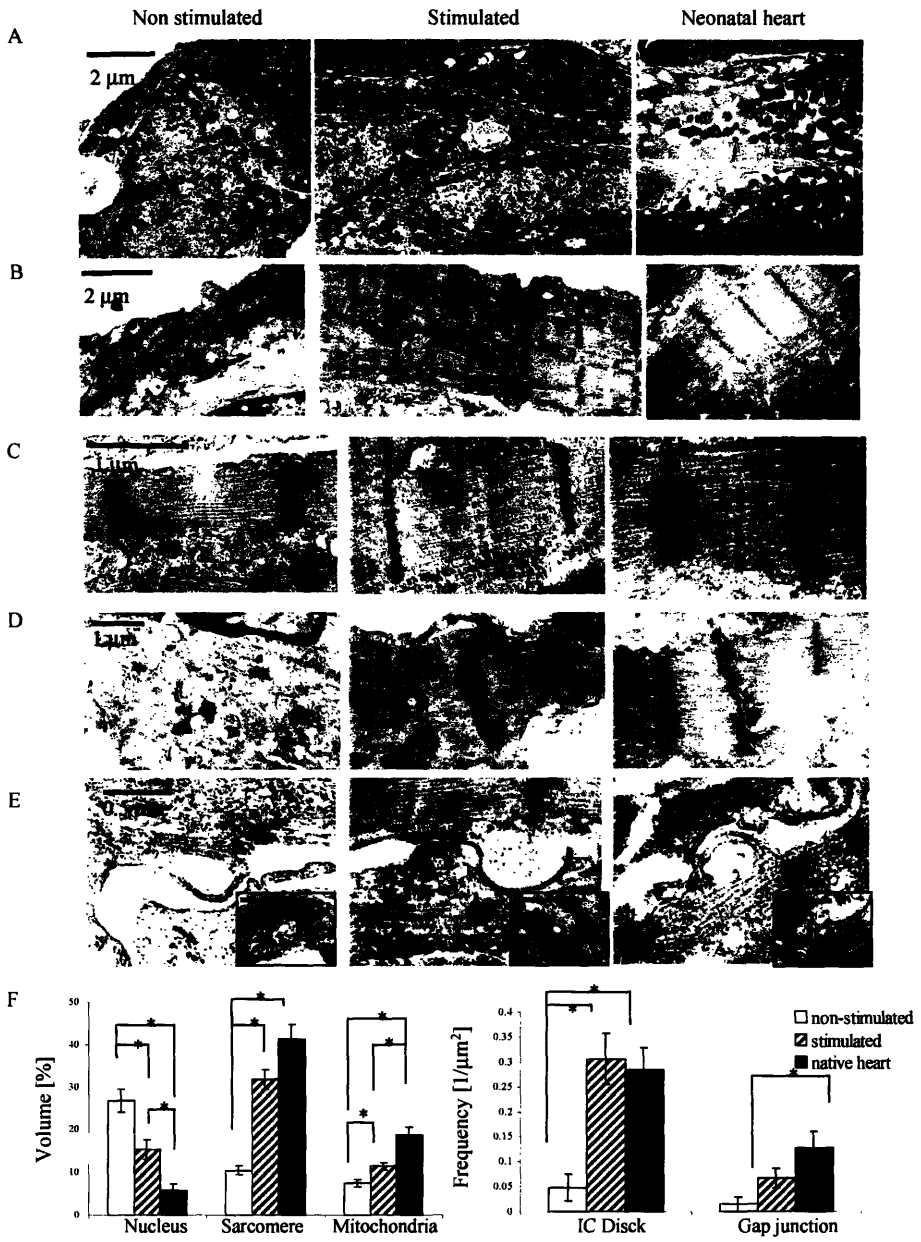

Figure 5.3. Ultrastructural features of stimulated and non-stimulated constructs at the end of cultivation (8-day) as compared to the neonatal rat ventricle A) Overview of cell shape and orientation B) Overview of myofibrils C) Intercalated discs D) Structure of a sarcomere E) Gap Junctions E Inset) T-Tubule F) Morphometric analysis: Volume fractions occupied by nucleus, sarcomeres and mithochondria and Frequency of membrane junctions. Statistical analysis performed by Tukey's test with one way ANOVA (n=18-46). P<0.05 considered significant

DISCUSSION:

Excitation-contraction coupling is crucial for development and function of native myocardium. Tissue culture systems available thus far, failed to induce orderly excitation-contraction coupling during culture. As a result, engineered cardiac constructs did not exhibit fully differentiated phenotype and parallel cell alignment. We hypothesized that electrical field induced contractions of cardiac constructs during in vitro tissue culture will enhance functional assembly and level of differentiation of engineered myocardium.

A commercial cardiac stimulator was used to generate electrical signals in order to induce and maintain synchronous contractions of cultured tissues (square biphasic pulses, 2ms in duration, supra-threshold amplitude of 5V/cm, frequency of 1 Hz). The applied voltage gradient (5V/cm) was selected to be of the same order of magnitude as the endogenous electrical field gradients that naturally occur in animal tissues [36]. The square biphasic pulses 2 ms in duration are characteristic both for the native myocardium and the field stimulation of cardiac monolayers [35, 37]. Thereby, synchronous macroscopic contractions of cultured tissues were induced under controlled *in vitro* conditions by a physiologically relevant mechanism, using electrical signals designed to mimic those generated within the heart.

Constructs were first cultured without electrical stimulation, to allow the cells to recover from isolation during which the cells acquire a round shape and most of the cardiac proteins are lost or disassembled [30]. Electrical stimulation was initiated at 1, 3 or 5 days following cell seeding on scaffolds, and applied continuously for additional five days; non-stimulated, otherwise identical tissue constructs served as controls. The progression of tissue assembly was assessed at various hierarchical levels: molecular (expression levels, amounts and distributions of cardiac proteins), cellular (cell number, viability, metabolism), ultrastructural (morphology of cells and nuclei, development of sarcomeres, distribution and frequency of gap junctions, intercalated discs, mitochondria, and microtubules), and functional (contractile activity, trans-membrane potentials). All construct properties were compared to those measured for neonatal heart ventricles.

Stimulated constructs exhibited superior contractile properties: significantly higher amplitude of contraction and maximum capture rate and lower excitation threshold compared to the unstimulated constructs (**Figure 5.1**). The basis for improved contractile properties was improved tissue morphology (**Figure 5.2**) and ultrastructure (**Figure 5.3**). In stimulated constructs cells expressing cardiac markers were elongated and arranged in parallel compared with the initial (day 3) and non-stimulated constructs which had round scattered cells. In addition the stimulated constructs had remarkably well developed ultrastructure with sarcomeres aligned

in parallel myofibrils, and abundance of mitochondria and glycogen. Non-stimulated constructs had poorly developed, non-oriented sarcomeres and small number of mitochondria (**Figure 5.3**).

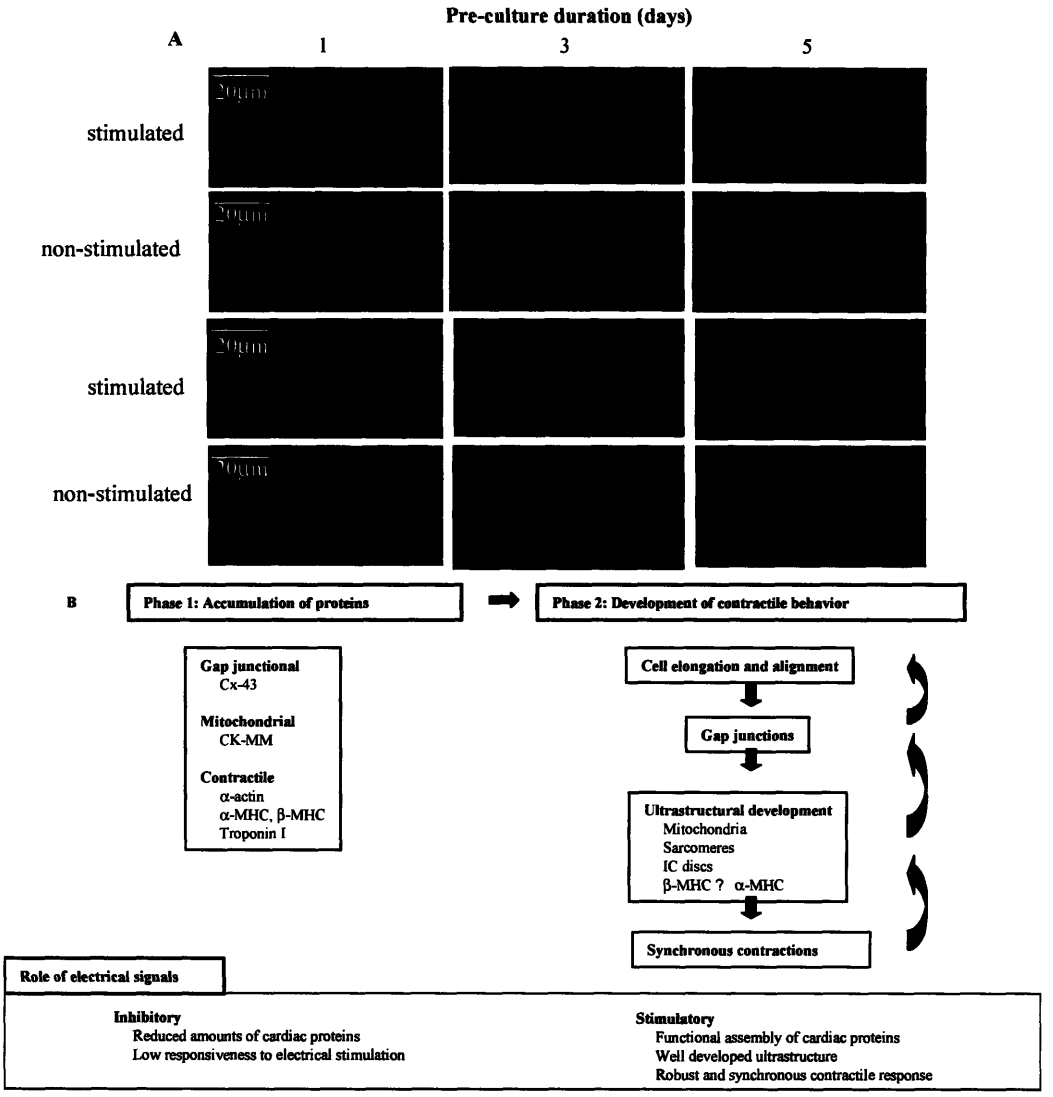

Figure 5.4. Temporal dependence of cell morphology on days of preculture and proposed mechanism on the role of electrical stimulation in functional assembly of engineered myocardium. A) Electrical stimulation of constructs at 5V, 50bpm and 2ms pulse duration was initiated 1,3 or 5 days after seeding, and maintained for additional 5 days. Resulting constructs were stained for connexin-43 (green), α-MHC (red) and nuclei (blue) and compared to the otherwise identical but unstimulated controls. B) Proposed mechanism for the effect of electrical field stimulation on the assembly of functional myocardium

The collected experimental evidence is consistent with a concurrent, interactive and progressive development of the conductive and contractile apparati in electrically stimulated tissue constructs (**Figure 5.4b**). Applied extracellular electric fields resulted in a non-uniform transmembrane potential with hyperpolarization at the anode end, depolarization at the cathode end, and the largest membrane depolarization in the cells aligned in the direction of the field [38, 39]. At Day 3, oval cells aligned in the direction of the field would be the first to generate action potentials and start contracting. As a result of field stimulation, processes form at the cells' ends [40]and lamelopodia extende toward the cathode in the direction of the field [41], causing cell elongation. The extension processes and cell elongation increase the probability that the neighboring cells meet, and establish connections through gap junctions. Although Cx-43 is present in the cells from day 3 (Western blots, **Figure 5.1f**), it is localized in the cytosol of round segregated cells (histology, **Figure 5.2d**) suggesting the absence of functional connexons. Cytoskeletal rearrangement that leads to cell elongation and extension may be similar to that described for electrical stimulation of endothelial cells [42]and mediated through PI3K-Akt pathways.

Once the gap junctions are established, electrical signals propagate through both the extracellular matrix and intracellular space, and lead to the stronger, more synchronous contractions and the formation of aligned myofibrils. The organization of contractile apparatus parallels embryonic development, in which contractile proteins are first laid down within the cells before contractions begin, and then organized into sarcomeres, resulting increased contractile force [43].

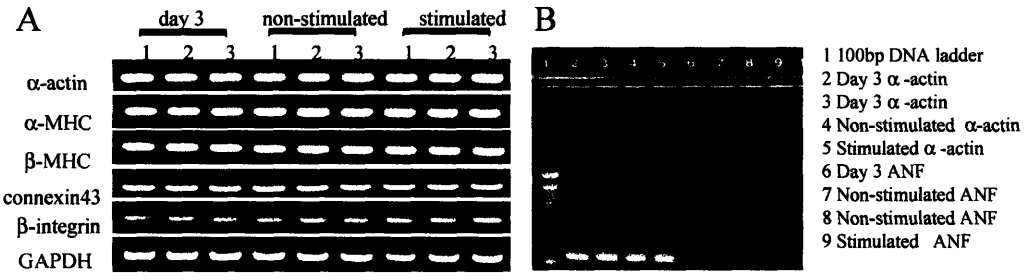

Figure 5.5. Expression of a number of cardiac proteins as assessed by RT-PCR

Induction and sensing of stretch are crucial for the proper development and assembly of sarcomeres. In this study, non-stimulated constructs had thick, diffused Z-lines (**Figure 5.3c**) similar to those found in mice knockout for muscle LIM protein, a key Z-line protein for sensing of stretch and signal propagation [44]. In a previous study, cardiac constructs exposed to cyclic

stretch assembled myofibrils with compact Z-lines [30]. Importantly, induction of contraction by electrical stimulation ensures that calcium handling is unaltered [37] and that the capacity and density of L type Ca^{2+} channels are maintained [35].

The effects of electrical stimulation critically depended on the time of its initiation. During isolation, myocytes disassemble much of their myofilament structure, yielding round cells that are transiently incapable of contracting in response to electrical stimulation. After 3 days, the cells have attached to the matrix and reassembled the machinery for excitation-contraction coupling, as evidenced by occasional spontaneous contractions. The application of field stimulation at this time orchestrates the assembly of myofibrils, cell elongation and establishment of gap junctions. If stimulation is initiated too late (day 5), reassembly of contractile apparatus becomes difficult and cell elongation does not occur, consistent with the finding [45] that the longer the time myocytes were inhibited from contraction by L type channel blockers, the longer it took to reassemble actin cytoskeleton.

Important areas of future work include optimizing the conditions of electrical stimulation (frequency, field gradient, duration of stimulation), quantifying the effect of electrical field stimulation on other cell types present in the native myocardium (endothelial cells, fibroblasts), and testing the biological function and remodeling of the cardiac grafts after short-term and long-term implantation in injured myocardium.

REFERENCES:

1. Association, A.H., *Heart Disease and Stroke Statistics-2004 Update.* 2004.
2. Soonpaa, M.H. and L.J. Field, *Survey of studies examining mammalian cardiomyocyte DNA synthesis.* Circulation Research, 1998. 83(1): p. 15-26.
3. Reinlib, L. and L. Field, *Cell transplantation as future therapy for cardiovascular disease?: A workshop of the National Heart, Lung, and Blood Institute.* Circulation, 2000. 101: p. e182-e187.
4. Koh, G.Y., et al., *Differentiation and long-term survival od C2C12 myoblast grafts in heart.* Journal of Clinical Investigation, 1993. 92(3): p. 1115-1116.
5. Soonpaa, M.H., et al., *Formation of nascent intercalated disks between grafted fetal cardiomyocytes and host myocardium.* Science, 1994. 264: p. 98-101.
6. Li, R.K., et al., *Cardiomyocyte transplantation improved heart function.* Annals of Thoracic Surgery, 1996. 62: p. 654-660.
7. Taylor, D.A., et al., *Regenerating functional myocardium: improved performance after skeletal myoblast transplantation.* Nature Medicine, 1998. 4: p. 929-933.
8. Reinecke, H., et al., *Survival, integration, and differentiation of cardiomyocyte grafts: a study in normal and injured rat hearts.* Circulation, 1999. 100(2): p. 193-202.
9. Sakai, T., et al., *Fetal cell transplantation: a comparison of three cell types.* Journal of Thoracic and Cardiovascular Surgery, 1999. 118(4): p. 715-724.

10. Condorelli, G., et al., *Cardiomyocytes induce endothelial cells to trans-differentiate into cardiac muscle: implications for myocardium regeneration.* Proceedings of the National Academy of Sciences USA, 2001. 98(19): p. 10733-10738.
11. Etzion, S., et al., *Influence of embryonic cardiomyocyte transplantation on the progression of heart failure in a rat model of extensive myocardial infarction.* Journal of Molecular and Cellular Cardiology, 2001. 33(7): p. 1321-1330.
12. Orlic, D., et al., *Bone marrow cells regenerate infarcted myocardium.* Nature, 2001. 410(5): p. 701-705.
13. Menasche, P., et al., *Myoblast transplantation for heart failure.* Lancet, 2001. 357(9252): p. 279-280.
14. Muller-Ehmsen, J., et al., *Rebuilding a damaged heart: long-term survival of transplanted neonatal rat cardiomyocytes after myocardial infarction and effect on cardiac function.* Circulation, 2002. 105(14): p. 1720-1726.
15. Muller-Ehmsen, J., et al., *Survival and development of neonatal rat cardiomyocytes transplanted into adult myocardium.* Journal of Molecular Cellular Cardiology, 2002. 34(2): p. 107-116.
16. Roell, W., et al., *Cellular cardiomyoplasty improves survival after myocardial injury.* Circulation, 2002. 105(20): p. 2435-2441.
17. Akins, R.E., et al., *Cardiac organogenesis in vitro: Reestablishment of three-dimensional tissue architecture by dissociated neonatal rat ventricular cells.* Tissue Engineering, 1999. 5(2): p. 103-118.
18. Bursac, N., et al., *Cardiac muscle tissue engineering: toward an in vitro model for electrophysiological studies.* American Journal of Physiology: Heart and Circulatory Physiology, 1999. 277(46): p. H433-H444.
19. Carrier, R.L., et al., *Cardiac tissue engineering: cell seeding, cultivation parameters and tissue construct characterization.* Biotechnology and Bioengineering, 1999. 64: p. 580-589.
20. Eschenhagen, T., et al., *Three-dimensional reconstitution of embryonic cardiomyocytes in a collagen matrix: a new heart model system.* FASEB Journal, 1997. 11: p. 683-694.
21. Fink, C., et al., *Chronic stretch of engineered heart tissue induces hypertrophy and functional improvement.* FASEB Journal, 2000. 14: p. 669-679.
22. Leor, J., et al., *Bioengineerred cardiac grafts: A new approach to repair the infarcted myocardium?* Circulation, 2000. 102(suppl III): p. III56-III61.
23. Kofidis, T., et al., *In vitro engineering of heart muscle: Artificial myocardial tissue.* Journal of Thoracic and Cardiovascular Surgery, 2002. 124(1): p. 63-69.
24. Li, R.-K., et al., *Survival and function of bioengineered cardiac grafts.* Circulation, 1999. 100(Suppl II): p. II63-II69.
25. Li, R.-K., et al., *Construction of a bioengineered cardiac graft.* Journal of Thoracic and Cardiovascular Surgery, 2000. 119: p. 368-375.
26. Papadaki, M., et al., *Tissue engineering of functional cardiac muscle: molecular, structural and electrophysiological studies.* American Journal of Physiology: Heart and Circulatory Physiology, 2001. 280(Heart Circ. Physiol. 44): p. H168-H178.
27. Radisic, M., et al., *High density seeding of myocyte cells for tissue engineering.* Biotechnology and Bioengineering, 2003. 82(4): p. 403-414.
28. Radisic, M., et al., *Medium perfusion enables engineering of compact and contractile cardiac tissue.* American Journal of Physiology: Heart and Circulatory Physiology, 2004. 286: p. H507-H516.
29. Shimizu, T., et al., *Fabrication of pulsatile cardiac tissue grafts using a novel 3-dimensional cell sheet manipulation technique and temperature- responsive cell culture surfaces.* Circulation Research, 2002. 90(3): p. e40-e48.

30. Zimmermann, W.H., et al., *Tissue engineering of a differentiated cardiac muscle construct.* Circulation Research, 2002. 90(2): p. 223-230.
31. Zimmermann, W.H., et al., *Cardiac grafting of engineered heart tissue in syngenic rats.* Circulation, 2002. 106(12 Suppl 1): p. I151-I157.
32. Severs, N.J., *The cardiac muscle cell.* Bioessays, 2000. 22(2): p. 188-199.
33. Ivester, C.T., et al., *Contraction accelerates myosin heavy chain synthesis rates in adult cardiocytes by an increase in the rate of translational initiation.* Journal of Biological Chemistry, 1995. 270(37): p. 21950-21957.
34. Olivetti, G., P. Anversa, and A.V. Loud, *Morphometric study of early postnatal development in the left and right ventricular myocardium of the rat. II. Tissue composition, capillary growth, and sarcoplasmic alterations.* Circulation Research, 1980. 46(4): p. 503-512.
35. Berger, H.J., et al., *Continual electric field stimulation preserves contractile function of adult ventricular myocytes in primary culture.* American Journal of Physiology-Heart and Circulatory Physiology, 1994. 266(1 Pt 2): p. H341-H349.
36. Nuccitelli, R., *Endogenous ionic currents and DC electric fields in multicellular animal tissues.* Bioelectromagnetics, 1992. Suppl 1: p. 147-157.
37. Holt, E., et al., *Electrical stimulation of adult rat cardiomyocytes in culture improves contractile properties and is associated with altered calcium handling.* Basic Research in Cardiology, 1997. 92(5): p. 289-298.
38. Tung, L., N. Sliz, and M.R. Mulligan, *Influence of electrical axis of stimulation on excitation of cardiac muscle cells.* Circulation Research, 1991. 69(3): p. 722-730.
39. Tung, L. and J.R. Borderies, *Analysis of electric field stimulation of single cardiac muscle cells.* Biophysical Journal, 1992. 63(2): p. 371-386.
40. Kato, S., et al., *Growth effects of electrically stimulated contraction on adult feline cardiocytes in primary culture.* American Journal of Physiology-Heart and Circulatory Physiology, 1995. 268(6 Pt 2): p. H2495-24504.
41. Erickson, C.A. and R. Nuccitelli, *Embryonic fibroblast motility and orientation can be influenced by physiological electric fields.* Journal of Cell Biology, 1984. 98(1): p. 296-307.
42. Zhao, M., et al., *Electrical stimulation directly induces pre-angiogenic responses in vascular endothelial cells by signaling through VEGF receptors.* Journal of Cell Science, 2004. 117(Pt 3): p. 397-405.
43. Siedner, S., et al., *Developmental changes in contractility and sarcomeric proteins from the early embryonic to the adult stage in the mouse heart.* Journal of Physiology, 2003. 548(Pt 2): p. 493-505.
44. Knoll, R., et al., *The cardiac mechanical stretch sensor machinery involves a Z disc complex that is defective in a subset of human dilated cardiomyopathy.* Cell, 2002. 111(7): p. 943-955.
45. Sharp, W.W., et al., *Contractile activity modulates actin synthesis and turnover in cultured neonatal rat heart cells.* Circulation Reserach, 1993. 73(1): p. 172-183.

6. SEQUENTIAL CULTIVATION OF CARDIAC MYOCYTES AND CARDIAC FIBROBLAST SUBPOPULATIONS RESULTS IN ROBUST CONTRACTILE RESPONSE OF ENGINEERED CARDIAC TISSUE

INTRODUCTION:

Native myocardium consists of several cell types of which 1/3 are myocytes and most of the non-myocytes are fibroblasts [1]. Cardiac myocytes are the largest cells in the myocardium, they occupy ~90% of the volume and are responsible for synchronous contractions of the ventricles. The main roles of cardiac fibroblasts are to secrete the components of the extra-cellular matrix (ECM) and transmit mechanical force by the receptor mediated connections to the ECM [2]. The myocardial ECM consists of a fibrillar collagen network, with predominant collagen type I and III, a basement membrane, proteoglycans, glycosaminoglycans and a variety of bioactive molecules [3]. The exact composition of the ECM is regulated by a cross-talk between myocytes and fibroblasts [2]. Recent studies demonstrated that cardiac fibroblasts can propagate electrical stimuli over the distances on the order of 100μm via gap junctional communications [4].

Early attempts to engineer cardiac tissue involved the use of cell suspension enriched for myocytes (80-90%) by pre-plating. [5, 6]. The engineered cardiac constructs exhibited markers of cardiac differentiation and were able to propagate electrical signals over several millimeters. The velocity of signal propagation increased with the fraction of myocytes in the starting cell suspension [7] However, neither the force of contraction nor the amplitude of macroscopic contractile response were investigated. Zimmerman et al. [8]recognized the importance of the presence of multiple cell types in cultivating heart tissue in the presence of phasic stretch. The engineered heart tissue based on a mixed cell population exhibited robust contractile force and positive ionotropic response. Akhyari et al. [9]detected the presence of newly synthesized collagen network in the tissue constructs based on passaged human pediatric heart cells, illustrating the importance of fibroblasts in remodeling scaffolds *in vitro*. However, both studies investigated only one cell composition and the ratio of cardiac myocytes to cardiac fibroblasts was not quantified.

We hypothesized that the co-culture of cardiac fibroblasts and cardiac myocytes will enhance functional assembly of the engineered cardiac constructs by enabling scaffold remodeling and active cross-talk between cells. Cardiac fibroblasts and myocytes were separated by pre-plating and applied to the poly(glycerol sebacate) scaffolds (biorubber) separately, synchronously (unseparated) or serially (fibroblasts pretreatment followed by addition of myocytes). Although, the presence of fibroblasts significantly improved the amplitude of

contraction of the engineered cardiac tissue, the pretreated group exhibited lower excitation threshold and improved construct composition and morphology.

MATERIALS AND METHODS:

Cell isolation:

Cardiomyocytes were obtained from 1 - 2 day old neonatal Sprague Dawley (Charles River) rats according to procedures approved by the Institute's Committee on Animal Care, as previously described [5]In brief, ventricles were quartered, incubated overnight at 4°C in a 0.06 % (w/v) solution of trypsin in Hank's Balanced Salt Solution (HBSS, Gibco), and subjected to a series of digestions (3 min, 37°C, 150 rpm) in 0.1 % (w/v) solution of collagenase type II in HBSS. The cell suspension from the digestions were collected and labeled "unseparated cells". To separate myocytes and fibroblasts the cell suspension was centrifuged (750 rpm, 5 min), and the pellet was resuspended in Dulbecco's Modified Eagle's Medium (DMEM, Gibco) containing 4.5 g/L glucose supplemented with 10% FBS, 10 mM HEPES, 2 mM L-glutamine and 100 units/ml penicillin. The cells from the pellet were pre-plated in T75 flasks for one 75 min period to enrich for cardiomyocytes. Cells that remained unattached were labeled "cardiomyocytes". The attached cells were propagated for 3-7 days in culture, trypsinized as described previously [10]and labeled "fibroblasts".

Construct preparation:

Porous biorubber, poly(glycerol-sebacate), scaffolds were prepared by salt leaching technique. Disc 5mm diameter x 2 mm thick were sterilized by 70% ethanol overnight followed by 4hr in 95% ethanol and 1 hr in 100% ethanol. Ethanol was removed by vacuum filtration and the scaffolds were rinsed in phosphate buffered saline (PBS, Gibco) for 1-4 hr followed by 1hr in FBS. For construct pretreatment with fibroblasts, $1 \cdot 10^6$ fibroblasts were resuspended in 10µl Matrigel® (BD) and applied to the scaffold as described previously [10]The constructs were pretreated in six well plates (1 construct/well) for 5 days in 5 ml of culture medium at 25 rpm. Cell free scaffolds were kept in culture medium in identical conditions.

At the end of pretreatment cell-free scaffolds were seeded with $3 \cdot 10^6$ unseparated cells (US) or $3 \cdot 10^6$ cardiomyocytes (CM) using Matrigel ®. Scaffold pretreated with fibroblasts were seeded with $2 \cdot 10^6$ cardiomyocytes (CF+CM). The constructs were suspended on needles in 150 ml spinner flasks (Bellco) (6 constructs/flask) and cultivated for 6 days in 60 ml of culture medium. Stirring at 30 rpm was initiated after 24 hr in culture. As a control we used constructs at the end of pretreatment (CF0) and fibroblasts constructs at the end of culture in spinner flasks (CF). (**Table 6.1**). Culture medium was exchanged by 100% after 3 days in spinner flask culture.

Table 6.1. Experimental design. All constructs were seeded with the same number of cells ($3 \cdot 10^6$). Myocytes and fibroblasts are added simultaneously (US), separately (CM group and CF group) or serially (CF+CM).

Pretreatment **5 days, six well plates, 25 rpm**	**Culture** **6 days, spinner flasks , 30rpm (group designation)**
$1 \cdot 10^6$ Fibroblast fraction (CF0)	No cells added (CF)
No cells	$3 \cdot 10^6$ unseparated cells (US)
No cells	$3 \cdot 10^6$ cardiomyocyte fraction (CM)
$1 \cdot 10^6$ Fibroblast fraction	$2 \cdot 10^6$ cardiomyocyte fraction (CF+CM)

Assessment:

Cell composition:

The relative ratio of fibroblasts to myocytes in original cell suspensions was assessed by labeling of intracellular markers in conjunction with fluorescence activated cell sorting. (FACS). The cells separated by preplating were fixed and premeabilized with the solution of acetone and methanol (3:2) at –20°C. To identify cardiomyocytes the cell suspension in 5%FBS/PBS (10^6cells/ml) was incubated with mouse anti-troponin I (Clone 23C6, 1:100, Biodesign) or mouse anti-sarcomeric α-actin (clone 5C5, 1:100, Sigma) for 30 min on ice, rinsed and incubated with fluorescein conjugated horse anti-mouse IgG for additional 30 min on ice (1:400, Vector Laboratories). To identify fibroblasts the cells were labeled with Cy 3 conjugated mouse anti-vimentin (clone V9, 1;200, Sigma) for 30 min on ice. The fluorescence was read on FACScan (Becton Dickinson). Unlabeled cells and cells labeled with secondary antibody only served as controls.

Biochemical and metabolic assessment:

Medium samples were taken at the end of pretreatment and after 3 and 6 days in spinner flask culture and analyzed for glucose, lactate using a glucose and L-lactate analyzer Model 2300 STAT plus (Yellow Spring Instrument, [5])and for lactate dehydrogenase levels (LDH) using a commercially available kit (LDH-L, Chiron Diagnostics, Carrier et al. 1999)

Samples for DNA, total protein and Western blot were taken at the end of pretreatment (CF0) and at the end of culture (CF, US, CM CF+CM) weight and frozen in liquid nitrogen. They were homogenized in a buffer (1N NH_4OH , 2% Triton X-100) by Mini-bead beater with 6 cycles 10s cycles at 25 rpm. After centrifugation for 10 minutes at 12,000 *g* at 4°C, the homogenates were stored at -80°C for further analysis.

For DNA assay, the homogenate was incubated at 37°C for 10 min and then diluted with 10 mM Tris-1 mM EDTA buffer containing 100 mM NaCl (1:20). After centrifugation at 2,500g for 30 min, the supernatant to measure DNA content fluorometrically by Hoescht dye binding [5].

Total protein was measured by a commercially available kit (Bio-Rad) as previously described [5, 6].

Contractile response:

The contractile function of engineered cardiac constructs was evaluated by monitoring contractile activity upon electrical stimulation at 200X magnification using a microscope (Nikon Diaphot) at the end of cultivation period as described [11]. Each constructs was placed in a 60 mm Petri dish containing of 120 ml Tyrode's solution (140 mM NaCl, 5.4 mM KCl, 0.33 mM NaH_2PO_4, 1.8 mM $CaCl_2$, 1 mM $MgCl_2$, 5 mM HEPES, 5.5 mM D-glucose, pH 7.4) between two carbon rods (Ladd Research Instruments) connected to a cardiac stimulator (Nihon Kohden). The measurements were done at room temperature. The stimuli (square pulses, 2 ms duration) were applied at a rate of 60 bpm starting at amplitude of 1 V that was gradually increased until the excitation threshold (ET) was reached and the entire construct was observed to beat synchronously. Maximum capture rate (MCR) was determined at 200% of ET by increasing the stimulation frequency until the paced contractions ceased or became irregular. For evaluation of contraction amplitude, video recorded beating sequences (1-5 min) were digitized at the rate of 30 frames/s. The "face-sectional" area of each construct was determined as function of time using image analysis software (Scion Image). Amplitude of contraction was expressed as fractional area change.

Histology and immunohistochemistry

Constructs were sampled at the end of pretreatment and cultivation, rinsed in PBS, and fixed in 10% neutral buffered formalin (Sigma-Aldrich) for 6-12 hrs. Samples were embedded in paraffin, sectioned at 5 μm, and stained with hematoxylin and eosin (H + E) for general evaluation. All samples were face sectioned within the first 100 μm. Staining for cardiac (troponin I, sarcomeric α-actin, connexin-43) and fibroblast markers (vimentin and prolyl-4-hydroxylase) in n=2-6 samples per group was used to assess cell distribution and tissue organization.

For immunofluorescence, sections were depariffinized and antigen was retrieved by heat treatment for 20 minutes at 95°C in decloacking chamber (Biocare Medical), blocked with 10% horse serum (Vector Laboratories) for 40 minutes at RT, then incubated for 1 hour at 37°C with the following primary antibodies diluted in PBS containing 0.5% Tween 20 and 1.5% horse serum: polyclonal rabbit troponin I (Chemicon 1:200), polyclonal rabbit anti-Connexin-43 (Chemicon, 1:50), mouse anti-prolyl-4-hydroxylase β subunit (Clone 6-9H6, Chemicon 1:50), mouse anti sarcomeric α-actin (clone5C5, 1;100, Sigma) and mouse anti-vimentin Cy3

conjugated. (clone V9, Sigma, 1:100). Subsequently, the slides were rinsed in PBS and incubated with the appropriate secondary antibodies (all from Vector Laboratories) for 30 minutes at 37°C: fluorescein conjugated goat anti-rabbit IgG (1:200) for Cx-43 and TnI visualization and fluorescein conjugated horse anti-mouse IgG (1:200) for 30 min at 37oC. The sections were counterstained with DAPI and coverslipped (Vectorshield mounting medium with DAPI). Neonatal rat ventricles and bovine articulate cartilage served as positive control and negative control, respectively. For double staining the slides stained with sarcomeric α-actin were blocked with 10% NHS as described above and incubated with mouse Cy3 conjugated anti-vimentin. Construct architecture and cell distribution were assessed from stained tissue sections using a fluorescent microscope (Axioplan, Zeiss) and Open Lab software. For quantification of relative ratio of fibroblasts to myocytes, 1-4 pictures were taken at 40x from each section (n=2-5 sections per group). The number of red (fibroblasts), green cells (myocytes) and blue nuclei was counted by three independent observers.

Western blots

Construct homogenates were diluted (1;2) in Laemni buffer (Bio-Rad) containing 5% mercaptoethanol and 2% SDS and boiled for 5 minutes to denature proteins. They were separated on 4-20% Tris-glycine minigels (Invitrogen) *using 1x Tris/Glycine/SDS running buffer* at a constant voltage of 100 V for 2 hours at room temperature. Two or three independent constructs from each group were analyzed to compare the expression of the protein bands, and each lane was loaded with the same protein concentration (20 μg). SeeBlue® Plus2 pre-stained standards (Invitrogen) was used as a protein size marker. Eluted proteins were electroblotted in 1x Tris/Glycine/SDS running buffer (Bio-Rad) onto polyvinylidene difluoride membranes (Bio-Rad) at 100 V for 60 minutes at room temperature in a Bio-Rad Trans-Blot cell. Blots were first incubated with 5% nonfat dry milk in 0.1%Tween 20/PBS (PBS-T) at room temperature for 1 hour to block non-specific binding and then, for an additional 1hr at 50 rpm, with the appropriate primary antibody. The primary antibodies were: polyclonal rabbit anti-connexin-43 (Chemicon), diluted 1:40 in PBS-T and polyclonal rabbit anti-troponin I (Chemicon) diluted 1:100 in PBS-T. Blots were washed five times with PBS-T and incubated 1 hour at room temperature with sheep anti-rabbit IgG antibodies (Sigma). After five additional washes, the immunocomplexes were developed using enhanced horseradish peroxidase-luminol chemiluminescence (ECL Western blotting detection reagents, Amersham) and detected after exposure to photographic film (Hyperfilm-ECL) for 5-30 seconds. Band intensity was quantified by an image analysis software (Scion Image).

Statistical analysis of multiple experimental groups was performed using Tukey's test followed by one way ANOVA for pairwise comparisons; $p<0.05$ was considered significant. Normality and equality of variance were tested for all data sets.

RESULTS:

The starting cell populations had different ratios of fibroblasts to myocytes. (**Figure 6.3a**) The unseparated (US) cell suspension obtained by heart digestion had ~30% of myocytes and ~44% of vimentin positive cells, although the difference between the two values was not statistically significant. The fibroblast group, obtained by expanding the cells attached to the tissue culture plastic during pre-plate consisted of significantly more cells (~75%) expressing vimentin and than those (6-18%)expressing cardiac markers (troponin I and α-actin). The suspension that remained unattached after one pre-plate was slightly but not significantly enriched for myocytes with equal fractions of cells expressing cardiac markers. (41-45%) to those expressing vimentin (~40%).

Glucose consumption rate per construct (**Table 6.2**) was comparable in the group seeded with the unseparated cells and cardiomyocyte group and it was higher in the group pretreated with fibroblasts. The values expressed per 10^6 cells (0.24μmol/10^6cells/hr for CF0, 0.09 for US 0.08 for CM and 0.19 for CF+CM group) are on the order of those reported previously [11, 12]. Molar ratio of lactate produced to glucose consumed (**Table 6.2**) was over 2 during the pretreatment in six well plates consistent with the anaerobic cell metabolism and it decreased to 1.6-1.7 during culture in spinner flask, reflecting better oxygen supply to all of the construct surfaces. Regardless, the metabolism was still in the anaerobic range most likely due to the limitations of the oxygen supply to the center of the construct. The levels of LDH increased during cultivation and were significantly higher in the US and CM group compared to the pretreatment group, indicating increased levels of cell damage.

Table 6.2. Metabolic properties of the constructs during pretreatment and culture. Data are averages ± se n= 3-12. *Significantly higher than pretreatment by Dunn's test.

	Lactate produced/glucose Consumed L/g [mol/mol]	Glucose consumption rate g[μmol/cons/day]	Lactate dehydrogenase release LDH [u/cons/day]
Pretreatment	2.43 ± 0.21	0.11 ± 0.01	0.007 ± 0.001
CM	1.67 ± 0.40	0.08 ± 0.02	0.042 ± 0.015*
US	1.62 ± 0.17	0.11 ± 0.03	0.055 ± 0.013*
CF+CM	1.70 ± 0.22	0.18 ± 0.06	0.037 ± 0.012

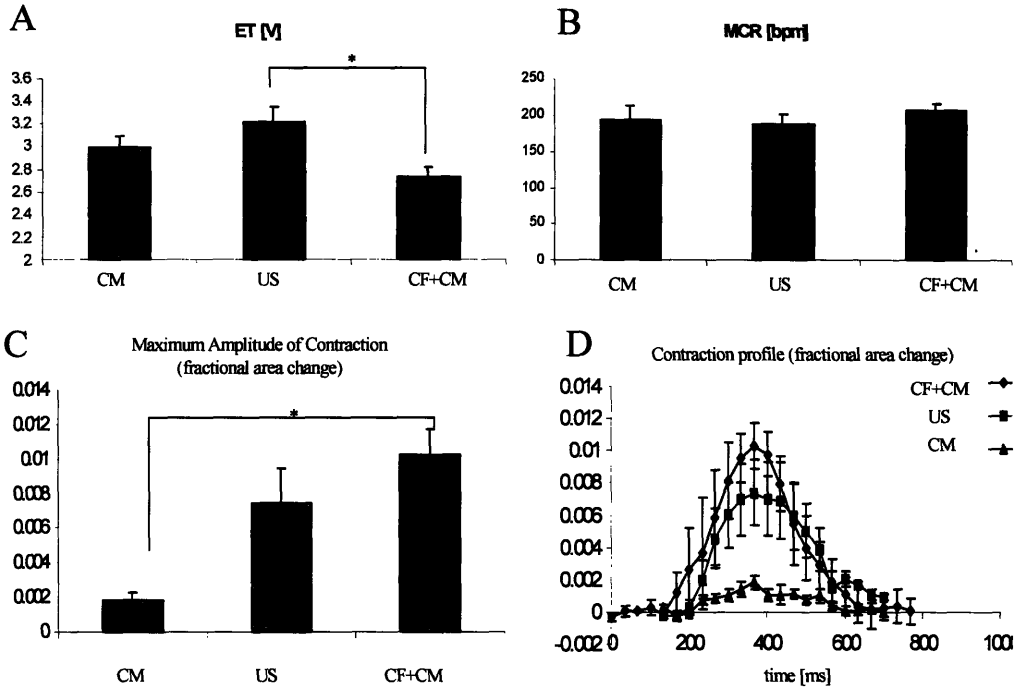

*Figure 6.1. Contractile properties of constructs at the end of cultivation a) Excitation threshold (ET), b) Maximum capture rate (MCR) c) Maximum amplitude of contraction d) Contraction time course. Data are averages± se, n=2-10. *Significantly different by Tukey's test*

We were able to reproducibly induce synchronous contractile response to electrical pacing in groups seeded with myocytes alone (CM), unseparated cells (US) and group pretreated with fibroblasts followed by the addition of myocytes (CF+CM). Constructs that contained mostly fibroblasts, at the end of pretreatment (CF0) and the control group at the end of cultivation (CF) could not be induced to contract synchronously. Occasional contractions of individual fibers were observed at voltages between 5-8V. The group pretreated with fibroblasts followed by addition of myocytes (CF+CM) had the lowest excitation threshold (**Figure 6.1a**) and the highest amplitude of contraction (**Figure 6.1c, d**) compared with the CM and US group. The excitation threshold was significantly higher in the US group compared to the CF+CM group and the amplitude of contraction was significantly lower in the CM group compared to the CF+CM group. Maximum capture rate was comparable in all groups (**Figure 6.1b**).

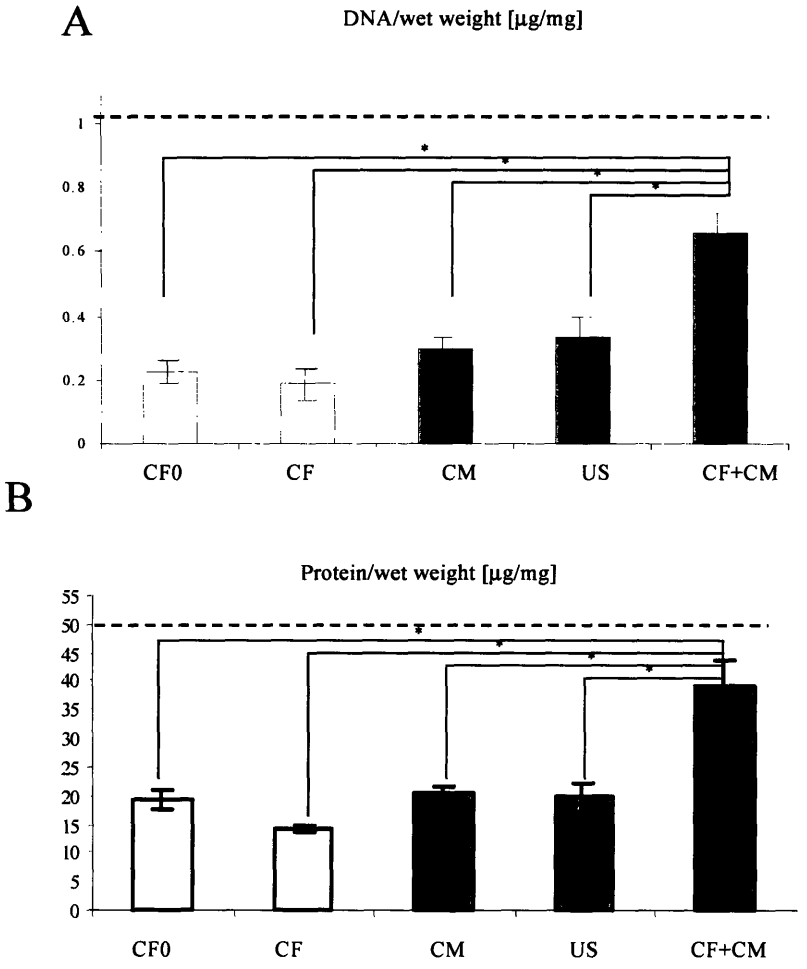

*Figure 6.2 Construct composition. Data are averages ±se n=3 *Significantly different ($p<0.05$) by Tukey's test and one way ANOVA.*

DNA content per wet weight of CF+CM group was significantly higher compared to the all other groups and the two fibroblast controls (CF0, CF, CM, US), and comparable to that measured for native neonatal ventricle by [5]. (**Figure 6.2a**). Total cell number was comparable in the US, CM and CF+CM group (~10^6cells); CF0 and CF group had about ~$0.5 \cdot 10^6$ cells. Construct wet weights were as follows: 26±3 mg for CF0, 28±3 for CF, 39±2 for CM, 43±5 for US and 17±4 for CF+CM. Protein content was ~2 times higher in the CF+CM group that in the other groups (**Figure 6.2b**) and comparable to that measured for the native ventricle [5], while the remaining groups had protein content inferior to that present in the native ventricle.

Assessment of cell fractions from α-actin/vimentin co-stained sections indicated that the ratio of myocytes to fibroblasts was maintained during pretreatment with fractions comparable in the CF0 group to those of the original "fibroblast" cell suspension. (**Figure 6.3b**) The constructs seeded with "unseparated" cell suspension also maintained the ratio fibroblasts to myocytes with approximately equal cell fractions and statistically similar to those of the original cell suspension. The group seeded with myocytes alone (CM) and the group pretreated with fibroblasts followed by the addition of myocytes (CF+CM) had a significantly higher fraction of myocytes compared to the fibroblasts at the end of spinner flask cultivation and the ratio of myocytes to fibroblasts was comparable in these two groups.

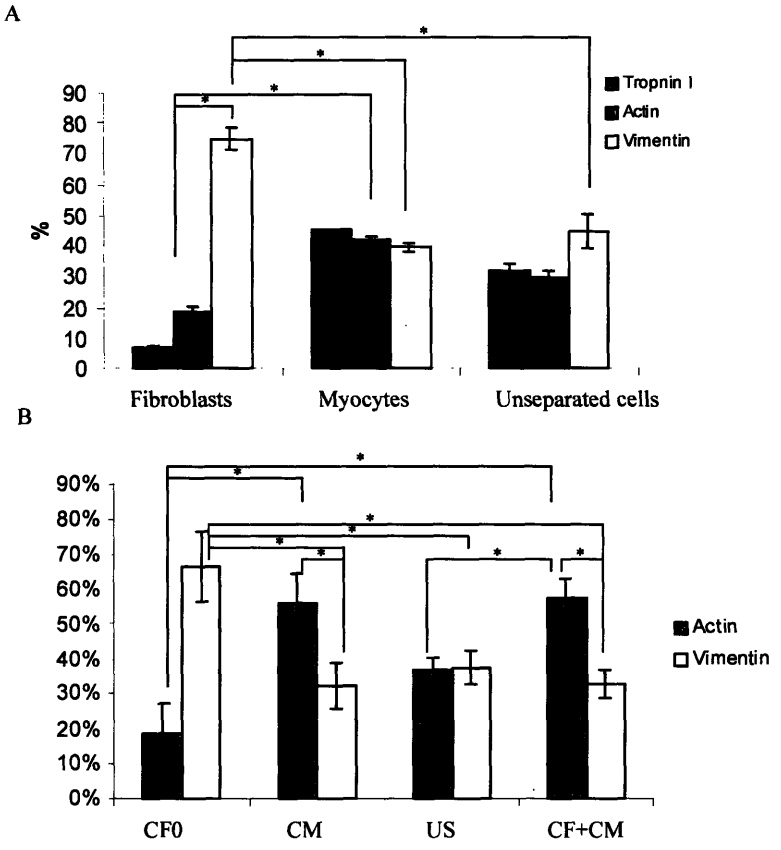

*Figure 6 3. Composition of initial cell suspension and constructs A) Percentages of myocytes and fibroblasts in initial cell populations as determined by FACS B) Percentages of fibroblasts and myocytes in the constructs at the end of pretreatment and culture as determined by morphometry. Data are averages±se n=2-16 *Significantly different ($p<0.05$) as determined by Tukey's test and one-way ANOVA*

After cultivation in spinner flasks, 100-200μm thick layer of tissue was formed at the outer-surfaces of the tissue construct. Constructs based on fibroblasts only showed cell clustering in

clumps or fiber like structure at the surfaces of the constructs. (**Figure 6.4a**) Constructs from the CM, US and CF+CM group had relatively continuous layer of tissue covering the construct.

Co-staining for sarcomeric α-actin/vimentin (**Figure 6.4b**) indicated that the vimentin positive cells (fibroblasts) were present at the outer surfaces of the tissue construct in the contact with culture medium while the sarcomeric α-actin positive cells were located in the interior within the myofiber-like structures. CF+CM group had the largest compact α-actin positive regions. These compact regions of myocytes were present in the CM and US group constructs but they were smaller and scattered around the face section.

Vimentin positive cells (**Figure 6.4c**) were dominant in the group seeded with the "fibroblast" cell suspension forming scar-like tissue. In addition to covering the surface of the tissue construct, they were scattered between the myocytes in the deeper layers of the tissue in the CM, CF+CM and US group. A thick fibrous capsule occasionally formed at the contact between the construct and the stainless steel needle used to suspend the constructs (**Figure 6.4b, CF+CM**).

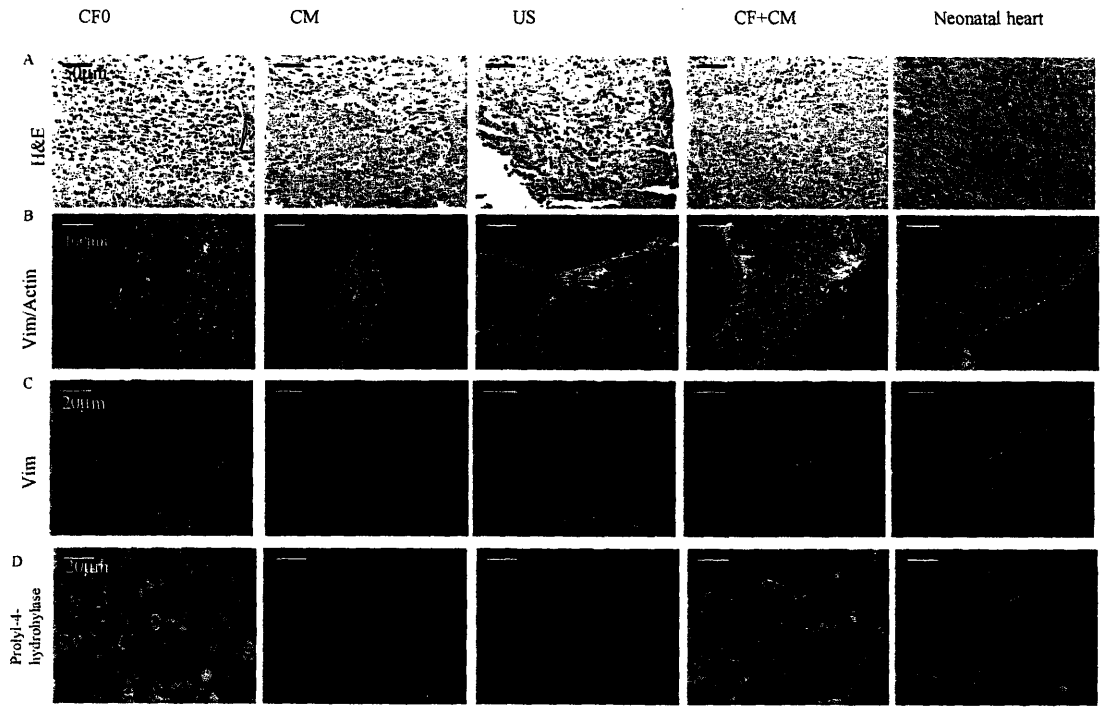

Figure 6.4 Tissue morphology and expression of cardiac and fibroblast markers. Constructs were paraffin embedded and face sectioned within first 100μm. A) Hematoxylin and Eosin staining B) Vimentin and actin double staining to identify fibroblasts and myocytes respectively C) Vimentin staining at higher magnification to identify fibroblast morphology D)Prolyl-4-hydroxylase to identify collagen secreting fibroblasts

Cells expressing cardiac Troponin I (**Figure 6.5a, b**) were present in the constructs based on the "fibroblast" cell suspension but they were sparse and with "star-like" morphology not typical for cardiac myocytes. Troponin I (TnI) positive cells were frequent in the constructs from the CM group, they had elongated morphology but there was no parallel alignment. In the US group cells expressing TnI were elongated and arranged in parallel in short domains interrupted by larger domains not expressing cardiac TnI, whereas in CF+CM group TnI positive cells formed large domains of compact tissue with elongated cells aligned in parallel.

Fibroblasts expressing prolyl-4-hydroxylase (**Figure 6.4d**), an enzyme responsible for collagen deposition, were detectable in all groups except in the constructs from the CM group. The presence was very low in the constructs from the US group, and significant in the constructs based on fibroblasts alone. In the CF+CM group, the cells expressing prolyl-4-hydroxylase were scattered within the compact layer of tissue consisting predominantly of myocytes.

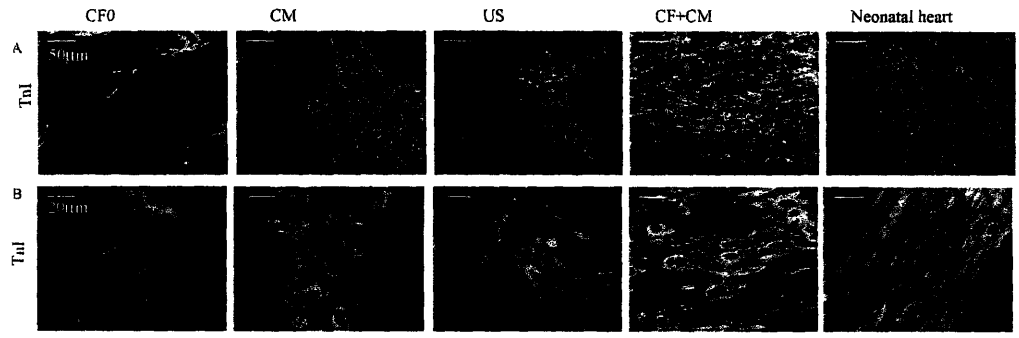

Figure 6.5. Expression of cardiac Troponin I.

Connexin –43, a gap junctional protein, was almost undetectable in the constructs based on fibroblasts (CF0, CF), while it was present in the compact regions of tissue in the CM, US and CF+CM group (**Figure 6.6**). In these regions connexin distribution appeared punctuate, characteristic of the neonatal rat heart.

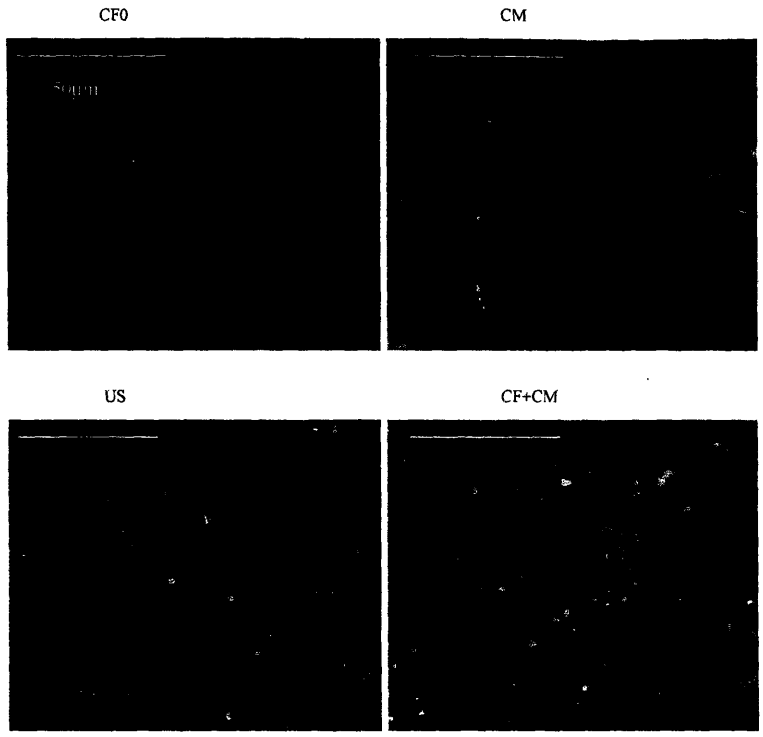

Figure 6.6. Expression of cardiac Connexin-43 .

Western blotting for cardiac markers, connexin-43 and troponin I confirmed the presence of these proteins in the original cell suspension based on unseparated cells and the cardiomyocyte enriched fraction (**Figure 6.7a, b**). In the starting cell suspension, the relative amount was significantly higher in the cardiomyocyte fraction and unseparated fraction compared to the fibroblasts fraction (**Figure 6.7c**), consistent with the composition determined by FACS (**Figure 6.3a**). Constructs from US, CM and CF+CM group had higher relative band intensities for Troponin I compared to the CF0 and CF group (**Figure 6.7c**). The amount of Connexin-43 was consistently low in all initial cell populations, and progressively increased with time in culture reaching maximum values in CM and CF+CM group (**Figure 6. 7c**).

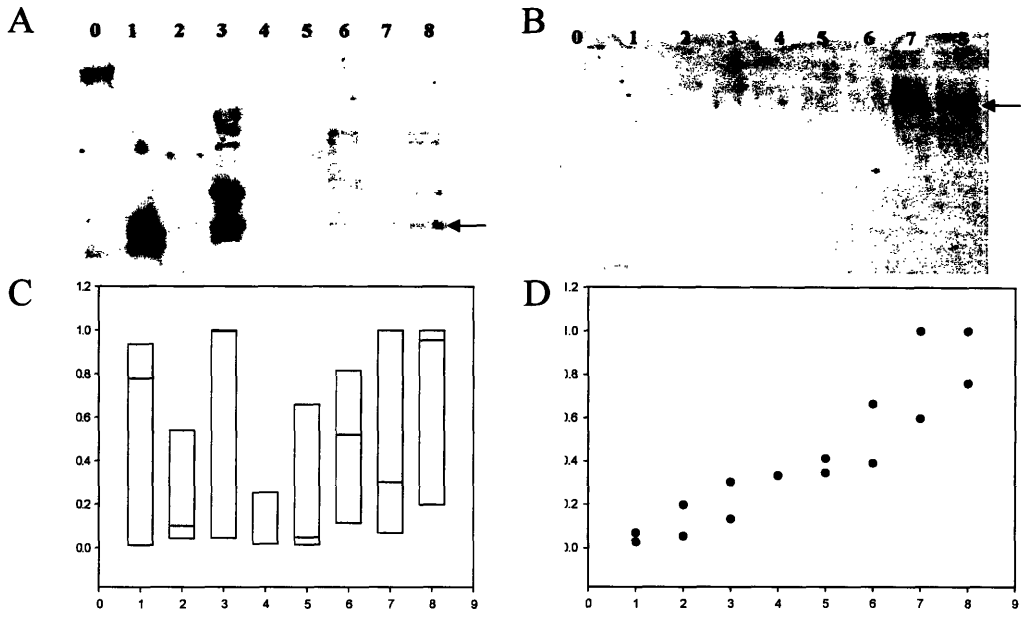

Figure 6.7 Cardiac specific proteins. Western blots for cardiac troponin I (A) and connexin-43 (B) in freshly isolated cells and constructs. Arrows indicate bands of interest. Plots of relative band intensities for troponin I (C Box Plot, median 25th and 75th percentile, n=3), and connexin-43 (D, n=2). The strongest band is assigned value of 1.0-marker lane, 1-unseparated cells, 2-fibroblast fraction, 3-cardiomyocyte fraction, 4-CF0 construct, 5-CF6 construct, 6-CM construct, 7-US construct,
8-CF+CM construct.

DISCUSSION:

Cardiac fibroblasts contribute to a considerable proportion of cells present in the native myocardium [1] The main role of fibroblasts is to secrete the components of the ECM and transmit mechanical force [2]. In monolayer cultures of heart cells, fibroblasts are usually removed before plating in order to prevent the overgrowth during culture. By analogy, in early tissue engineering approaches, fibroblasts were routinely removed before culture and the scaffolds were seeded with enriched suspensions of myocytes (80-90%) [6]. The engineered cardiac tissue should ideally reproduce structure and function of the native myocardium and presence of multiple cell types is one of the hallmarks of the native tissue.

We hypothesized that the co-culture of cardiac fibroblasts and cardiac myocytes will enhance functional assembly of the engineered cardiac constructs by enabling scaffold remodeling and active cross-talk between cells. The cells isolated form the neonatal rat hearts were used as unseparated cell suspension, or separated in predominantly myocyte and predominantly fibroblast (**Figure 6.3a**) fraction by preplating. In our experimental design,

unseparated cell suspension was applied to the biorubber scaffolds (US), myocyte fraction alone was applied (CM) or myocytes were applied following the pretreatment of the scaffold with fibroblasts (CF+CM).

As expected, the groups that had higher numbers of fibroblasts added to the scaffold (US, CF+CM) had more robust contractile response, with the highest amplitude of contraction observed in the CF+CM group (**Figure 6.1c,d**). Maximum capture rate was comparable in all of the groups (**Figure 6.1b**), but it was lower than the values reported for the similar constructs previously [11] most likely due to the slightly lower duration of culture and the fact that these measurements were taken at the room temperature. Consistent with the previous reports, US group had higher excitation threshold than the CM group (**Figure 6.1a**) but unexpectedly, the CF+CM group had statistically the lowest excitation threshold.

The superior contractile properties in the CF+CM group had the biochemical and morphological basis. The DNA content of CF+CM group was significantly higher (**Figure 6.2a**) compared to the other groups and comparable to that of the native heart, most likely contributing to the decrease in the excitation threshold. Higher cellularity was correlated to the lower excitation threshold in a previous study [11]. Consistent with the lower excitation threshold is the high amount of the connexin-43 identified in Western blots for CM and CF+CM group (**Figure 6.7d**). The release of LDH as a measure of cell damage was the highest in the US group (**Table 6.2**), which was consistent with the low cellularity and high excitation threshold observed in this group.

The protein content (**Figure 6.2b**) and metabolic activity (**Table 6.1**) was almost two times as high in the CF+CM group compared to the other groups, most likely enabling the cells to develop active force necessary for the high amplitude of construct contraction. Glucose consumption rate as a measure of metabolic activity correlated well with the amplitude of contraction with lowest values measured for CM group and the highest measured for CM+CF group.

The amplitude of contraction correlated well with the orientation of the myocytes on the construct surfaces. In the CF+CM group the cells expressing cardiac markers (**Figure 6.4b, Figure 6.5a,b**), troponin I and sarcomeric α-actin were aligned in parallel in compact regions resembling the myofibers in the native myocardium, allowing for a synchronous and vigorous contractile response. In the US group, parallel alignment of the myocytes was observed in some regions while myocytes in the CM group lacked a specific orientation, yielding low amplitude of contraction.

The overwhelming difference between the CF+CM group and the CM group was that CM group contained almost no cells expressing prolyl-4-hydroxylase (**Figure 6.4g**), indicting that the fibroblasts present in the CM constructs were not involved in the deposition of collagen as a component of the extracellular matrix. In the US group prolyl-4-hydroxylase cells were present at low quantities, while the CF+CM group had a considerable fraction of prolyl-4-hyrdoxylase cells scattered among the myocytes. In all groups vimentin positive cells were lining the interface between the construct and culture medium (**Figure 6.4b**) thereby protecting the myocytes from the turbulent environment present in the spinner flask. However, in the CF+CM group the fibroblasts in the tissue interior were actively involved in scaffold remodeling and deposition of ECM components.

The initial ratio of fibroblasts to myocytes (F/M) in the CM group was 0.9 (**Figure 6.3a**) and it decreased to 0.6 after 6 days in culture (**Figure 6.3b**). In the US group the F/M was 1.5 and decreased to 1.0, while the CF+CM group had initial ratio of 1.2 (**Figure 6.3a,b**) that decreased to 0.6. The data indicate that in all constructs fibroblasts were preferentially lost compared to the myocytes, perhaps due to the involvement in scaffold remodeling. Although the ratio of fibroblasts to myocytes was the same at the end of cultivation in the CF+CM and CM group, the improved contractile properties in the CF+CM group can be attributed to the improved morphology.

The presented data suggest that the presence of fibroblasts as well as the extracellular components secreted by the fibroblasts significantly improve the properties of the engineered heart tissue. When seeded at lower density during pretreatment, cardiac fibroblasts have enough time to recover from the isolation procedure and start remodeling the polymeric scaffold by secreting components of extracellular matrix and soluble factors. When myocytes are added to a scaffold conditioned in such manner they encounter environment similar to that of the native ventricle from which they have been isolated and supportive of the tissue assembly. It appears, that when the myocytes and fibroblasts are seeded at the high density simultaneously (US) they do not receive appropriate cues to engage in the scaffold remodeling and tissue assembly perhaps due to the competition for oxygen. Constructs obtained from the myocyte enriched group (CM) have even less chance of remodeling the scaffold due the lower number of fibroblasts present, and although they maintain DNA levels they fail to accumulate protein as would be expected during maturation *in vivo*.

In conclusion, this study demonstrates that preconditioning of polymeric scaffolds with fibroblasts creates an environment supportive of the assembly of heart tissue and improves the contractile properties of engineered constructs.

REFERENCES:

1. Nag, A.C., *Study of non-muscle cells of the adult mammalian heart: a fine structural analysis and distribution.* Cytobios, 1980. **28**(109): p. 41-61.
2. Sussman, M.A., A. McCulloch, and T.K. Borg, *Dance band on the Titanic: biomechanical signaling in cardiac hypertrophy.* Circulation Research, 2002. **91**(10): p. 888-898.
3. Burlew, B.S. and K.T. Weber, *Cardiac fibrosis as a cause of diastolic dysfunction.* Herz, 2002. **27**(2): p. 92-98.
4. Gaudesius, G., et al., *Coupling of cardiac electrical activity over extended distances by fibroblasts of cardiac origin.* Circulation Research, 2003. **93**(5): p. 421-428.
5. Carrier, R.L., et al., *Cardiac tissue engineering: cell seeding, cultivation parameters and tissue construct characterization.* Biotechnology and Bioengineering, 1999. **64**: p. 580-589.
6. Bursac, N., et al., *Cardiac muscle tissue engineering: toward an in vitro model for electrophysiological studies.* American Journal of Physiology: Heart and Circulatory Physiology, 1999. **277**(46): p. H433-H444.
7. Papadaki, M., et al., *Tissue engineering of functional cardiac muscle: molecular, structural and electrophysiological studies.* American Journal of Physiology: Heart and Circulatory Physiology, 2001. **280**(Heart Circ. Physiol. 44): p. H168-H178.
8. Zimmermann, W.H., et al., *Tissue engineering of a differentiated cardiac muscle construct.* Circulation Research, 2002. **90**(2): p. 223-230.
9. Akhyari, P., et al., *Mechanical stretch regimen enhances the formation of bioengineered autologous cardiac muscle grafts.* Circulation, 2002. **106**(12 Suppl 1): p. I137-I142.
10. Radisic, M., et al., *High density seeding of myocyte cells for tissue engineering.* Biotechnology and Bioengineering, 2003. **82**(4): p. 403-414.
11. Radisic, M., et al., *Medium perfusion enables engineering of compact and contractile cardiac tissue.* American Journal of Physiology: Heart and Circulatory Physiology, 2004. **286**: p. H507-H516.
12. Casey, T.M. and P.G. Arthur, *Hibernation in noncontracting mammalian cardiomyocytes.* Circulation, 2000. **102**(25): p. 3124-3129.

7. BIOMIMETIC APPROACH TO CARDIAC TISSUE ENGINEERING: OXYGEN CARRIERS AND CHANNELED SCAFFOLDS

INTRODUCTION

In vascularized tissues, such as myocardium, oxygen is supplied by convection of blood through a capillary network and diffusion into the tissue space surrounding each capillary. At physiological conditions, oxygen dissolved in blood plasma accounts for ~1.5% of total oxygen content of the blood [1, pg. 90]. Majority of oxygen carrying capacity of the blood comes from hemoglobin, a natural oxygen carrier that ensures that sufficient oxygen is supplied to the tissue in a single pass of blood though a capillary network at low flow rates (Re=1).

In current cardiac tissue engineering approaches, tissue constructs were cultivated immersed in culture medium in dishes [2], bioreactors [3-5], and in some cases in the presence of mechanical stretch [6-8]. In all cases, oxygen transport through the tissue was largely governed by molecular diffusion, which can support only a thin (100 – 200 μm) surface layer of functional tissue, and leaves construct interior hypoxic and acellular.

Cell distribution was markedly improved by seeding and cultivation in perfused cartridges, due to the efficient supply of oxygen to cells throughout the constructs [9-11]. However, the convective component of oxygen supply was provided by medium flow through the tissue compartment. In a recent study [12] perfusion of culture medium through a single syngeneic aorta embedded in the center of tissue engineered construct significantly improved metabolic activity and viability of cardiac cells. Although, the compartment for medium flow was separated in this case, the vessel diameter was too high to mimic the capillary network present in native myocardium.

Our objective was to provide *in vivo*-like oxygen supply to the cells within engineered cardiac constructs, and thereby enhance functional cell assembly (**Table 7.1**). To mimic the capillary network, cells were cultured on an elastic, highly porous scaffold with a parallel array of channels. To mimic oxygen supply by hemoglobin, the channel array was perfused with culture medium supplemented with synthetic oxygen carriers (Oxygent^{TM}). Oxygent^{TM} is a is a 32%v/v phospholipid stabilized emulsion of perfluorooctyl bromide as a principal component and a small percentage of perfluorodecyl bromide [13]. Constructs perfused with unsupplemented culture medium served as controls. Since they are immiscible with the aqueous phase of culture medium perfluorocarbon (PFC) particles serve as rechargeable oxygen reservoirs. As oxygen is depleted from the aqueous phase of culture medium it is replenished by diffusion from PFC particles. Overall, the oxygen partial pressures measured in the aqueous phase of unsupplemented and PFC-

supplemented culture medium are the same. The PFC particles replenish oxygen consumed by the cells without increasing oxygen concentration in culture medium. As a result, the total oxygen content of the PFC supplemented medium is higher, supporting higher cell density per single pass through the channel array.

Table 7.1. Biomimetic approach to cardiac tissue engineering: main factors of the in vivo myocardial environment and their *in vitro* counter parts.

	In vivo	IN VITRO
Cells	High density (~10^8cells/cm^3) Multiple cell types (myocytes, fibroblasts, endothelial cell)	High density (~$0.3 \cdot 10^8$cells/cm^3) Multiple cell types (myocytes, fibroblasts)
Geometry	Capillary network (~7μm diameter, ~30μm spacing)	Parallel channel array (335 μm diameter, 364μm spacing)
Mass transport modes	Convection: Blood flow ~500μm/s Diffusion in tissue space	Convection: Medium flow ~500μm/s Diffusion in construct space
Oxygen carriers	Hemoglobin (arterial blood) O_2 dissolved in plasma 130μM O_2 as oxyhemoglobin 8500μM O_2 total 8630μM	5.4% PFC emulsion (at 160mmHg and 37°C) O_2 dissolved in aqueous phase 220μM O_2 in PFC particles 230μM O_2 total 450μM

MATERIALS AND METHODS:

Cell isolation: Cardiomyocytes were obtained from 1 - 2 day old neonatal Sprague Dawley (Charles River) rats according to procedures approved by the Institute's Committee on Animal Care, as previously described [4]. In brief, ventricles were quartered, incubated overnight at 4°C in a 0.06 % (w/v) solution of trypsin in Hank's Balanced Salt Solution (HBSS, Gibcco), and subjected to a series of digestions (3 min, 37°C, 150 rpm) in 0.1 % (w/v) solution of collagenase type II in HBSS. The cell suspension from the digestions was collected. To separate myocytes and fibroblasts the cell suspension was centrifuged (750 rpm, 5 min), and the pellet was resuspended in Dulbecco's Modified Eagle's Medium (DMEM, Gibco) containing 4.5 g/L glucose supplemented with 10% FBS, 10 mM HEPES, 2 mM L-glutamine and 100 units/ml penicillin. The cells from the pellet were pre-plated in T75 flasks for one 75 min period to enrich for cardiomyocytes. Cells that remained unattached were labeled "cardiomyocytes". The attached cells were propagated for 3-7 days in culture, trypsinized as described previously [10] and labeled "fibroblasts".

Scaffold: Porous poly(glycerol-sebacate) scaffolds were by salt leaching technique. Briefly, PGS solution in tetrahydrofuran was poured into a Teflon mold filled with NaCl particles of desired sizes. The mold was transferred to a vacuum oven and cured at 120 °C and 100 mTorr. The resulted material was soaked in deionized water to remove the NaCl particles. Scaffolds with porosity up to 91% can be obtained after removal of water An array of cubically packed parallel channels was bored on 120Watt CO_2 laser cutting/engraving system. Discs 5-6mm diameter x 2 mm thick were sterilized by 70% ethanol overnight followed by 4hr in 95% ethanol and 1 hr in 100% ethanol. Ethanol was removed by vacuum filtration and the scaffolds were rinsed in phosphate buffered saline (PBS, Gibco) for 1-4 hr followed by 1hr in FBS. Channel diameter and spacing was determined from the light micrographs using image analysis software (Scion Image).

Construct preparation and culture: For scaffold preconditioning with fibroblasts, 0.5-$1 \cdot 10^6$ fibroblasts were resuspended in 10µl Matrigel® (BD) and applied to the scaffold as described previously [10]. The constructs were pretreated in six well plates (1 construct/well) for 4 days in 5 ml of culture medium at 25 rpm. At the end of preconditioing, $2.3 \cdot 10^6$ cardiomyocytes in 15 µl of Matrigel® was added to the construct as described (Chapter 6) and allowed to gel for 30 min at 37oC. The constructs were cultivated for additional 3 days in the perfusion loops as described previously. [10, 11]. Briefly, the constructs were tightly fitted inside the 5 mm ID, 10 mm OD silicone tubing rings, placed between two stainless steel screens and positioned into 1.5 ml polycarbonate perfusion cartridges (kindly donated by the Advanced Tissue Sciences, La Jolla, CA; one scaffold per cartridge). The screens (85% open area) provided mechanical support during perfusion and the silicone ring routed the culture medium through the central area of the construct. Constructs were subjected to unidirectional medium flow at 0.1 mL/min provided by the IsmaTec multichannel peristaltic pump (**Figure 7.1A**). Total volume of culture medium in the gas exchanger tubing, medium bag and cartridge was 30 ml. To investigate the effect of presence of oxygen carriers, 3 ml of Oxygent™ was added to the 27 ml of culture medium, kindly donated by the Alliance Pharmaceuticals Corps, San Diego CA. Unsupplemented culture medium served as a control. A total of 7 rat litters was used in 7 independent experiments with n = 4 - 6 constructs per experiment.

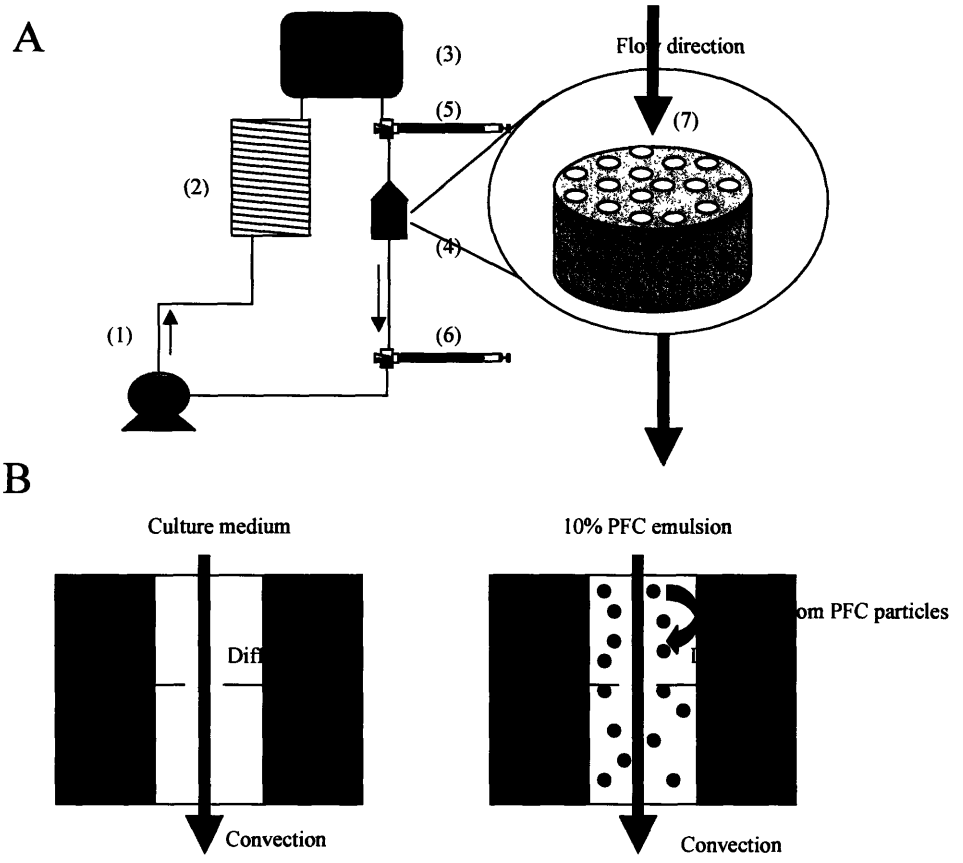

Figure 7.1.Schematics of the model system. ***(A) Perfusion loop.*** *Channeled biorubber scaffolds (7) preconditioned with cardiac fibroblasts were seeded with cardiac myocytes and placed into perfusion cartridges (4) between two debubbling syringes (5,6). Medium flow (0.1 ml/min) was provided by a multi-channel peristaltic pump (1) and gas exchange was provided by a coil of thin silicone tubing (3m long) (2). Loops were placed in the 37oC/5%CO_2 incubator vertically, so that the reservoir bag (3) also served as a bubble trap.* ***(B) Main modes of oxygen transport*** *in the channeled construct perfused with culture medium include convection through the channel lumen and diffusion into the construct space surrounding each channel. Medium supplemented by 10%PFC emulsion is replenished by the release of oxygen from the PFC particles into the culture medium phase which is governed by Henry's law.*

Measurement of PFC concentration: Since perfusion loops were placed vertically during culture so that the medium reservoir bag acts as a bubble trap there was a some precipitation of the heavier PFC emulsion in the lower part of the loop (perfusion cartridge and gas exchanger). To determine the exact concentration of circulating PFC, lower part of the loop was sectioned off at the end of cultivation, the medium was collected and the concentration of emulsion was determined spectrophotometrically. For standard curve, PFC emulsion (Oxygent^{TM})

was diluted at known concentrations in culture medium. The resulting standard emulsions were further diluted in phosphate buffer saline (1:10), and the absorbance was read at 970 nm (wavelength corresponding to the maximum absorbance as determined from wavelength scans).

Biochemical and metabolical assessments: Medium samples were taken at the end of pretreatment and cultivation and analyzed for glucose, lactate using a glucose and L-lactate analyzer Model 2300 STAT plus (Yellow Spring Instrument, [4]) and for lactate dehydrogenase levels (LDH) using a commercially available kit (LDH-L, Chiron Diagnostics, [4]). Gas composition and pH at the inlet to perfusion cartridge was measured from medium samples using a gas blood analyzer (Model 1610, Lexington, MA). Oxygen concentration at the outlet of the perfusion cartridges was measured by inline ruthenium based oxygen sensors, kindly donated by Payload Systems, Inc.

Samples for DNA, total protein and Western blot were taken at the end culture, weighted and frozen in liquid nitrogen. They were homogenized in an extraction buffer (1N NH_4OH , 2% Triton X-100) by Mini-bead beater (Biospec, Bartlesville, OK) with 6 cycles 10s duration at 25 rpm. After centrifugation for 10 minutes at 12,000 *g* at 4°C, the homogenates were stored at -80°C for further analysis. For DNA assay, the homogenate was incubated at 37°C for 10 min and then diluted with 10 mM Tris-1 mM EDTA buffer containing 100 mM NaCl (1:20). After centrifugation at 2,500g for 30 min, the supernatant to measure DNA content fluorometrically by Hoescht dye binding [4]. Total protein was measured by a commercially available kit (Bio-Rad) as previously described [3, 4].

Contractile response: The contractile function of engineered cardiac constructs was evaluated by monitoring contractile activity upon electrical stimulation at 200X magnification using a microscope (Nikon Diaphot) at the end of cultivation period. Each constructs was placed in a 60 mm Petri dish containing of 120 ml Tyrode's solution (140 mM NaCl, 5.4 mM KCl, 0.33 mM NaH_2PO_4, 1.8 mM $CaCl_2$, 1 mM $MgCl_2$, 5 mM HEPES, 5.5 mM D-glucose, pH 7.4) between two carbon rods (Ladd Research Instruments) connected to a cardiac stimulator (Nihon Kohden). The measurements were done at room temperature. The stimuli (square pulses, 2 ms duration) were applied at a rate of 60 bpm starting at amplitude of 1 V that was gradually increased until the excitation threshold (ET) was reached and the entire construct was observed to beat synchronously. Maximum capture rate (MCR) was determined at 200% of ET by increasing the stimulation frequency until the paced contractions ceased or became irregular.

Scanning electron microscopy: At the end of cultivation samples were fixed in formalin overnight, rinsed in PBS and assessed for cell distribution and morphology using an environmental scanning electron microscope (Philips/FEI XL30 FEG-SEM).

*Western blots:*Construct homogenates were diluted (1:2) in Laemni buffer (Bio-Rad) containing 5% mercaptoethanol and 2% SDS and boiled for 5 minutes to denature proteins. They were separated on 4-20% Tris-glycine gel (Invitrogen) using 1x Tris/Glycine/SDS running buffer (Bio-Rad) at a constant voltage of 100 V for 2 hours at room temperature. Four independent constructs from each group were analyzed to compare the expression of proteins and each lane was loaded with the same total protein concentration (20 μg). SeeBlue® Plus2 pre-stained standards (Invitrogen) was as a protein size marker. The gel was electroblotted in 1x Tris/Glycine/Methanol blotting buffer (Bio-Rad) onto polyvinylidene difluoride membranes (Bio-Rad) at 100 V for 1 hour at room temperature in a Trans-Blot cell (Bio-Rad). Blots were first incubated with 5% nonfat dry milk in 0.1% Tween 20/PBS (PBS-T) at room temperature for 1 hour to block non-specific binding and then, for an additional 1 hour at 50 rpm, with the appropriate primary antibody. The primary antibodies were: (1) polyclonal rabbit anti-Connexin-43 (Chemicon), diluted 1:40 in PBS-T and (2) polyclonal rabbit anti-troponin I (Chemicon), diluted 1:100 in PBS-T. Blots were washed five times with PBS-T and incubated 1 hour at room temperature with sheep anti-rabbit IgG antibodies (Sigma). After five additional washes, the blot was developed using enhanced horseradish peroxidase-luminol chemiluminescence (ECL Western blotting detection reagents, Amersham) and the immunocomplexes were detected after exposure to photographic film (Hyperfilm-ECL, Amersham) for 5-30 seconds. Band intensity was quantified by an image analysis software (Scion Image).

Histology and Immunohistochemistry: Constructs were sampled at the end of pretreatment and cultivation, rinsed in PBS, and fixed in 10% neutral buffered formalin (Sigma-Aldrich). Samples were embedded in paraffin, sectioned at 5 μm, and cross-sectioned or faced sectioned and stained with hematoxylin and eosin (H + E) for general evaluation. Staining for cardiac (troponin I, connexin-43) and fibroblast markers (vimentin) used to assess cell distribution and tissue organization.

For immunofluorescence, sections were depariffinized and antigen was retrieved by heat treatment for 20 minutes at 95°C in deckloacking chamber (Biocare Medical), blocked with 10% horse serum (Vector Laboratories) for 40 minutes at RT, then incubated for 1 hour at 37°C with polyclonal rabbit anti-Connexin-43 (Chemicon, 1:40), or with a mixture of polyclonal rabbit troponin I (Chemicon 1:200) and mouse anti-vimentin Cy3 conjugated. (clone V9, Sigma, 1:100) for double staining. All antibodies were diluted in PBS containing 0.5% Tween 20 and 1.5%

horse serum. For Connexin-43 and Troponin-I visualization, the slides were rinsed in PBS and incubated with fluorescein conjugated goat anti-rabbit IgG (1:200) for 30min at 37°C. The sections were counterstained with DAPI and coverslipped (Vectorshield mounting medium with DAPI). Neonatal rat ventricles and bovine articulate cartilage served as positive control and negative control, respectively. Construct architecture and cell distribution were assessed from stained tissue sections using a fluorescent microscope (Axioplan, Zeiss) and Open Lab software.

Statistical analysis was done using SigmaStat 3.0 (SPSS). All data sets were tested for normality and equality of variance. Statistically significant differences were determined by Students t-test or by Rank sum test. $P<0.05$ was considered significant.

RESULTS

Precipitation of heavy PFC particles in the lower portions of the perfusion loop resulted in the effective volume fraction of the circulating PFC emulsion of $5.4 \pm 0.3\%$. Oxygen partial pressure in culture medium in the PFC group was lower than in the culture medium group (**Table 7.2**). There were no significant differences in levels of pCO_2 and pH and in the glucose metabolism between the groups supplemented with PFC emulsion and perfused with pure culture medium (**Table 7.2**). The release of lactate dehydrogenase (LDH), a measure of cell damage, was significantly lower in the group perfused with PFC emulsion as compared to the group perfused with culture medium alone, indicating less cell death in the PFC group.

After 3 days of culture, constructs from both groups were able to respond by synchronous contractions to the electrical field stimulation provided by a cardiac stimulator. Excitation threshold was significantly lower (**Figure 7.2A**), the maximum capture rate was slightly but not significantly lower in the PFC group as compared to the group cultivated with culture medium alone (**Figure 7.2B**).

Table 7.2. Medium gas composition and metabolic properties of cardiac constructs cultivated in the conventional culture medium or culture medium supplemented with PFC emlusion. * Significant difference between two groups by t-test ($p<0.05$), n=3-10, avg±se

PARAMETER	***CULTURE MEDIUM***	PFC EMULSION
pO_2 in [mmHg]	161.8 ± 1.7	155.6 ± 0.5 *
pO_2 out [mmHg]	117 ± 6	127 ± 5
pCO_2 in [mmHg]	40.5 ± 3.2	41.5 ± 3.5
pH in	7.40 ± 0.10	7.4 ± 0.12
Glucose consumption rate [μmol/hr/construct]	0.26 ± 0.03	0.20 ± 0.04
Lactate produced/Glucose consumed [mol/mol]	0.95 ± 0.04	0.72 ± 0.20
Lactate Dehyrdogenase [10^{-3} U/hr/construct]	1.63 ± 0.12	1.08 ± 0.07 *

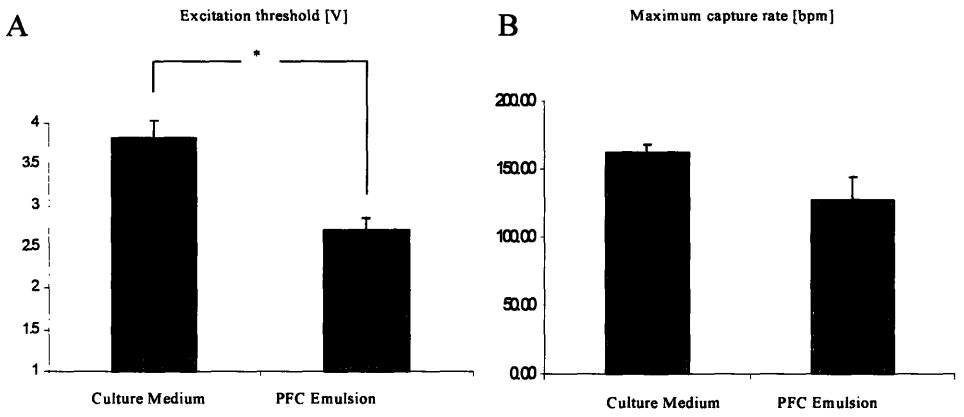

Figure 7.2. Contractile properties of cardiac constructs *cultivated in with conventional culture medium and with culture medium supplemented with PFC emulsion. *Significant difference between Two groups by t-test ($p<0.05$), n=4-7, Ave ± SE*

Consistent with the higher excitation threshold, DNA content per construct was significantly higher (~60%) in the group cultivated with PFC emulsion compared to the culture medium alone (**Figure 7.3A**). Construct wet weight was higher in the group perfused with PFC emulsion (24.9 ± 1.7mg) compared to the group perfused with pure culture medium (16.4mg, 16.0mg 19.1-median; 25^{th} and 75^{th} percentile). Although the protein content per construct was slightly higher in the PFC group compared to the culture medium group (0.74 ± 0.10 mg vs. 0.62 ± 0.04 mg respectively), Protein/DNA ratio as a measure of hypertrophy was lower but not significantly in

the PFC compared to the culture medium group (**Figure 7.3B**).

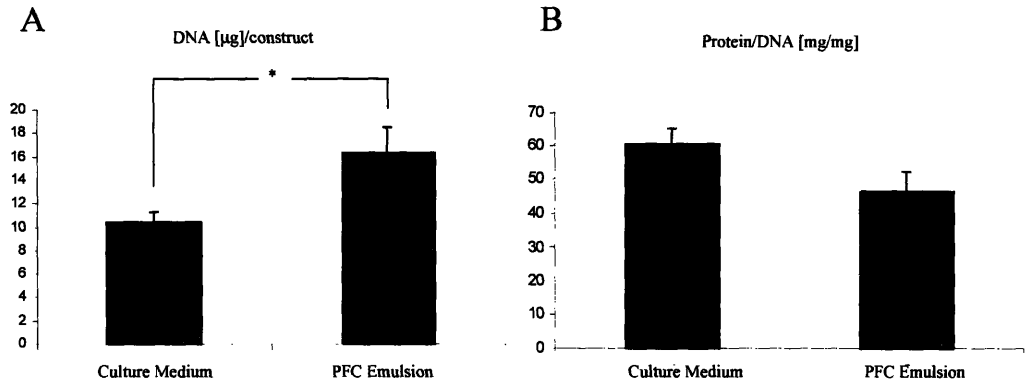

Figure 7.3. Protein and DNA content of cardiac constructs *cultivated in with conventional culture medium and with culture medium supplemented with PFC emulsion. *Significant difference between Two groups by rank-sum test ($p<0.05$), $n=4$, Ave ± SE*

Scanning electron microscopy of the laser machined poly(glycerol-sebacate) revealed the presence (**Figure 7.4 A,B**) of a cubically packed parallel channel array. As determined from light micrographs of dry scaffold, average channel diameter was 377 ± 52 μm (Ave ± SD) and wall-to-wall spacing was 222μm (median) (25^{th} percentile 210 μm, 75^{th} percentile 279 μm). The pores in the channel walls remained open during cultivation allowing for nutrient and oxygen exchange with the surrounding tissue space. (**Figure 7.4 B**). After 3 days in culture dense cell patches were covering the surface and the pores of the tissue constructs in both groups (**Figure 7.4C,D**). Scanning electron microscopy of the construct interior revealed the presence of cell patches throughout the construct cross-sections in both groups. (**Figure 7.4 E,F**). Although, large number of open channels with cells coating the walls was present in both groups (**Figure 7.4 G,H**) cell density was higher in the PFC group as compared to the culture medium group. As assessed from the fluorescent micrographs of the wet constructs, the average channel diameter after cultivation was comparable in both groups and significantly smaller than that before cultivation and the channel wall-to-wall spacing became slightly higher (335 ± 46μm and 364μm (median) (25^{th} percentile 341 μm, 75^{th} percentile 402 μm) respectively). The constructs thickness was estimated from histological cross-sections to be 2.08 ± 0.2 mm (Ave ± SD).

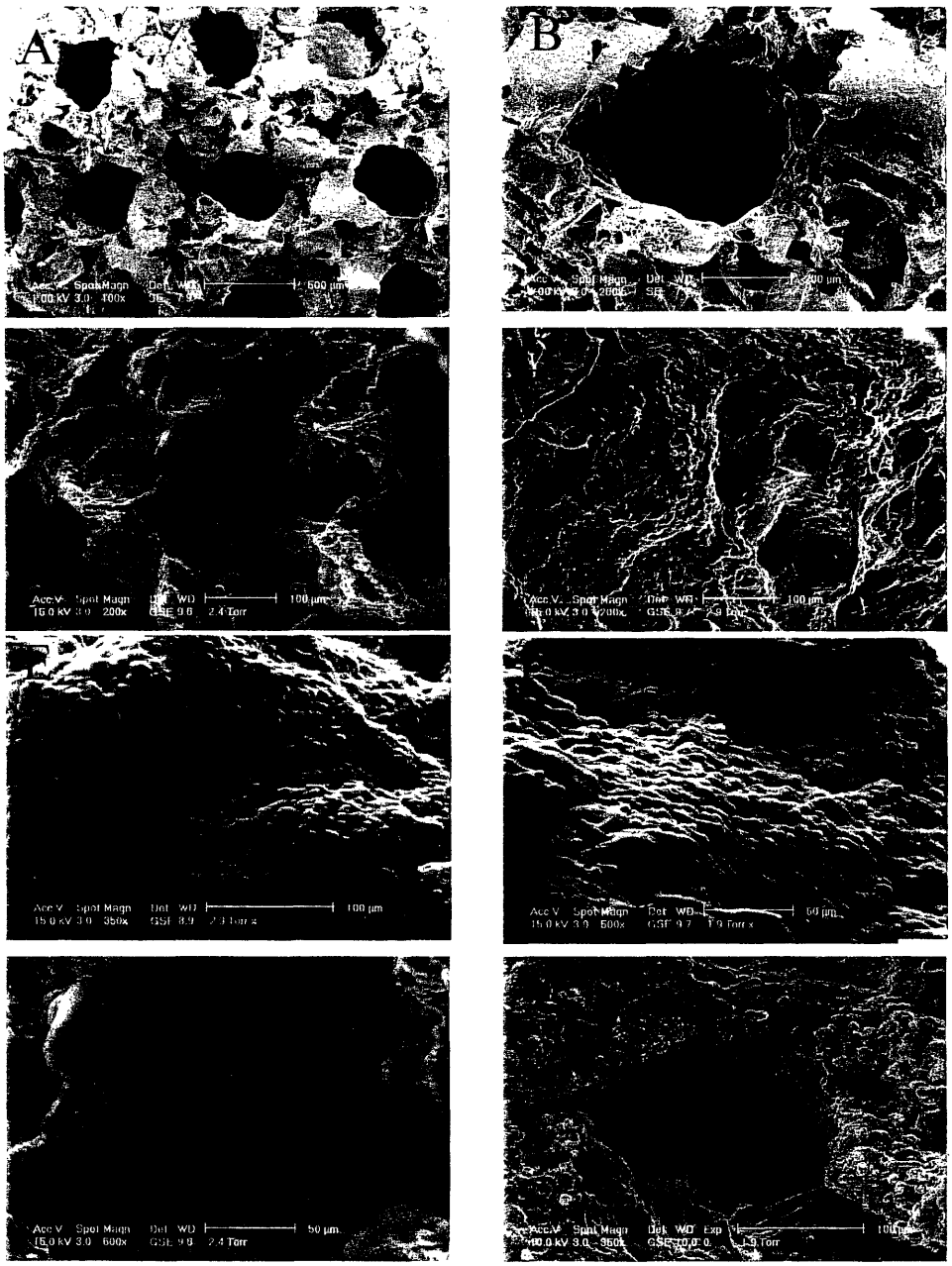

Figure 7.4. Scanning electron micrographs *of biorubber scaffold with a parallel channel array (A,B) and cardiac constructs cultivated in the standard culture medium (C,E,G) or culture medium supplemented with PFC emulsion (D,F,H). Face veiw (C,D); cross-section (E,F) and examples of representative channels (G,H)*

The presence of gap junctions was detected in both groups by staining for cardiac Connexin-43 (**Figure 7.5A**). Double staining for cardiac troponin I and vimentin indicated that the constructs consisted of mixture of cardiac myocytes and cardiac fibroblasts although, the myocytes appeared to constitute the majority of cell population (**Figure 5A**). Western blotting for cardiac markers confirmed the presence of cardiac Troponin I and gap junction protein connexin 43 (**Figure 7.5B**). Image analysis of the bands, indicated higher relative presence of troponin I and connexin 43 in the group supplemented with PFC emulsion compared to the culture medium alone (**Figure 7.5C**).

DISCUSSION

In native vascularized tissues, high cell density (~10^8 cells/cm^3) is supported by the flow of oxygen rich blood trough a dense capillary network (**Table 7.1**). Oxygen diffuses from the blood into the tissue space surrounding each capillary. Since the solubility of oxygen in plasma at 37°C is very low (130μM in arterial blood), the presence of a natural oxygen carrier, hemoglobin increases the total oxygen content of blood by carrying 65 times more oxygen than the blood plasma alone (8,630 μM). Under physiological conditions, only a fraction of oxygen is depleted from the blood in a single pass through capillary network. The difference in oxygen concentration in plasma between arterial and venous blood is ~76μM, and approximately 2,680 μM of oxyhemoglobin is depleted [1]. We report a biomimetic *in vitro* culture system in which cardiac tissue is engineered using a scaffold with parallel channel array (to mimick the role of capillary network) and synthetic oxygen carriers, perfluorooctyl bromide emulsion.

Unlike hemoglobin, which has binding sites for oxygen, oxygen content in neat perfluorooctyl bromide ($C_8F_{17}Br$) is governed by Henry's law, with liner relationship between atmospheric pO_2 and oxygen concentration. Solubility of oxygen in neat $C_8F_{17}Br$ is ~17 times higher than solubility of oxygen in water. Since neat PFCs are immiscible with water, preparations that are used as oxygen carriers in e.g blood substitutes have to be emulsified and stabilized with appropriate surfactants [13]. Oxygent™ used in this work is a 32v/v% (60%w/v), perfluroctyl bromide emulsion with average particle size of 0.2μm. [13].

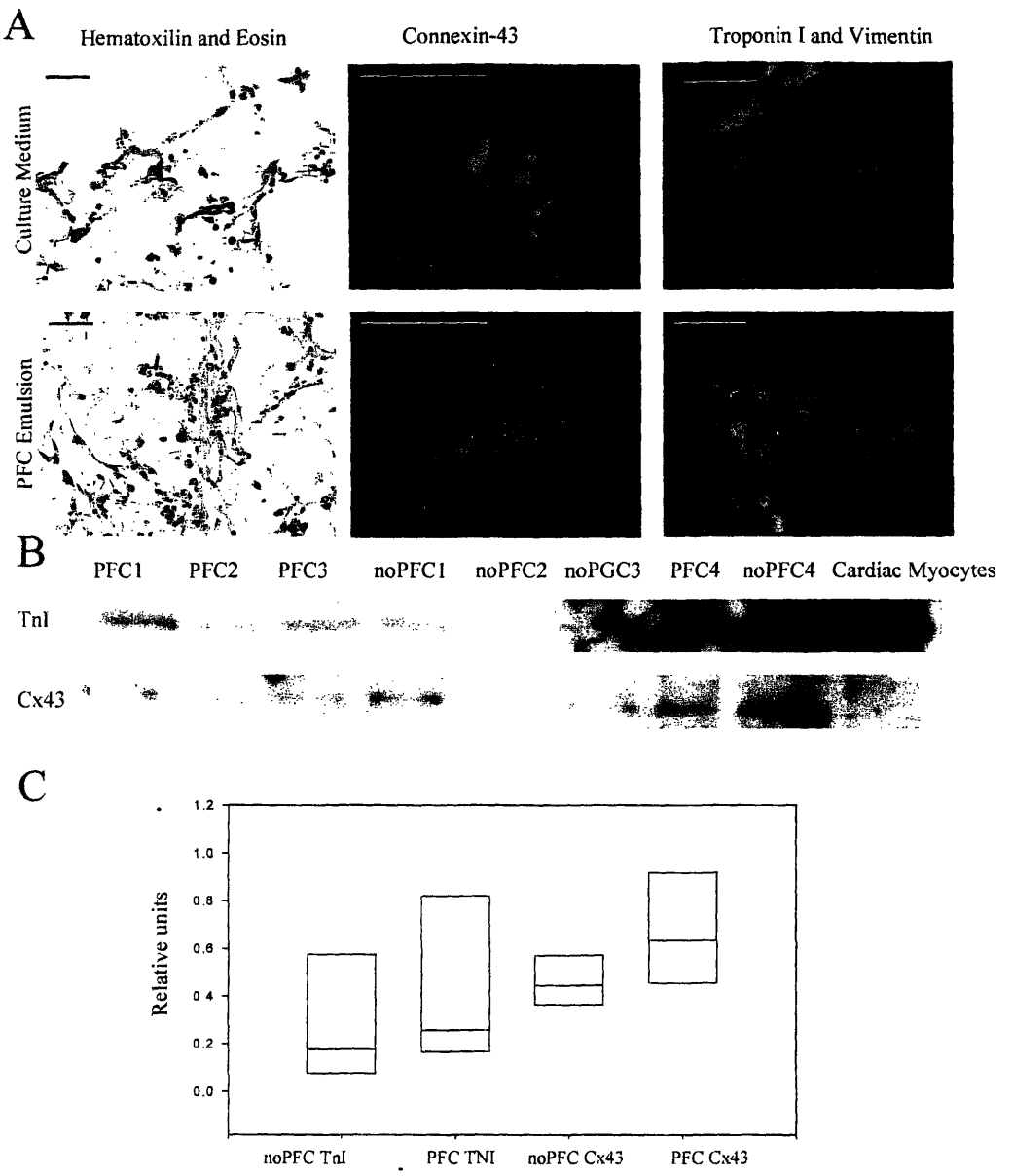

Figure 7.5. Expression of cardiac markers: Troponin I and connexin-43 in cardiac constructs cultivated in the presence of standard culture or medium supplemented with PFC emulsion. (a)Tissue architecture as assessed by HandE staining of cross-sections through the center. Presence of connexin-43 (green dots), Troponin I (green) and Vimenin (red). Scale bar 50μm. (b) Western blots (c) Box plot (median, 25th,75th percentile) of relative band intensities. The strongest band is assigned values of 1, the remaining bands are expressed as fraction of the strongest band.(n=4 per group)

Culture medium supplemented with Oxygent™, PFC emulsion, was perfused at the linear velocity similar to that in the capillary network (560μm/s) through a scaffold with parallel channel array. Since neat perfluorocarbon has ~2 times higher density than water, the emulsion precipitates in the lower portions of the perfusion loop, yielding circulating PFC concentration of 5.4%v/v. At those conditions total oxygen content of the medium supplemented with PFC is approximately twice as high as that of the unsupplemented culture medium. (**Table 7.1**).

As the medium flows through the channel array, oxygen is depleted from the aqueous phase of the culture medium by diffusion into the construct space where it is used in cardiac myocyte respiration (**Figure 7.1 A,B**). Depletion of oxygen in the aqueous phase acts as a driving force for the release of oxygen from the PFC particles, thereby contributing to the maintenance of higher oxygen concentrations in the medium. (**Figure 7.1 B**). Due to the small size of PFC particles, the release of oxygen from the PFC phase into the aqueous phase is a very fast process, and estimated not to be rate limiting in this system (Chapter 8). For comparison, in un-supplemented culture medium, oxygen is depleted faster since there is no oxygen carrier phase that acts as a reservoir. For a detailed model of oxygen profiles and transport processes in the tissue construct with and without the PFC emulsion please see Chapter 8.

Supplementation of the culture medium with PFC emulsion did not have significant effects on pH and pCO_2 at the inlet of the perfusion cartridge (**Table 7.2**). Both were maintained within the physiological range and were indistinguishable from the values measured for the unsupplemented culture medium. Lower partial pressure of oxygen at the inlet of the perfusion cartridge was consistent with the fact that PFC supplemented culture medium requires longer residence time in the gas exchanger (i.e longer gas exchanger) in order to fully equilibrate with the atmospheric oxygen.(**Table 7.2**). At the outlet of perfusion cartridge, higher oxygen partial pressure in the PFC group was consistent with the increased total oxygen content in the PFC group compared to the culture medium group. Overall, change in the partial pressure of oxygen in the aqueous phase was almost two times higher in the group perused with pure culture medium (45mmHg), compared to the group perfused with the PFC emulsion (28mmHg), consistent with ~2 times higher total oxygen content in the PFC emulsion.

At the flow rate of 0.1 ml/min, total oxygen concentration consumed from the culture medium was estimated to be 62 μM and total oxygen consumed from the PFC supplemented medium was higher, 82 μM (aqueous phase +PFC phase). Improved delivery of oxygen to the tissue constructs resulted in significantly higher DNA content in the PFC supplemented group compared to the unsupplemented group (**Figure 7.3A**). The corresponding number of cells per construct in the PFC group was $1.36 \cdot 10^6$ and for culture medium group it was $0.87 \cdot 10^6$,

indicating that the cell number decreased during culture in both groups from the initial number of seeded cells ($3 \cdot 10^6$), but at slower rate in the PFC group. Less cell damage and death in the PFC group is also consistent with the significantly lower levels of LDH release (**Table 7.2**).

Although, protein content was higher in the PFC supplemented group compared to the culture medium alone (0.74 ± 0.10 mg vs. 0.62 ± 0.04 mg respectively) oxygen consumption per unit of protein was comparable in both groups (11nmol/min/mg protein for PFC and 10 nmol/min/mg protein of culture medium group) and comparable to the previously reported values [14]. Glucose metabolism was comparable in both groups, with slightly lower consumption rates in the PFC group (**Table 7.2**) and lower L/G ratio indicative of more aerobic cell metabolism compared to the culture medium group (**Table 7.2**). Consistent with the improved oxygen supply is also higher ratio of oxygen/glucose consumed in the PFC group compared to the culture medium alone (2.4 mol/mol vs. 1.4mol/mol respectively).

Resulting cell density in the PFC group was higher than in the culture medium alone ($0.43 \cdot 10^8$ cells/cm^3 vs. $0.27 \cdot 10^8$ cells/cm^3), but it was still lower than the values we reported previously (~1 10^8cells/cm^3) for perfusion of constructs based on collagen sponges [11]. Most likely, the reason is a higher affinity of cells for collagen scaffold compared to the biorubber scaffold, resulting in improved cell attachment in collagen scaffolds. However, poor mechanical properties of collagen and large degree of swelling (approximately 30% immediately following hydration in culture medium, [10]) do not allow for creation of a channel array. Cell attachment onto biorubber can be improved by functionilizing the scaffold e.g through the addition of RGD domains without compromising mechanical properties such as elastomeric behavior and low degree of swelling.

As a result of higher cell density in the constructs cultivated with the PFC supplemented culture medium, enhanced electrical coupling of cardiac myocytes, improved the maintenance of differentiated phenotype as assessed by higher expression of cardiac troponin I and connexin-43 (**Figure 7.5 A,B,C**) and improved contractile properties of engineered constructs in the PFC group compared to the culture medium group (**Figure 7.2 A**).

At the end of cultivation most of the channels remained open with walls coated with dense patches of cells (**Figure 7.4**). Although cells were present between the channels, a compact and continuous layer of tissue was not formed. In order to achieve that scaffolds can be seeded with higher number of cells, constructs can be cultivated for longer time periods so that the cells have an opportunity to elongate and the scaffold can be optimized for cell attachment and migration by e.g addition of RGD domains. At the end of cultivation, channel diameter was significantly

smaller compared to the channel diameter in the dry scaffold not only due to the cell infiltration but also due to the small degree of swelling.

In summary, we developed a biomimetic culture system in which cardiac fibroblasts and myocytes are co-cultured on scaffolds with parallel channel array that mimics the role of capillary network perfused at 500μm/s with the culture medium supplemented with the PFC oxygen carrier that mimics the role of hemoglobin. Although the supplementation of PFC emulsion increased total oxygen content of the medium by 100% it was still significantly lower than oxygen content of the blood. The increase in oxygen content had an effect on cell density and DNA content that was ~60% higher in the PFC group compared to the culture medium group. As a result, contractile properties and protein expression were improved in the PFC group.

REFERENCES:

1. Fournier, R.L., *Basic Transport Phenomena in Biomedical Engineering.* 1998, Philadelphia: Taylor & Francis. p. 24.
2. Li, R.-K., et al., *Construction of a bioengineered cardiac graft.* Journal of Thoracic and Cardiovascular Surgery, 2000. 119: p. 368-375.
3. Bursac, N., et al., *Cardiac muscle tissue engineering: toward an in vitro model for electrophysiological studies.* American Journal of Physiology: Heart and Circulatory Physiology, 1999. 277(46): p. H433-H444.
4. Carrier, R.L., et al., *Cardiac tissue engineering: cell seeding, cultivation parameters and tissue construct characterization.* Biotechnology and Bioengineering, 1999. 64: p. 580-589.
5. Papadaki, M., et al., *Tissue engineering of functional cardiac muscle: molecular, structural and electrophysiological studies.* American Journal of Physiology: Heart and Circulatory Physiology, 2001. 280(Heart Circ. Physiol. 44): p. H168-H178.
6. Akhyari, P., et al., *Mechanical stretch regimen enhances the formation of bioengineered autologous cardiac muscle grafts.* Circulation, 2002. 106(12 Suppl 1): p. I137-I142.
7. Eschenhagen, T., et al., *Three-dimensional reconstitution of embryonic cardiomyocytes in a collagen matrix: a new heart model system.* FASEB Journal, 1997. 11: p. 683-694.
8. Zimmermann, W.H., et al., *Tissue engineering of a differentiated cardiac muscle construct.* Circulation Research, 2002. 90(2): p. 223-230.
9. Carrier, R.L., et al., *Perfusion improves tissue architecture of engineered cardiac muscle.* Tissue Engineering, 2002. 8(2): p. 175-188.
10. Radisic, M., et al., *High density seeding of myocyte cells for tissue engineering.* Biotechnology and Bioengineering, 2003. 82(4): p. 403-414.
11. Radisic, M., et al., *Medium perfusion enables engineering of compact and contractile cardiac tissue.* American Journal of Physiology: Heart and Circulatory Physiology, 2004. 286: p. H507-H516.
12. Kofidis, T., et al., *Pulsatile perfusion and cardiomyocyte viability in a solid three-dimensional matrix.* Biomaterials, 2003. 24(27): p. 5009-5014.
13. Kraft, M.P., J.G. Riess, and J.G. Weers, *The design and engineering of oxygen-delivering fluorocarbon emulsions*, in *Submicron Emulsions in Drug Targeting and Delivery*, S. Benita, Editor. 1998, Harwood Academic Publishers: Amsterdam. p. 235-333.

14. Yamada, T., et al., *Oxygen consumption of mammalian myocardial-cells in culture - measurements in beating cells attached to the substrate of the culture dish.* Analytical Biochemistry, 1985. 145(2): p. 302-307.

8.MATHEMATICAL MODEL OF OXYGEN DISTRIBUTION IN ENGINEERED CARDIAC TISSUE WITH PARALLEL CHANNEL ARRAY PERFUSED WITH CULTURE MEDIUM SUPPLEMENTED WITH SYNTHETIC OXYGEN CARRIERS

INTRODUCTION:

The key parameter in engineering functional 3D tissues in vitro is oxygen supply [1-3]. In native rat heart, oxygen is supplied by diffusion from capillaries that are spaced ~20 μm apart[4]. Since the solubility of oxygen in plasma is low, the oxygen carrier, hemoglobin increases total oxygen content of blood and therefore increases the mass of tissue that can be supported in a single pass through capillary network The average oxygen concentration in arterial blood is 130μM and in the venous blood it is 54 μM [1].

In conventional tissue engineering approaches, cells are supported on polymer scaffolds to form tissue constructs immersed in culture medium. Oxygen dissolved in the medium is transported by diffusion from the surface of the tissue construct into its interior. The medium is re-oxygenated via a gas exchanger [5], by aeration or by membrane exchange [2]. Diffusion alone is capable of providing enough oxygen for ~100 μm thick outer layer of a tissue construct while the interior remains relatively acellular or becomes necrotic due to hypoxia [6].

To resolve this problem a perfusion bioreactor system has been developed [7]. In such a system the entire construct is directly perfused with culture medium, and the transport of oxygen from the medium to the cells occurs via both diffusion and convection. However, the solubility of oxygen in water at 37 °C is not enough to satisfy metabolic demand of large number of cells (e.g. $5 \cdot 10^8$ cells/cm^3 construct) at low flow rates (e.g. 0.5 ml/min/cm^2). Increasing the flow rate increases the shear stress exerted on the cells, which in turn can decreases viability and cell number. To provide enough oxygen for thick constructs at low flow rates, it is necessary to have a pool of oxygen in the medium, available to quickly meet changing local oxygen demand. By utilizing synthetic oxygen carriers (perfluorocarbons), the length of tissue construct that can be supported per single pass through perfusion bioreactor at a given flow rate will be increased.

Our main hypothesis is that functional assembly of engineered cardiac tissue will be enhanced by increasing local oxygen concentration in the tissue space within the physiological range (up to 220μM). This hypothesis is consistent with the observation that cardiac constructs cultivated in perfusion at ~80μM exhibit weaker presence of cardiac markers, and poorer organization of contractile apparatus compared to the constructs cultivated at ~220μm [8]. In addition it was demonstrated that isolated cardiomyocytes begin to downregulate energy using processes at oxygen concentrations as high as 70μM[9].

In order to test this hypothesis, we recently reported a biomimetic *in vitro* tissue culture system in which neonatal rat heart cells were cultured on an elastic, highly porous scaffold with a parallel array of channels perfused with culture medium supplemented with the a synthetic oxygen carrier (Oxygent™, perfluorocarbon emulsion -PFC). In this system, the parallel channel array mimics the role of capillary network and the PFC emulsion mimics the role of hemoglobin. Constructs perfused with unsupplemented culture medium served as controls.

In this paper a steady state mathematical model that relates distribution of oxygen within the engineered tissue construct to the medium flow rate, partial pressure of oxygen and mass fraction of oxygen carrier is derived and solved using the finite element method. The model was used to compare oxygen distribution in the experimentally obtained channeled cardiac tissue constructs perfused with pure culture medium and with PFC supplemented culture medium. In addition, the model was used to define optimum scaffold geometry and flow conditions necessary to cultivate cardiac constructs of physiologically high cell density (10^8cells/cm^3) and clinically relevant thickness (0.5cm). As a part of assumption validation resistances to the transport of oxygen were compared in each phase, indicating that the transfer of oxygen from the PFC phase into the aqueous phase was not rate limiting. Addition of PFC emulsion improved oxygen transport by improving apparent average velocity and by increasing effective diffusivity.

GOVERNING EQUATIONS

Let C_p and C_a be oxygen concentrations in the PFC and aqueous phase respectively in a system depicted in **Figure 8.1** and ϕ fraction of PFC emulsion.. Assuming that the drops are (i) small enough that the concentration is nearly uniform within a given drop and (ii) each drop is very nearly in equilibrium with the adjacent media, the total O_2 concentration at any point in the emulsion is:

$$C_{total} = (1-\phi)C_a + \phi C_p \tag{1}$$

Since by definition partition coefficient is $K=C_p/C_a$:

$$C_{total} = [1+(K-1)\phi]C_a \tag{2}$$

Treating the emulsion as a homogenous fluid of constant density conservation of equation for oxygen at steady state can be expressed as:

$$\mathbf{v}_a \cdot \nabla C_t = -\nabla \mathbf{J} \tag{3}$$

where $\mathbf{v}_a$ is velocity and **J** is the flux of oxygen relative to $\mathbf{v}_a$ (the diffusive flux).The diffusive flux can be expressed in terms of either C_{total} or C_a; the latter is preferable since C_a is more convenient for matching concentrations at the emulsion-tissue interface. Choosing C_a gives:

$$\mathbf{J} = -D_{eff}\nabla^2 C_a \tag{4}$$

where D_{eff} is effective diffusivity, defined by [10, pg191] ::

$$D_{eff} = \frac{D_a}{K_{eff}}\left(1+3\left(\frac{\gamma-1}{\gamma+2}\right)\phi\right) \tag{5}$$

In **Eq. 5** D_a is diffusivity of aqueous phase of culture medium, $\gamma=KD_p/D_a$ and $K_{eff}=1$ for the case when emulsion concentration is based upon the continuous phase concentration.

Combining **Eq. 1-4** the steady state oxygen conservation equation becomes:

$$[1+(K-1)\phi]\mathbf{v}_a \cdot \nabla C_a = -D_{eff}\nabla^2 C_a \tag{6}$$

Similarly, the conservation equation for oxygen in the tissue space can be expressed as:

$$\mathbf{v}_t \cdot \nabla C_t = -D_t \nabla^2 C_t + R \tag{7}$$

where R is oxygen consumption rate according to the Michaelis-Mentent kinetics:

(8)

$$R = -\frac{V_{max} C_t}{K_m + C_t}$$

Since permeability of channels is significantly greater than the permeability of tissue space, it is reasonable to assume that radial velocity component can be neglected in the channel and that there is no convection in the tissue space [11]. In order to confirm this assumption, hydraulic permeability of channel-free biorubber scaffold was experimentally estimated to be 8.1 ± 0.4 10^{-12} m^2 [(m3/s)/m2] [(Pa s) m/Pa] (please refer to experimental section).

Based on Darcy permeability, the average axial velocity in the scaffold space was estimated to be 1.7 10^{-4}cm/s. The scaffold axial Pe number was calculated as::

$$Pe_s = \frac{U_z^s (R_t - R_c)}{D_a} \tag{9}$$

For the experimentally obtained channel geometry, Pe_s=0.09. For the proposed thick scaffold (0.5cm) with dense packing of narrow channels (100μm channel diameter and 100μm channel spacing), the estimated scaffold axial velocity was 4.7 10^{-4}cm/s (at the highest flow rate investigated) and Pe_s number was 0.095. As Matrigel/cell suspension is added to the scaffold it is expected that the permeability of the tissue space and axial tissue Peclet number would decrease even further. The value of 0.095 is the upper bound of the tissue Pe number obtainable in this system, thus justifying the assumption of no convection in the tissue space.

Accordingly, the conservation equations for oxygen in the channel lumen can be rewritten as:

(10)

$$[1+(K-1)\phi]\cdot v_z(r)\frac{\partial C_a}{\partial z}=D_{eff}\left[\frac{1}{r}\frac{\partial}{\partial r}\left(r\frac{\partial C_a}{\partial r}\right)+\frac{\partial^2 C_a}{\partial z^2}\right]$$

This governing equation is of the same form as Equation 15 given in Shah and Mehra [12] except that they did not take effective diffusivity into account. Although axial diffusion can be neglected in **Eq. 10** due to the relatively high value of Pe, the software used for numerical solution considered axial diffusion automatically. Governing equation for oxygen distribution in the tissue region can be expressed as:

(11)

$$0=D_t\left[\frac{1}{r}\frac{\partial}{\partial r}\left(r\frac{\partial C_t}{\partial r}\right)+\frac{\partial^2 C_t}{\partial z^2}\right]+R$$

The equations are subject to the following boundary conditions presented in **Table 8.1.**

Table 8.1 Boundary conditions

CHANNEL	TISSUE ANNULUS	
$C_a(r,0)=C_{in}$	$C_t(r,0)=C_{in}$	Measured bulk O_2 concentration at the construct entrance
$C_a(r,L)=C_{out}$ or $\frac{\partial C_a(r,L)}{\partial z}=0$	$C_t(r,L)=C_{out}$ or $C_t(r,L)=\frac{\int_0^{R_c} C_a(r,L)v_z r dr}{\int_0^{R_c} v_z r dr}$	Measured bulk O_2 concentration at the construct outlet (used for experimental conditions) Bulk O_2 concentration at the outlet not measured, Neumann boundary condition imposed for the concentration in culture medium at the outlet, mixing-cup concentration for the outlet culture medium imposed at the outlet of tissue space (used for predictions)
$\partial C_a/\partial r(0,z)=0$	$\partial C_t/\partial r(R_t,z)=0$	symmetry conditions
$D_a\frac{\partial C_a}{\partial r}(R_c,z)=D_t\frac{\partial C_t}{\partial r}(R_c,z)$	$C_a(R_c,z)=C_t(R_c,z)$	Equal flux of O_2 at the interface, concentrations of O_2 in the medium and the tissue are the same

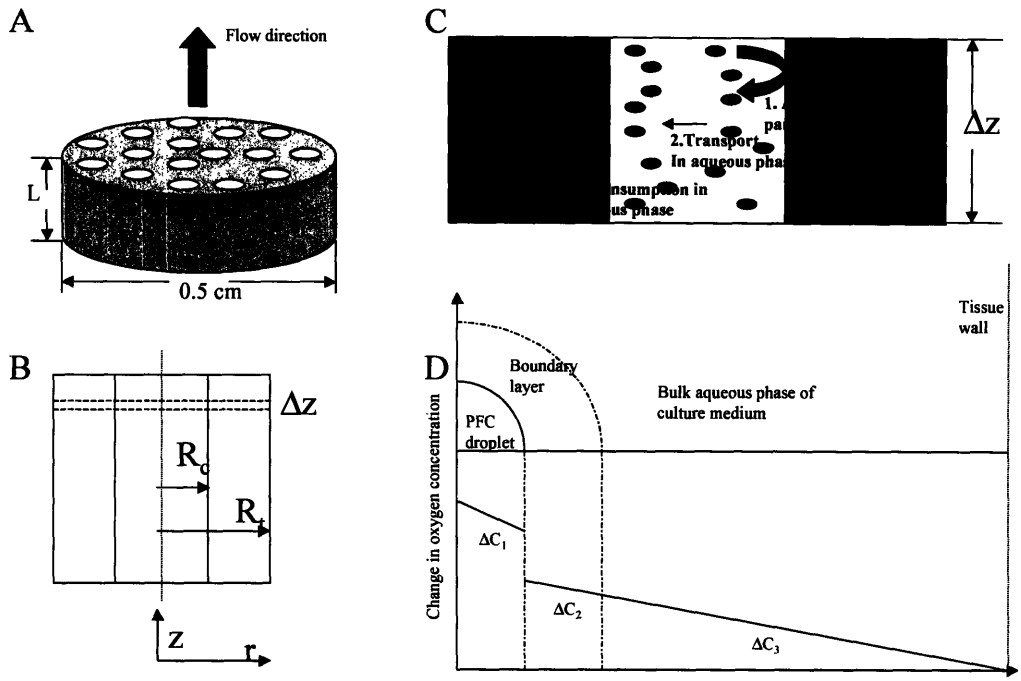

Figure 8.1. Schematics of the construct with parallel channel array (A) cross section of one channel (B) main transport processes in a differential channel layer (C) and concentration differences considered for the analysis of resistances (D).

METHODS:
Experimental studies

Cultivation of the cardiac tissue constructs:
Porous poly(glycerol-sebacate) scaffolds were fabricated by means of a salt leaching technique. Briefly, PGS solution in tetrahydrofuran was poured into a Teflon mold filled with NaCl particles of desired sizes. The mold was transferred to a vacuum oven and cured at 120 °C and 100 mTorr. The resulting material was soaked in deionized water to remove the NaCl particles. Scaffolds with porosity up to 91% were obtained after removal of water. An array of cubically packed parallel channels was bored using a 120Watt CO_2 laser cutting/engraving system (Model X-660, Universal Laser Systems, Scottsdale AZ). Discs 5-6mm diameter x 2 mm thick were sterilized by 70% ethanol overnight followed by 4hr in 95% ethanol and 1 hr in 100% ethanol. Ethanol was removed by vacuum filtration and the scaffolds were rinsed in phosphate buffered saline (PBS, Gibco) for 1-4 hr followed by 1hr in FBS (Fetal Bovine Serum, Gibco). Channel diameter and spacing was determined from the light micrographs using image analysis software (Scion Image)

Cells were isolated from neonatal rat ventricles as described previously [8]. For scaffold preconditioning with fibroblasts, $0.5\text{-}1\cdot10^6$ fibroblasts were resuspended in 10µl Matrigel® (BD) and applied to the scaffold as described previously [13]. The constructs were pretreated in six well plates (1 construct/well) for 4 days in 5 ml of culture medium at 25 rpm. At the end of preconditioning, $2.3\cdot10^6$ cardiomyocytes in 15 µl of Matrigel® was added to the construct, and allowed to gel for 30 min at 37°C. The constructs were cultivated in the perfusion loops for additional 3 days as described previously. [14]. Briefly, the constructs were tightly fitted inside the 5 mm ID, 10 mm OD silicone tubing rings, placed between two stainless steel screens and positioned into 1.5 ml polycarbonate perfusion cartridges (kindly donated by the Advanced Tissue Sciences, La Jolla, CA; one scaffold per cartridge). The screens (85% open area) provided mechanical support during perfusion and the silicone ring routed the culture medium through the central area of the construct. Constructs were subjected to unidirectional medium flow at 0.1 mL/min provided by the IsmaTec multichannel peristaltic pump. The total volume of culture medium in the gas exchanger tubing, medium bag and cartridge was 30 ml. To investigate the effect of presence of oxygen carriers, the 27 ml of culture medium was mixed with 3ml of perfluorocarbon (PFC) emulsion (Oxygent™, kindly donated by the Alliance Pharmaceuticals Crops, San Diego, CA). Unsupplemented culture medium served as a control. A total of 7 rat litters were used in 7 independent experiments with n = 4 - 6 constructs per experiment.

Gas composition and pH at the inlet to perfusion cartridge was measured from medium samples using a gas blood analyzer (Model 1610, Lexington, MA). Oxygen concentration at the outlet of the perfusion cartridges was measured by in-line ruthenium based oxygen sensors (kindly donated by Payload Systems). The fraction of circulating PFC emulsion was determined by sectioning-off the lower portions of the loop, collecting the culture medium with PFC emulsion and determining the absorbance of dilute emulsion at 970nm.

At the end of cultivation constructs were collected and evaluated for protein, DNA content, contractile response, cell distribution and expression of cardiac markers. Fluorescent micrographs of the wet constructs were used in conjunction with an image analysis program (Scion image) to determined channel diameter and spacing after culture. Construct diameter and height was determined from histological sections.

Evaluation of hydraulic permeability of biorubber scaffold:

For evaluation of hydraulic permeability, a 5mm thick piece of biorubber scaffold without the channels was fitted into perfusion cartridge with 5mm diameter of open area, and connected to the water reservoir via silicone tubing and 3 way stop-cock. The water reservoir was placed at the height of 1.195m in order to provide a constant pressure head. To determine flow rate, the water draining from the perfusion cartridge upon the opening of 3 way stop cock was collected at timed intervals. Flow around the scaffold was prevented by fixing the scaffold between silicone gaskets as described previously [14]. The measurement was performed at room temperature (22°C). Hydraulic permeability was determined based on Darcy's law (**Eg.12**).

$$\frac{Q}{A} = -\frac{k}{\mu}\frac{\Delta P}{\Delta L} \qquad (12)$$

In Eq. 12, Q is volumetric flow rate, A is the area of empty open cross-section, μ is viscosity of water, ΔP is pressure drop and ΔL is scaffold thickness.

MODEL PARAMETERS:

A mathematical model was implemented for the set of experimental conditions summarized in **Table 8.2**. Average number of channels per construct was calculated based on the measurements of channel radius, spacing and construct diameter. The flow rate and average velocity per channel was calculated based on the imposed flow rate (0.1 ml/min) and the number of channels. Maximum oxygen consumption (Vmax) rate was calculated based on the protein content, scaffold volume (without channels) and maximum consumption rate per unit protein reported for non-beating monolayers of neonatal rat cardiomyocytes [15]. The non-beating rather than beating values were used due to the observation that constructs usually do not exhibit spontaneous contractions within the first three days of cultivation. The fraction of circulating PFC emulsion droplets (ϕ) was higher than the nominal fraction (5.4vol % vs. 3.2%) due to some settling in the lower portions of the loop. The circulating PFC fraction was determined spectrophotometrically after the medium was collected from the lower portions of the loop.

In addition, mathematical modeling was used to predict oxygen concentration profiles in tissue constructs of clinically relevant thickness (0.5cm) with various channel geometry (diameter and spacing), flow rates, cell density and concentration of circulating PFC emulsion. The main goal was to determine channel geometry and culture conditions (flow rate and concentration of

PFC emulsion) that would yield high oxygen concentrations in the tissue space at physiologically high cell densities (10^8cell/cm^3).

In one case, oxygen concentration profiles were compared in a 0.5 cm thick tissue construct with 330μm channel diameter, 370μm wall-to-wall spacing perfused at the average linear velocity per channel of 0.049cm/s (or 0.1ml/min bulk flow) with culture medium supplemented with 0, 3.2, 6.4 vol% PFC emulsion (0, 10 or 20 vol% of Oxygent™). The channel geometry and flow conditions used for these simulations were the same as those utilized in experimental studies. The simulations were performed at two cell densities: $0.27 \cdot 10^8$ cells/cm^3 which is a low value measured experimentally and $1 \cdot 10^8$ cells/cm^3 which is a physiologically relevant density. The cells were assumed to be uniformly distributed around the channel. The corresponding maximum oxygen consumption rate (Vmax) was calculated to be 8.8 and 33 μM/s respectively, based on 60mg prot/μg DNA ([8]) and 27.6 nmolO_2/mg protein/min. Culture medium at the inlet to the construct was assumed fully saturated with atmospheric oxygen with an oxygen concentration of 222.47 μM.

In another case, oxygen concentration profiles were compared in a 0.5 cm thick tissue construct with 100μm channel diameter, 100μm wall-to-wall spacing perfused at the average linear velocity per channel of 0.049cm/s or 0.135 cm/s (corresponding to 0.11ml/min and 0.31 ml/min of bulk flow respectively) with culture medium supplemented with 0, 3.2, 6.4 vol% PFC emulsion (0, 10 or 20% of Oxygent™). Such a fine channel array was not produced experimentally due to the limitations associated with the laser cutting/engraving system, but represent the target value in scaffold design necessary for high oxygen concentration in the tissue space. Cell density in the tissue space was set to be physiological (10^8cells/cm^3, Vmax=33μM/s, Km=6.875μM). At the low volume fractions of PFC used in the simulation (ϕ=0.033-0.064) the viscosity of PFC supplemented culture medium is maintained at the values comparable to that of water (~1cp, [16]). The average velocity of culture medium was chosen so that the shear stress at the walls was less than 1dyn/cm^2 which is below the range (1.6-3.3 dyne/cm^2) reported to induce decreased viability in hybridoma and human embryonic kidney cells [17, 18].

Table 8.2. Model parameters used to predict oxygen concentration profiles in a cardiac tissue construct based on channeled biorubber scaffolds and perfused with pure culture medium or culture medium supplemented with PFC emulsion as described in experimental section.

PARAMETER	*VALUE*	*SOURCE*
R_c (channel radius)	165μm	measured
R_t (tissue radius)	370 μm	measured
L (construct length)	2mm	measured
Number of Channels	40 for cubic packing	$N=R^2\pi/(2r_t)^2$ Rc=0.5cm, construct radius
U (average velocity per channel)	0.049 cm/s (0.1 ml/min)	Radisic et al TE1, set
Oxygen consumption	27.6nmol/mg protein/min	[15]
K_m	6.875μM	[9]
Protein amount	0.743mg (for PFC supplemented) 0.624mg (for pure culture medium)	measured
V_{max}	10.5 μM/s (for PFC supplemented) 8.8 μM/s (for pure culture medium)	Calculated
PFC in Oxygent™	32% v/v	Alliance Pharmaceuticals Corps
d (PFC droplet diameter)	0.2 μm	Alliance Pharmaceuticals Corps
Oxygent™ in culture medium	17.1%	measured
ϕ PFC emulsion droplets in culture medium	5.4vol%	
Solubility of oxygen in neat PFC	0.02mol/L	[1]
D_a (aquos oxygen diffusion coefficient)	$2.4\ 10^{-5}$ cm^2/s	[19]
D_t (tissue oxygen diffusion coefficient)	$2.0\ 10^{-5}$ cm^2/s	[7]
D_p (Oxygen diffusion coefficient in neat PFC)	$D_p=5.6\ 10^{-5}$ cm^2/s	[20]
C_{in} (inlet oxygen concentration in aqueous phase)	213.0 μM (for PFC supplemented) 222.5 μM (for pure culture medium)	measured
C_{out} (outlet oxygen concentration)	177.0 μM (for PFC supplemented) 152.6 μM (for pure culture medium)	measured

Important dimensionless numbers

In order to simplify the mathematical model, Re and Pe numbers were calculated for all investigated channel geometries and average velocities. The low values of Re and velocity entrance lengths (**Table 8.3**) indicate that the flow was laminar and fully developed over most of

the length of the channel for 0.2 and 0.5 cm thick constructs. Therefore, the velocity profile $v_z(r)$ in conservation equations is given by:

$$v_z(r)=2U(1-r^2/R_c^2) \quad (13)$$

Table 8.3 Important dimensionless numbers, mass transport and velocity entrance length for all of the channel dimensions and average velocities investigated.

	$Re=2\rho UR_c/\eta$	$L_v=R_c(1.18+0.112Re)$[10]	$Pe=2UR_c/D_a$	$L_m=r_c(1+0.1Pe)$[10,PG101]
R_c=0.0165cm U=0.049cm/s	0.23	0.020cm	67.4	0.128cm
R_c=0.005cm U=0.049cm/s	0.07	0.006cm	20.4	0.015cm
R_c=0.005cm U=0.135cm/s	0.19	0.006cm	56.2	0.033cm

Relatively high values of Pe numbers imply that axial diffusion within the channel can be neglected. For the conditions investigated experimentally (**Table 8.3** first row) approximately one half of the 0.2 cm thick construct was within the mass transfer entrance length. For this reason it was impractical to describe the transport within the channel with a single mass transfer coefficient.

Assumption validation for model parameters:

To justify the assumption of uniform oxygen concentration within PFC droplets and the local equilibrium between PFC and aqueous phase at every point along the channel length, the following processes have to be considered (**Figure 8.1C**):

1. Diffusion of oxygen inside the PFC droplet
2. Diffusion of oxygen from the PFC droplet to the surrounding aqueous phase of culture medium.
3. Transport of oxygen from the bulk fluid to the tissue wall.

There is a gradient in oxygen concentration from the center of PFC droplet to the drop/medium interface ($\Delta C1$), followed by the drop at the aqueous phase and a gradient through the boundary layer ($\Delta C2$) (**Figure 8.1D**). The ratio of these two concentration differences is proportional to the Biot number [10,pg83]:

$$Bi=\frac{k_2(d/2)}{KD_p}\sim\frac{\Delta C_1}{\Delta C_2} \quad (14)$$

In **Eq. 14**, k_2 is the mass transfer coefficient for the absorption of oxygen from the PFC droplet into the aqueous phase of culture medium, d is a diameter of PFC droplet and, K is the partition coefficient and D_p is diffusion coefficient of oxygen in neat PFC. Droplet mass transport coefficient can be expressed in terms of Sherwood number, Sh as:

$$Sh_d = \frac{k_2 \cdot d}{D_a} \tag{15}$$

In **Eq. 15** D_a is a diffusion coefficient for oxygen in the aqueous phase of culture medium. By combining Eq. 1 and Eq. 2 Biot number can be expressed as:

$$Bi = \frac{Sh_d D_a}{2KD_p} \tag{16}$$

Internal diffusion can be neglected for Bi<<1. Since PFC particles are of small diameter (0.2μm) it can be assumed that they move with the flow and Sh_d=2. For D_a=2.4 10^{-5} cm^2/s [7], D_p=5.6 10^{-5} cm^2/s [20] and K=20.3 (the ratio of oxygen solubilities at 760mmHg and 37°C in neat perfluorooctyl bromide and water), the Biot number in **Eq. 16** has value of 0.02 implying that the resistance to internal diffusion can be neglected.

To determine $\Delta C_2/\Delta C_3$ we will compare the rate of transport from the boundary layer around the PFC droplet to the bulk fluid and from the bulk fluid to the tissue wall (**Figure 8.1D**). in the differential channel layer of length Δz. Mass flow of oxygen from the PFC particles into the aqueous phase of culture medium can be described by the following equation:

$$r_2 = k_2 \cdot a_p \cdot \Delta C_2 \tag{17}$$

In **Eq. 17**, k_2 is the drop mass transport coefficient as defined in 2 and a_p is surface area of all PFC droplets in the control volume considered.

$$a_p = S_p \cdot N_p = 6\pi \frac{R_c \Delta z \phi}{d} \tag{18}$$

In **Eq. 18** S_p is the surface area of one droplet, N_p is number of all of the PFC droplets in the control volume considered, R_c is channel radius and ϕ is volume fraction of PFC emulsion. By combining **Eq. 17**, **Eq. 18** and **Eq 15** with Sh_d=2 mass flow of oxygen from the PFC to aqueous phase can be expressed as:

$$r_2 = 12\pi \Delta C_2 \frac{D_a R_c \Delta z \phi}{d} \tag{19}$$

Mass flow of oxygen, r_3, from the bulk phase of culture medium to the channel wall can be described as:

$$r_3 = k_3 \Delta C_3 (2\pi R_c \Delta z) \tag{20}$$

In **Eq. 20**, k_3 is a mass transport coefficient that is related to the channel Sherwood number Sh_c

$$Sh_c = \frac{2k_3 R_c}{D_{eff}} \tag{21}$$

.Effective diffusivity, D_{eff} is given by Eq. 5. Eq. 5 neglects interparticle interactions which should be fine for the dilute emulsion investigated ($\phi<0.1$). For the condition investigated in this paper culture medium is supplemented by 10-20% of Oxygent^{TM}, an emulsion kindly donate by Allianace Pharmaceuticals, Corps. Oxygent^{TM} is 32vol% PFC emulsion, resulting in ϕ=0.032-0.064. For the given conditions, with γ=47.3 D_{eff}=1.09-1.18D_a. At steady state r_2=r_3:

$$12\pi\Delta C_2 \frac{D_a R_c \Delta z \phi}{d} = k_3 \Delta C_3 (2\pi R_c \Delta z) \tag{22}$$

As a result the ratio of ΔC_2 to ΔC_3 can be expressed as:

$$\frac{\Delta C_2}{\Delta C_3} = \frac{Sh_c}{12\phi}\left(\frac{D_{eff}}{D_a}\right)\left(\frac{d}{R_c}\right)^2$$

Accordingly for the range of ϕ=0.032-0.064 and D_{eff} in the range of (1.09-1.18)D_a, the ratio of $\Delta C_2/\Delta C_3$ will be in the range (4.17-2.26)$10^{-6}Sh_c$.

The value of the channel Sherwood number was calculated for the: constant concentration at the channel wall and constant flux at the wall. Since there is consumption of oxygen at the channel wall the real boundary condition is mixed or Robin boundary condition and the Sherwood number for this case falls in between the values obtained for constant flux and constant concentration boundary condition. [10, pg.392].

To estimate Sh_c up to the value of mass transfer entrance length (0.128mm) **Eq. 23** and **Eq. 24**, both applicable for the fully developed velocity profile, were used for constant concentration and constant flux boundary condition respectively [10, pg. 384].

$$Sh_c = 1.357\left(\frac{R_c}{y}\right)^{1/3} Pe^{1/3} \tag{23}$$

$$Sh_c = 1.640\left(\frac{R_c}{y}\right)^{1/3} Pe^{1/3} \tag{24}$$

Beyond the mass transport entrance length (which is most of the construct for the 100μm diameter channels) the values of 3.576 and 4.360 for Sherwood number were used for constant concentration and constant flux boundary condition respectively. The resulting values, all bellow 10^6 are summarized in **Table 8.4**

Table 8.4. Channel Sherwood number

Sh_c (constant concentration at the wall)		**Sh_c (constant flux at the wall)**	
L<Lm		L<Lm	
L [cm]	Sh	L [cm]	Sh
0.03	4.524	0.03	5.568
0.06	3.591	0.06	4.419
0.09	3.137	0.09	3.860
0.12	2.850	0.12	3.507
L>Lm		L>Lm	
0.12-0.2	3.576	0.12-0.2	3.660

Consequently since Sh_t is many orders of magnitude less than 10^6 over most of the tube length at the conditions investigated, $\Delta C_2 << \Delta C_3$ over most of the tube length except very near to the entrance where $Sh_t \rightarrow \infty$. Since $\Delta C_1 << \Delta C_2$, than also $\Delta C_1 << \Delta C_3$. Therefore, absorbance from the PFC droplets into the aqueous phase is not the rate limiting step and local equilibrium can be assumed at every point in the channel.

Numerical Method

Finite element method was used to solve the model with a commercial software package FEMLAB (Comsol Inc., Burlington, MA) using built in 2D variable general form PDE. This PDE template takes into account diffusion in both axial and radial direction in the channel.

Symmetry planes (Neumann boundary condition) were placed at the boundaries between the domains and in the channel center-line. **(Figure 8.1B).** Dirichlet boundary condition was imposed at the entrance and at the exit of the tissue construct. Since Pe number for this problem was high, the transport was convection dominated in the channel subdomain. In order to stabilize the discrete scheme streamline diffusion was added.

Since the source term in the convection-diffusion equation follows Michaelis-Menten kinetics and is non-linear, the equations had to be solved using a stationary non-linear solver. The algorithm solves the equation by an affine invariant form of the damped Newton method. The Jacobian that is needed for the nonlinear iterations is set to be calculated exactly using symbolic math toolbox. The maximum number of iterations was set to 25, minimum step size to 10^{-4} and the tolerance for convergence is set to 10^{-6}. The convergence was tested by refining the mesh.

In order to validate the model, oxygen profile in the center (L/2) of the tissue space with cells respiring at Vmax, was compared to the one dimensional analytical solution with zero order kinetics.

As demonstrated in governing equations **(Eq. 10)** and **Table 8.5**, PFC emulsion contributes to the enhancement of mass transfer by increasing effective diffusivity, and the convective term (apparent average veolicty). To illustrate this effect, simulations were performed in a densely packed channel array (100μm channel diameter, 100 μm wall-to-wall spacing), perfused at 0.135cm/s with culture medium supplemented with 0, 3.2 % and 6.4 % of PFC emulsion. For simplicity the oxygen consumption in the tissue region was assumed to follow zero order kinetics at 18μM/s (corresponding to cell density of ~0.5 10^6cells/cm^3). In each case contribution of effective diffusivity alone, convective term alone and the combined effect of both terms was investigated. Volume averaged and minimum oxygen concentration as well as the mixing-cup culture medium concentration at the outlet were compared.

RESULTS

The effect of PFC emulsion on oxygen concentration in engineered cardiac tissue

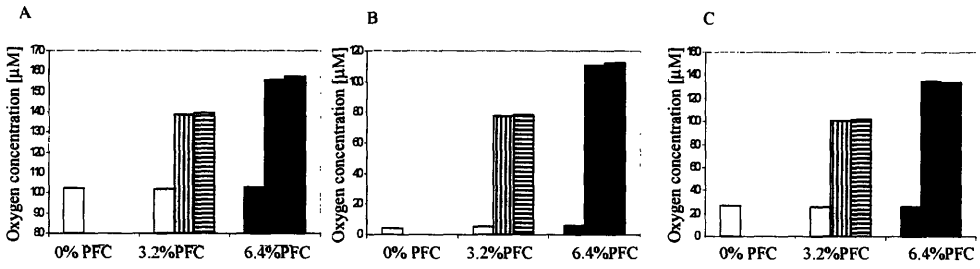

Figure 8.2. Effect of PFC emulsion on the oxygen concentration in the engineered cardiac tissue. A) Volume average oxygen concentration in the tissue space, B) Minimum oxygen concentration in the tissue space C) Mixing-cup outlet oxygen concentration in the aqueous phase of the culture medium. Oxygen concentration was calculated for a densely packed channel array (100 μm channel diameter, 100 μm wall-to-wall spacing). Oxygen consumption rate in the tissue space was set at 18μM/s and was assumed to follow zero order kinetics. The velocity of culture medium was 0.135cm/s. 0%PFC white bar, 3.2%PFC gray bars. 6.2%PFC red bars. For 3.2 and 6.4% of PFC, contribution of effective diffusivity alone was compared to the contribution of convective term (vertical lines) and the combined effect of both terms (horizontal lines).

The presence of PFC emulsion increased volume averaged and minimum oxygen concentration in the tissue space as well as the bulk oxygen concentration at the outlet from channel lumen. Volume averaged concentration in the tissue space increased roughly linearly between 0 and 6.4 % of PFC emulsion (R^2=0.9586). Minimum oxygen concentration in the tissue

space was increased by 19.5 times with addition of 3.2% PFC and 28 times by addition of 6.4% PFC. Concurrently with the increase in the concentration in the tissue space, the concentration in the culture medium increased as well. Addition of 3.2% -6.4%of PFC emulsion, increased the outlet bulk medium aqueous concentration by 3.8-5 times respectively. As illustrated in the **Figure 8.2**, ~96.7-98.7% of the increase in the minimum and volume averaged oxygen concentration can be contributed to the increase in the convective term, with the reminder of the increase associate with the increase in effective diffusivity.

Model solution and validation

Oxygen distribution in one half of the tissue construct perfused with pure culture medium and culture medium supplemented with PFC emulsion, as described in experimental section (**Table 8.2**), is presented in **Figure 8.3. A, B**. The convergence was tested by increasing mesh size from 141 triangles and 92 nodes to 9024 triangles and 4677 nodes, with no significant changes in the oxygen profile (**Figure 2C**). In the last two refinements, the values agreed up to four significant digits. In addition for zero order kinetics, the agreement between the simulated oxygen profile in the tissue space (at L/2=0.1cm) and one dimensional analytical solution was in three significant digits.

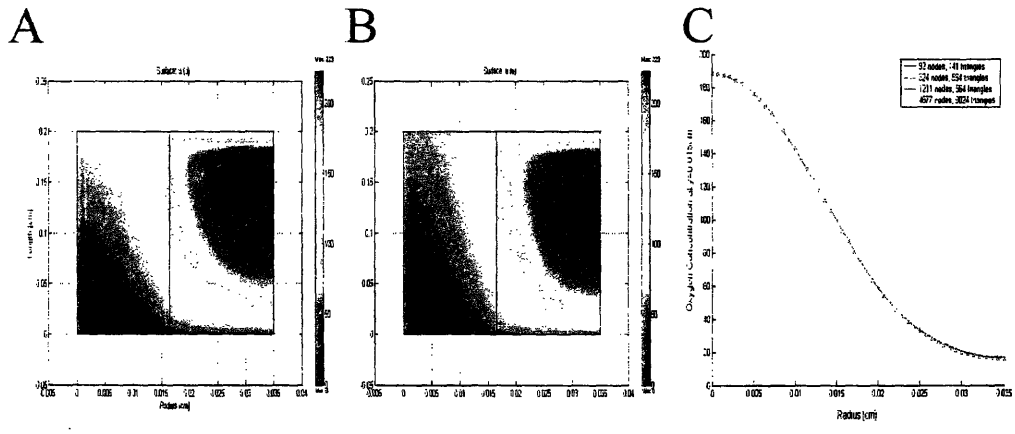

Figure 8.3. Model solution and validation. Distribution of oxygen concentration (μM) in a channel and tissue space perfused with culture medium alone (A) or culture medium supplemented with5.4 vol% PFC emulsion (B) with experimentally determined parameters (Table 8.2). Convergence demonstrated in (C) corresponds to the concentration at 0.15 cm of construct length in (A). One half of channel and tissue space shown in all panels.

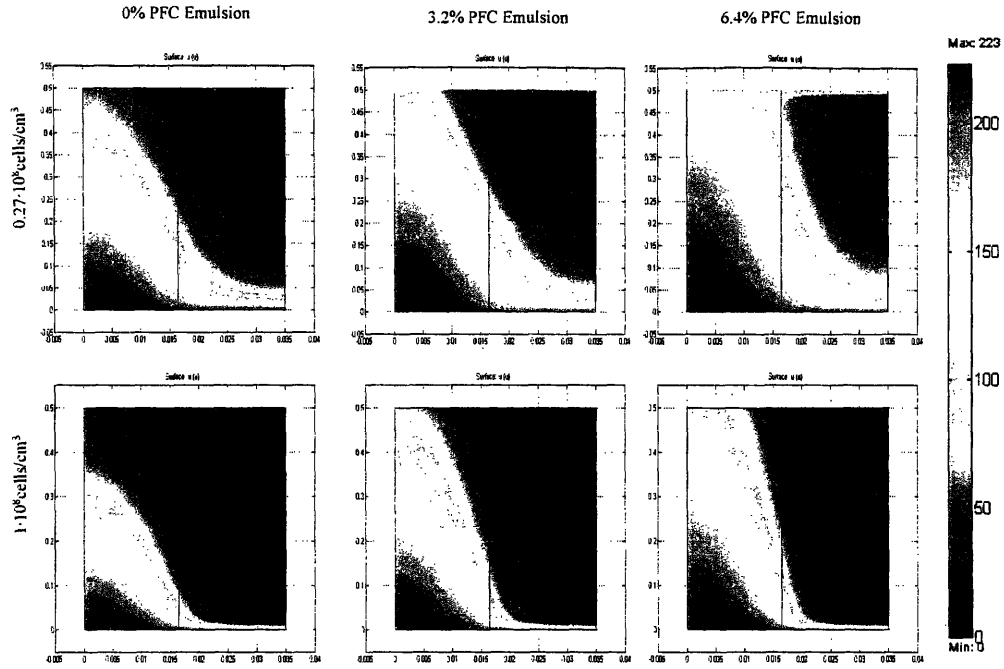

Figure 8.4. Comparison of predicted oxygen concentration profiles (μM) in a channel array supplemented with 0, 3.2, or 6.4% PFC emulsion. Cell density in the tissue space was set to the low value measured experimentally ($0.27 \cdot 10^8$ cells/cm3) and the physiological cell density ($1 \cdot 10^8$ cells/cm3). Channel array dimensions (330 μm channel diameter, 360 μm wall-to-wall spacing, and the average velocity of culture medium (0.049cm/s) correspond to the experimentally obtained values. One half of the channel and surrounding tissue space shown, array length [cm] vs. radius [cm].

Oxygen profiles in the cardiac tissue constructs at experimental conditions

At the inlet of the tissue construct oxygen concentration in the channel lumen in the pure culture medium and PFC supplemented culture medium is comparable and slightly lower in the tissue space of the PFC group due to the higher cell density. At the height of 0.1cm the concentrations become comparable in both lumen and the tissue space, while at 0.15 cm higher oxygen concentration is observed in the lumen of the channel perfused with the PFC supplemented culture medium compared to the pure culture medium. Finally at 0.19cm higher oxygen concentration is observed in both tissue space and the channel lumen for the PFC supplemented culture medium, demonstrating the benefits of supplementation for thicker constructs of higher cell density.

In the channel lumen, oxygen concentration in the aqueous phase of culture medium was higher in the PFC supplemented medium compared to the pure medium However, in the tissue

space the differences in oxygen concentration were present at small depths while at higher depths there were no significant differences, indicating that even with perfluorocarbons it is necessary to have channels spaced closely in order to avoid oxygen limitations.

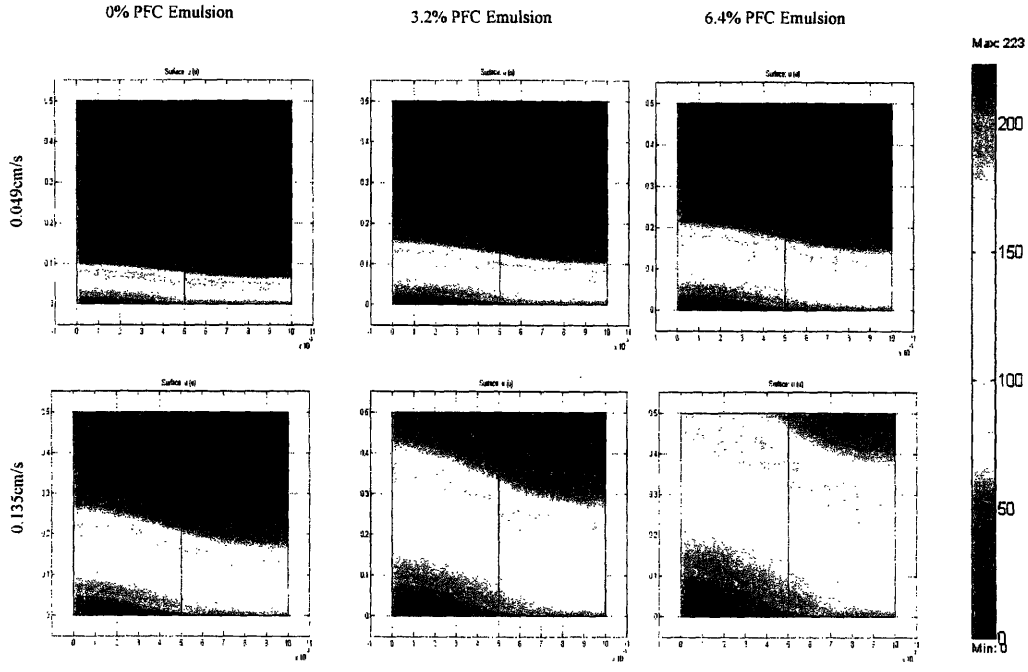

Figure 8.5. Comparison of predicted oxygen concentration profiles (μM) in a channel array supplemented with 0, 3.2, or 6.4% PFC emulsion at physiological cell density ($1 \cdot 10^8$cells/cm3) at the low (0.049cm/s) and high (0.135 cm/s) average velocities of culture medium. Channel array dimensions are 100 μm channel diameter, 100μm wall-to-wall spacing. One half of the channel and surrounding tissue space shown, array length [cm] vs. radius [cm].

Model predictions to aid in scaffold and culture conditions design

In order to determine conditions necessary to provide high oxygen concentration to the tissue space with physiologically high cell density ($1 \cdot 10^8$cells/cm^3) and clinically relevant thickness (0.5cm), we varied channel geometry, flow rate and fraction of PFC emulsion.

In one case channel geometry and flow rate corresponded to the experimentally obtained values: 330μm channel diameter, 370 μm wall-to-wall spacing and 0.049cm/s average channel velocity (**Figure 8.4**). At both cell densities investigated ($0.27 \cdot 10^8$ cells/cm^3 and $1 \cdot 10^8$cells/cm^3) oxygen concentration in the channel lumen and the tissue space increased with the increase in the circulating PFC fraction. For lower cell density at 6.4vol% PFC most of the tissue space had

oxygen concentration above 50 μM, the value roughly corresponding to the venous blood. However, at the high cell density most of the tissue space 50-100μm away from the channel was deprived of oxygen even at 6.4vol%PFC, in spite of the high oxygen concentrations present in the channel lumen (**Figure 8.4**).

In order to address the problem, oxygen profiles were modeled in a channel array consisting of channels 100μm in diameter and 100 μm wall-to-wall spacing at physiologically high cell density $1 \cdot 10^8$cells/cm^3. At 0.049 cm/s oxygen concentration increased significantly in both tissue space and channel lumen with the increase in circulating PFC emulsion from 0 to 6.4%% (**Figure 8.5**). However, in order to satisfy the demand of the entire 0.5 cm thick piece of tissue, average fluid velocity had to be increased to 0.135 cm/s.

Oxygen transport improvements with the presence of PFC emulsion

The presence of 3.2-6.4 vol% Oxygent™ (3.2-6.4 vol% PFC emulsion droplets) increases the effective diffusivity of the culture medium by 9-18%. In addition convective term is increased by 62-123% which is equivalent to the comparable increase in average fluid velocity. Therefore, both the transport in axial and radial direction is improved compared to the presence of the culture medium alone.

Table 8.5: Oxygen transport improvements in the presence of PFC emulsion

CIRCULATING PFC FRACTION (OXYGENT™ FRACTION)	CONVECTIVE TERM $[1+(K-1)\phi]$	EFFECTIVE DIFFUSIVITY EQ.11
0.000 (0.00)	1.00	D_a
0.032 (0.10)	1.62	$1.09D_a$
0.054 (0.17)	2.05	$1.15D_a$
0.064 (0.20)	2.23	$1.18D_a$

DISCUSSION:

We recently reported a biomimetic *in vitro* tissue culture system in which neonatal rat heart cells were cultured on an elastic, highly porous scaffold with a parallel array of channels perfused with culture medium supplemented with synthetic oxygen carrier (Oxygent™ perfluorocarbon emulsion). In this system, parallel channel array mimics the role of capillary network and the PFC emulsion mimics the role of hemoglobin. Constructs perfused with unsupplemented culture medium served as controls.

The main goal of this paper was to develop a steady state mathematical model that can be used to predict oxygen concentration profiles in channel lumen and tissue space surrounding each channel as a function of channel geometry, cell density, PFC emulsion content and flow rate. To simplify equations of continuity for oxygen constant density and diffusivity were assumed in each region. In addition it was assumed that there was no convection in the tissue space and that the rate of absorption of oxygen from the PFC phase into aqueous phase was not rate limiting.

The construct was divided into array of cubic domains with a channel in the center and tissue space surrounding the channel. One half of cross section of each domain with channel and tissue space surrounding it was modeled in 2D. The main modes of mass transfer in the channel were convection in axial direction and diffusion in radial direction based on the value of Peclet number (Pe) (**Table 8.3**). Solubility of oxygen in the perfluorocarbon phase is governed by Henry's law. Both axial and radial diffusion were taken into account in the tissue region. The consumption of oxygen in the tissue region occurs by Michaelis-Menten kinetics. Neumann boundary conditions were imposed at symmetry planes (channel center, and half distance between the domains). For all simulated cases Re was low and the flow was fully developed over most of the construct length (**Table 8.3**).

The assumption of no convection in the tissue space was validated by experimental evaluation of hydraulic permeability of empty channel-free biorubber scaffold. The obtained tissue Pe was 0.19. As Matrigel/cell suspension was added to the scaffold it is reasonable that the permeability of the scaffold and tissue Peclet number would decrease even further, justifying the assumption of no convection through the tissue space.

Simulations for the densely packed channel array with zero order kinetics (**Figure 8.2**) indicated that the presence of PFC emulsion at 3.2 and 6.4% significantly increased the volume averaged and minimum concentration in the tissue space, while maintaining higher oxygen concentration in the culture medium at the outlet. The majority of this increase (~98%) could be contributed to the increase in the convective term.

When cultivated in the presence of PFC emulsion (5.4 vol% circulating), the constructs had higher DNA and protein content (Chapter 7 **Table 7.1**) as well as the higher cells density compared to the unsupplemeted culture medium ($0.27 \cdot 10^8$ cells/cm^3 vs. $0.42 \cdot 10^8$cells/cm^3). As a result maximum oxygen consumption rate in the tissue space was higher for the PFC supplemented vs. unsupplemented culture medium (10.5 vs. 8.8 μM/s respectively). The comparison of modeled oxygen profiles in the tissue constructs (**Figure 8.3**) indicated that the differences in oxygen concentration between PFC supplemented and pure culture medium were more evident at higher construct thickness than closer to the entrance. Close to the entrance the

oxygen concentration in the tissue space was even slightly lower for the PFC supplemented culture medium due to the higher cell density. At the entrance to the tissue construct the concentration of oxygen in the aqueous phase of culture medium supplemented with PFC was slightly lower (~10μM) than in the pure culture medium, indicating that longer gas exchanger may be necessary for the complete reoxygenation of the culture medium supplemented with PFC emulsion.

Along the length of the channel lumen oxygen concentration of the PFC supplemented medium was higher than the non-supplemented (**Figure 8.3**) as well as in the tissue space at the channel wall (**Figure 8.3**). At about 75 μm within the channel wall these differences became less obvious and completely disappeared at x=0.035cm. Although oxygen supply to the construct was increased by the addition of PFC emulsion, so was the number of surviving cells, resulting in the increased oxygen consumption and approximately comparable oxygen concentration profiles over most of the construct volume.

In order to determine the effect of PFC emulsion on the oxygen profile in tissue space with the same cell density, we performed simulations at the existing channel geometry and flow rate with 0, 3.2, and 6.4% PFC (**Figure 8.4**). The low value of investigated cell density was $0.27 \cdot 10^8$ cells/cm^3 and the high was physiologically relevant value of $1 \cdot 10^8$ cells/cm^3. In both cases, oxygen concentration in the channel lumen and tissue space increased with the increase in the circulating PFC fraction. (**Figure 8.4**). However, at physiological cell densities, most of the tissue space beyond 50 μm away from the channel wall was deprived from oxygen even at 6.4%PFC emulsion.

In order to remedy this problem at high cell densities (10^8cells/cm^3), we investigated oxygen profiles in a 0.5 cm thick channel array with 100μm channel diameter and 100μm wall-to-wall spacing (**Figure 8.5**). The channel array used in our experiments (330μm channel diameter and 370μm wall-to-wall spacing) is the finest obtainable in 0.2cm thick scaffolds using the existing laser/cutting engraving system. In order to make thick scaffold (0.5 cm) with a fine channel array (100μm) the machining will have to be modified. Although the oxygen concentration in the tissue space increased considerably with the increase of circulating PFC concentration from 0-6.4%, we had to increase the flow rate in order to provide enough oxygen for the entire 0.5 cm thick construct. At our best conditions (0.135cm/s and 6.4%PFC) the oxygen is not depleted at any point in the scaffold and the minimum concentration of 33μM is approximately five times above the Km.

According to the developed mathematical model, addition of PFC emulsion increased convective term by the factor of $(K-1)\phi$, which is equivalent to the same increase in the average velocity. Therefore, at the given average velocity, culture medium with PFC will improve transport in the axial direction and support thicker construct, compared to the pure culture medium. In addition, higher oxygen solubility and diffusivity of PFC droplets, increased effective diffusivity of the supplemented culture medium by 9-18% compared to the pure culture medium, therefore improving the radial transport of oxygen.

In summary, a steady state mathematical model for oxygen concentration profile in a tissue constructs with a parallel channel array was developed as a function of concentration of PFC emulsion channel geometry, flow rate and cell density. The model was solved for a set of experimentally obtained conditions and used to predict oxygen concentration profiles in constructs of clinically relevant thickness (0.5 cm) and physiologically high cell densities. For the experimentally relevant parameters, the obtained cell density was higher when constructs were perfused with the PFC supplemented culture medium, leading to the increased oxygen consumption rate. Therefore, in spite of the improved delivery, the oxygen concentration profiles were comparable in the tissue space of the constructs cultivated with pure and PFC supplemented culture medium. The concentration in the channel lumen was higher in the PFC supplemented medium. At identical cell density the concentration in the tissue space increased with the increase in PFC concentration, flow rate and for finer channel arrays.

LIST OF SYMBOLS:

a_p-interfacial area of PFC droplets

Bi-Biot number

C_a-oxygen concentration in the aquos phase of the culture medium

C_{in}- aqueous phase oxygen concentration of the bulk culture medium at the inlet to the perfusion cartridge

C_{out}- aqueous phase oxygen concentration of the bulk culture medium at the outlet from the perfusion cartridge

C_p-oxygen concentration in the perfluorocarbon phase of culture medium

C_{total} –total oxygen concentration in the culture medium

d-diameter of a PFC droplet

Da-diffusivity in the aqueous phase of the culture medium

Deff -effective diffusivity of the culture medium

Dp-diffusivity in the perfluorocarbon phase of the culture medium

Dt-diffusivity in the tissue space

J-diffusive flux of oxygen

k2-mass transfer coefficient for the absorption of oxygen from the PFC droplet to the aquos phase

k3- channel mass transfer coefficient

K_{eff}-effective partition coefficient

K_m-Oxygen concentration at which consumption rate in the tissue space equals (½)V_{max}

K-partition coefficient

L-length of tissue construct (equivalent to channel length)

N_p-number density of PFC droplets

Pe-channel Pe number

Pe_s-scaffold Pe number

r_2-mass flow of oxygen from the PFC particles into the aqueous phase

r_3-mass flow of oxygen from the bulk culture medium to the channel wall

R_c-channel radius

Re-channel Re number

R_t-radius of the tissue space (defined from the channel center)

Sh_c-channel Sherwood number

Sh_d-droplet Sherwood number

S_p-surface area of one PFC droplet

U-average fluid velocity of the culture medium in the channel

$\mathbf{v_a}$-culture medium velocity in the channel

$\mathbf{v_a}$-culture medium velocity in the tissue space

V_{max}-Maximum oxygen consumption rate in the tissue space

v_z-axial velocity component of the culture medium in the channel

ΔC_1-oxygen gradient from the center of the PFC droplet to the droplet/aqueous phase interface

ΔC_2-oxygen gradient in the PFC droplet boundary layer

ΔC_3-oxygen gradient from the bulk fluid aqueous phase to the channel wall

Δz-thickness of a differential channel layer

ϕ-fraction of circulating PFC emulsion droplets

η-viscosity of culture medium

ρ-density of culture medium

REFERENCES

1. Fournier, R.L., *Basic Transport Phenomena in Biomedical Engineering.* 1998, Philadelphia: Taylor & Francis.
2. Obradovic, B., et al., *Gas exchange is essential for bioreactor cultivation of tissue engineered cartilage.* Biotechnology and Bioengineering, 1999. 63(2): p. 197-205.
3. Carrier, R.L., et al., *Effects of oxygen on engineered cardiac muscle.* Biotechnology and Bioengineering, 2002. 78: p. 617-625.
4. Rakusan, K. and B. Korecky, *The effect of growth and aging on functional capillary supply of the rat heart.* Growth, 1982. 46: p. 275-281.
5. Chromiak, J.A., et al., *Bioreactor perfusion system for the long-term maintenance of tissue engineered skeletal muscle organoids.* In Vitro Cellular & Developmental Biology - Animal, 1998. 34: p. 694-703.
6. Bursac, N., et al., *Cardiac muscle tissue engineering: toward an in vitro model for electrophysiological studies.* American Journal of Physiology: Heart and Circulatory Physiology, 1999. 277(46): p. H433-H444.
7. Carrier, R.L., et al., *Perfusion improves tissue architecture of engineered cardiac muscle.* Tissue Engineering, 2002. 8(2): p. 175-188.
8. Carrier, R.L., et al., *Cardiac tissue engineering: cell seeding, cultivation parameters and tissue construct characterization.* Biotechnology and Bioengineering, 1999. 64: p. 580-589.
9. Casey, T.M. and P.G. Arthur, *Hibernation in noncontracting mammalian cardiomyocytes.* Circulation, 2000. 102(25): p. 3124-3129.
10. Deen, W.M., *Analysis of Transport Phenomena.* 1998, New York: Oxford University Press.
11. Piret, J.M. and C.L. Cooney, *Model of oxygen transport limitations in hollow fiber bioreactors.* Biotechnology and Bioengineering, 1991. 37: p. 80-92.
12. Shah, N. and A. Mehra, *Modeling of oxygen uptake in perfluorocarbon emulsions. Some comparisons with uptake by blood.* ASAIO Journal, 1996. 42(3): p. 181-189.
13. Radisic, M., et al., *High density seeding of myocyte cells for tissue engineering.* Biotechnology and Bioengineering, 2003. 82(4): p. 403-414.
14. Radisic, M., et al., *Medium perfusion enables engineering of compact and contractile cardiac tissue.* American Journal of Physiology: Heart and Circulatory Physiology, 2004. 286: p. H507-H516.
15. Yamada, T., et al., *Oxygen consumption of mammalian myocardial-cells in culture - measurements in beating cells attached to the substrate of the culture dish.* Analytical Biochemistry, 1985. 145(2): p. 302-307.
16. Ni, Y., D.H. Klein, and T.J. Pelura, *Rheology of concentrated perfluorocarbon emulsions.* Biomaterials Artificial Cells and Immobilization Biotechnolology, 1992. 20(2-4): p. 869-871.
17. Kretzmer, G. and K. Schugerl, *Response of mammalian cells to shear stress.* Applied Microbiology and Biotechnology, 1991. 34(5): p. 613-616.
18. Stathopoulos, N.A. and J.D. Hellums, *Shear stress effects on human embryonic kidney cells in vitro.* Biotechnology and Bioengineering, 1985. 27: p. 1021-1026.
19. Geankoplis, C.J., *Transport Processed and Unit Operations.* 3rd ed. 1993, Englewood Clifs, NJ: Prentice-Hall.
20. Mates vanLobensels, E., et al., *Modeling diffusion limitation of gas exchange in lungs containing perfluorocarbon.* Journal of Applied Physiology, 1999. 86(1): p. 273-284.

9. SUMMARY AND FUTURE WORK

Summary

This Ph.D. thesis was motivated by the need to create functional cardiac tissue equivalents for the repair of impaired myocardium or studies of normal and pathological tissue function *in vitro*. Current tissue engineering approaches have been limited by diffusional oxygen supply, lack of physical stimuli and absence of multiple cell types characteristic of the native myocardium.

We hypothesized that functional, clinically sized (1-5 mm thick), compact cardiac constructs with physiologic cell densities can be engineered *in vitro* by mimicking cell microenvironment present in the native myocardium *in vivo*. The main factors in the myocardial environment include: high cell density (10^8cells/cm^3), multiple cell types, convective-diffusive oxygen supply with the presence of natural oxygen carrier, hemoglobin, and excitation-contraction coupling. During the course of this PhD thesis each of these factors was tested independently. The obtained results were summarized in six chapters (Chapter 3-8) of this thesis.

Since cardiac myocytes have limited ability to proliferate we developed methods of seeding cells at high densities while maintaining their viability (Chapter 3). This was achieved via a two step approach, in which cell/Matrigel suspension was inoculated onto collagen sponges followed by the alternating flow direction medium perfusion. Cultivation of cardiac constructs in the presence of convective-diffusive oxygen transport in perfusion bioreactors, maintained aerobic cell metabolism, viability and uniform distribution of cells expressing cardiac markers (Chapter 4). To improve cell morphology and functional tissue assembly cardiac constructs were cultivated with electrical stimulation of contraction in a physiologically relevant regime (Chapter 5). Orderly excitation-contraction coupling enabled formation of tissue with elongated cells aligned in parallel and with organized ultrastructure remarkably similar to the one present in the native heart. To investigate the effect of multiple cell types on the properties of engineered cardiac tissue cardiac fibroblasts and cardiac myocytes were cultivated synchronously, separately or serially (pretreatment of scaffolds with fibroblasts followed by the addition of myocytes) (Chapter 6). Pretreatment remarkably improved contractile response as well as biochemical and morphological properties of engineered cardiac tissue, most likely due to the deposition of extracellular matrix (e.g. collagen) and soluble factors that enhanced functional tissue assembly after addition of myocytes. Finally, in order to mimic capillary structure, cardiac fibroblasts and myocytes were co-cultured on a scaffold with a parallel channel array that was perfused with culture medium supplemented with synthetic oxygen carrier (perfluorocarbon, PFC, emulsion). The presence of PFC emulsion resulted in significantly higher cell density and improved contractile properties compared to the constructs cultivated in the culture medium alone,

presumably by increasing total oxygen content. (Chapter 7). Mathematical model of oxygen transport indicated that the release of oxygen from PFC particles was not rate limiting, and that the improvements in the oxygen transport were due to the increase in effective diffusivity of the culture medium supplemented with PFC emulsion and increase in the convective term proportional to the fraction of PFC particles. (Chapter 8)

In summary, each of the biomimetic factors applied alone, remarkably improved the properties of engineered cardiac tissue compared to the conventional tissue culture methods. All of the important structural and functional characteristics of the engineered cardiac tissue, high cell density, elongated cell morphology parallel cell alignment and contractility, were successfully addressed.

Future work

In this PhD thesis each of the listed biomimetic factors was tested independently. In the future work, it is necessary to combine these individual factors, in a single system. As a first step it is necessary to develop a bioreactor that would provide medium perfusion and electrical stimulation at the same time. Medium perfusion would enable high cell density and uniform distribution, while electrical stimulation would enable modulation of the level of cell differentiation and parallel cell alignment. The first step in the design of such a bioreactor would be a design of perfusion chamber with multiple wells for tissue construct, and electrodes built in the walls of the chamber (top-to-bottom or side-to-side depending on the desired cell orientation). Uniform medium flow can be provided by a porous platen of high resistance. In addition in such a system, mechanical stimulation can be provided by the pulsatile medium flow in conjunction with the pinch valve at the outlet from the perfusion chamber. Such a bioreactor would be useful in basic studies of the interaction between, electrical, mechanical and biochemical stimuli.

The cell co-culture can be expanded to include the third major cell type present in the native myocardium: endothelial cells. Channeled scaffolds, pretreated with fibroblasts can be seeded with cardiomyocytes and cultivated in the advanced bioreactor presented above. When the desired level of parenhymal tissue formation is achieved, endothelial cell can be injected to line the channels as described [1].

All of the work in this PhD, thesis has been performed with neonatal rat ventricular cells as a model system. Our overall goal is however, to repair human hearts and provide in vitro systems for study of human myocardium. Since adult cardiomyocytes have limited ability to proliferate [2] it is necessary to find autologous human cell source. It has been demonstrated recently, that with appropriate biochemical treatment bone marrow mesenchymal stem cells [3] and cells from adipose tissue [4, 5] can express some markers of cardiomyocyte phenotype. As a

part of future work it would be useful to study if undifferentiated cells from the autologous sources listed above can be turned into heart tissue using the biomimetic system presented in this thesis. Undifferentiated cells can be placed into 3D environment using the described gel inoculation system and collagen sponges, followed by cardiac-like electrical stimulation. As advanced bioreactors become available a range of mechanical, biochemical and electrical stimuli can be applied simultaneously, thereby potentially improving the level of differentiation.

Finally, it is necessary to evaluate the performance of engineered cardiac tissue in the long term and short term *in vivo* implantation studies. Previous implantation studies, showed moderate improvement and functional integration of the engineered cardiac constructs with the host myocardium [6-8]. Part of the problem may be that when implanted cardiac constructs do not communicate electrically with the rest of heart tissue. Contractions are relayed passively, instead by the action potential propagation. In the future work, it is necessary to check if pacing of the cardiac patch upon implantation via a pace-maker-like device would enhance the implantation outcome, and improve electro-mechanical coupling with the host myocardium.

Although, the routine treatment of impaired myocardium via tissue engineering may not become reality in our life-time, we will certainly address many of important biological questions by overcoming challenges necessary for successful implantation.

REFERENCES:

1. Niklason, L.E., et al., *Functional arteries grown in vitro.* Science, 1999. **284**(5413): p. 489-493.
2. Soonpaa, M.H. and L.J. Field, *Survey of studies examining mammalian cardiomyocyte DNA synthesis.* Circulation Research, 1998. **83**(1): p. 15-26.
3. Reyes, M., et al., *Purification and ex vivo expansion of postnatal human marrow mesodermal progenitor cells.* Blood, 2001. **98**(9): p. 2615-2625.
4. Rangappa, S., et al., *Transformation of adult mesenchymal stem cells isolated from the fatty tissue into cardiomyocytes.* Annals of Thoracic Surgery, 2003. **75**(3): p. 775-779.
5. Gaustad, K.G., et al., *Differentiation of human adipose tissue stem cells using extracts of rat cardiomyocytes.* Biochemical and Biophysical Research Communications, 2004. **314**(2): p. 420-427.
6. Li, R.-K., et al., *Survival and function of bioengineered cardiac grafts.* Circulation, 1999. **100**(Suppl II): p. II63-II69.
7. Leor, J., et al., *Bioengineerred cardiac grafts: A new approach to repair the infarcted myocardium?* Circulation, 2000. **102**(suppl III): p. III56-III61.
8. Zimmermann, W.H., et al., *Cardiac grafting of engineered heart tissue in syngenic rats.* Circulation, 2002. **106**(12 Suppl 1): p. I151-I157.